CHARACTERIZATION OF FIBROBLAST GROWTH FACTOR RECEPTOR TYPE I ISOFORMS IN *Xenopus laevis* EMBRYONIC DEVELOPMENT

GORDON W. NASH

Characterization of Fibroblast Growth Factor Receptor Type I Isoforms in *Xenopus laevis* Embryonic Development.

Gordon W Nash B.Sc.

A thesis submitted to the
School of Graduate Studies
in partial fulfillment of the
requirements for the degree of
Master of Science

Terry Fox Cancer Research Laboratories
Faculty of Medicine
Memorial University of Newfoundland

St. John's Newfoundland

Abstract

Fibroblast growth factor receptors are encoded by four genes, FGFR1-4, which are alternatively spliced to produce a large number of variant isoforms. This project was designed to investigate the molecular mechanism of the FGFR-VT+ isoform compared to its counterpart FGFR-VT- and the expression of four additional isoforms (FGFR-PS+, FGFR-PS-, α-FGFR1 and β-FGFR1). FGFR-VT- and FGFR-VT+ differ only by a dipeptide (Val^{423}-Thr^{424}) deletion. FGFR-PS- and FGFR-PS+ differ only by a dipeptide (Pro^{442}-Ser^{443}) deletion. α-FGFR and β-FGFR differ by the inclusion or exclusion of the first of the three immunoglobulin-like (Ig-like) loops.

Previous work has shown that overexpression of the VT+ form in *Xenopus* embryos resulted in posterior truncations, whereas embryos overexpressing the VT- form developed normally. In an effort to elucidate the molecular basis of these deformities, expression patterns of *Xenopus* molecular markers known to be important for the development of the anterior-posterior axis were investigated. Of the markers studied (BMP-4, Xenopus forkhead, Goosecoid, Mix-1, Noggin, Xenopus brachyury, Xwnt-8, Xenopus posterior), no difference in expression pattern was observed, as determined by RT-PCR.

Expression during early embryonic development of the FGFR variants PS+/PS- and α-FGFR1/β-FGFR1 were also examined by RT-PCR. Results suggested that PS- is more abundant than PS+ (1.3-1.8X higher) during early *Xenopus* development, however by stage 11.5 the ratio of PS-/PS+ approaches 1.0. Analysis of the Ig variants indicated that the α-FGFR1 form is the predominant transcript (2.5-4.1X higher) in early development. As development proceeds into tadpole stages, β-FGFR1 shows an increase in expression levels approaching that of α-FGFR1 at the same stage of development, with the ratio of α-FGFR1/β-FGFR1 approaching 1.0.

Acknowledgements

I would like to thank my supervisor, Dr. Laura Gillespie, for her support, encouragement, and insight. I would also like to thank my committee, Dr. Gary Paterno and Dr. Karen Mearow, for reviewing my thesis and support throughout my program. I also want to thank Gary for his insightfulness and technical support, as well as his comic relief. I would like to thank everyone in the Terry Fox Labs, especially Corinne, Paula and Artee for their technical assistance and support throughout my Masters program. I thank the staff of the Graduate Student Office for their assistance in completing this thesis. I thank my family and friends for their continued support, especially during these last few weeks. Adam, thanks for the friendly competition these past couple of months, it really helped get this thesis completed. Mandy, without your support I would have given up a long time ago, thank-you.

Table of Contents

List of Tables

List of Figures

List of Abbreviations

aFGF	acidic fibroblast growth factor
AIGF	androgen-induced growth factor
AP	ammonium persulfate
BEK	bacterially expressed kinase
bFGF	basic fibroblast growth factor
BMP-4	bone morphogenetic protein – 4
$Ca(NO_3)_2 \cdot 4H_2O$	calcium nitrate
cDNA	complementary deoxyribonucleic acid
CEK-2	chicken embryo kinase
cRNA	complementary ribonucleic acid
DAG	diacylglycerol
dATP	2'-deoxyadenosine-5'-triphosphate
dCTP	2'-deoxycytidine-5'-triphosphate
DEPC	diethyl pyrocarbonate
dGTP	2'-deoxyguanosine-5'-triphosphate
dH_2O	deionized water
DNA	deoxyribonucleic acid
DNase	deoxyribonuclase
dNTP	dinucleoside triphosphates
dpp	decapentaplegic
DTT	dithiothreitol
dTTP	2'-deoxythymidine-5'-triphosphate
EDTA	ethylene diamine tetraacetic acid
eFGF	embryonic fibroblast growth factor
FGF	fibroblast growth factor
FGFR	fibroblast growth factor receptor
GAF	glia-activating factor
Grb2	growth receptor-binding protein 2
gsc	goosecoid
H_2O_2	hydrogen peroxide
Hepes	N-[2-hydroxyethyl]piperazine-N'-[2-ethanesulfonic acid]
HLGAG	heparin-like glycosaminoglycans
IAA	isoamylalcohol
Ig	immunoglobulin
IP_3	inositol triphosphate
KCl	potassium chloride
KGF	keratinocyte growth factor
MAPK	mitogen-activated protein kinase
MBT	mid-blastula transition
MEK	Map kinase/ERK (extracellular signal-regulated protein kinase)
$MgSO_4 \cdot 7\ H_2O$	magnesium sulfate
Mix.1	mesoderm induced homeobox 1

MMLV-RT	Moloney Murine Leukemia Virus reverse transcriptase
mRNA	messanger RNA
NaBicard	sodium bicarbonate
NaCl	sodium chloride
NAM	normal amphibian medium
NaOAc	sodium acetate
NaOH	sodium hydroxide
NaOH	sodium hydroxide
PCR	polymerase chain reaction
PIP2	phosphatidyl-inositol-4,5-bisphosphate
PKA	protein kinase A
PKC	protein kinase C
PLC-γ	phospholipase C – gamma
Pro	proline
RNA	ribonucleic acid
RNase	ribonuclease
RT	reverse transcription
RTK	receptor tyrosine kinase
RT-PCR	reverse transcription polymerase chain reaction
SDS	sodium dodecyl sulfate
SDS-PAGE	sodium dodecyl sulfate – polyacrylamide gel electrophoresis
SEP	sperm entry point
Ser	serine
Sos	son of sevenless
SSB	sample loading buffer
TBE	tris, borate, EDTA buffer
TCA	trichloroacetic acid
TEMED	N, N, N', N'-tetramethylethylenediamine
TGF-β	transforming growth factor – beta
Thr	threonine
Val	valine
Xbra	xenopus brachyury
XFD	dominant negative mutant of XFGFR
XFGFR	xenopus fibroblast growth factor receptor
Xnr	xenopus nodal related
Xpo	xenopus posterior
XTC-MIF	XTC mesoderm inducing factor
Xwnt-8	xenopus wnt-8

Chapter 1
Introduction

1.1 Model System: *Xenopus laevis*

Xenopus laevis, the African clawed frog, has been used as a model system for the analysis of early vertebrate development for decades (Deuchar 1975; Jones and Smith 1999). *Xenopus laevis* present many features that make it appropriate for use in developmental biology studies: the females can be induced to lay large quantities of viable eggs both easily and repeatedly; the eggs are large (approximately 1 mm diameter) and this is favorable for such procedures as micro-injection and micro-dissection; *in vitro* fertilization using the shredded testes from a sacrificed male *Xenopus* provides large numbers of synchronously developing embryos; the rapid rate of development in *Xenopus* means that results can be obtained quickly; the yolk supply that each egg contains serves as an energy source permits the eggs to be cultured in relatively simple salt solutions. Mesoderm induction is the primary developmental process being studied in this project, but before describing it in detail, a brief overview of early *Xenopus* development will be presented.

1.2 Xenopus Development

An overview of *Xenopus laevis* lifecycle is pictorially represented in Figure 1.1. The unfertilized egg is already differentiated into an upper, pigmented half known as the animal hemisphere and a lower, unpigmented half known as the vegetal hemisphere, together forming a radially symmetrical sphere. Following fertilization of the egg by a

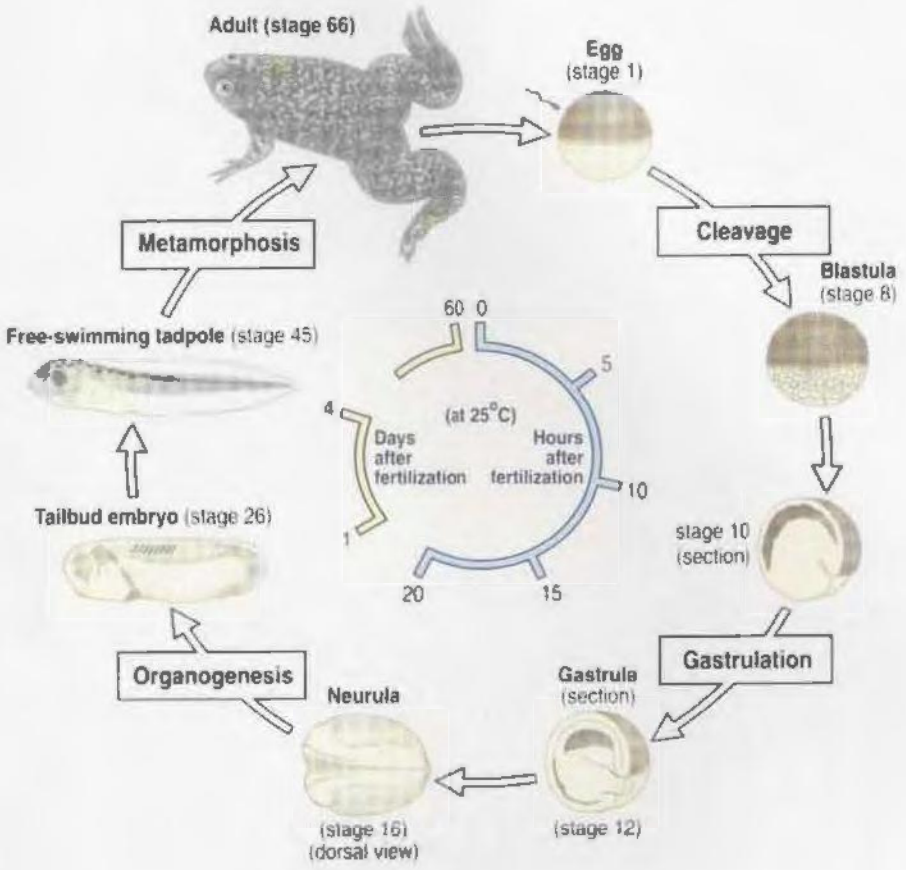

Figure 1.1: Life Cycle of *Xenopus laevis*. The inner scale represents the amount of time, in hours and days, required post-fertilization for *Xenopus* embryos to reach the standardized stages of development indicated, when cultured at 25°C. (from Principles of Development, Lewis Wolpert (1998))

sperm (Stage 1) a period of rapid cleavage commences. The cleavages are mitotic cell divisions which result in an increase in cell number without cell growth, hence a decrease in cell size. After approximately six hours of cell division, the embryo, now known as a blastula, has formed a fluid-filled cavity, the blastocoel, located above the larger yolk cells of the vegetal hemisphere (Stage 8). The germ layers – ectoderm, endoderm and mesoderm are now partly specified. During the next stage of development, gastrulation, the cells will undergo rearrangement as to achieve the proper orientation of the germ layers, with the endoderm moving inside, the mesoderm taking up the middle layer position and the ectoderm covering the entire surface of the embryo. Gastrulation is followed by neurulation, the stage during which the nervous system is established and other major body systems are specified at their future locations. These other body systems develop during the period referred to as organogenesis. Within three days post-fertilization the embryo has developed into a free-swimming tadpole. Over the course of the next fifty to sixty days the tadpole will undergo metamorphosis and develop into an adult frog. (Wolpert et al. 1998)

1.2.1 Fertilization and Post-Fertilization

Fertilization is achieved when a single sperm penetrates the egg at any point on the animal hemisphere, referred to as the Sperm Entry Point (SEP). The SEP defines the future dorso-ventral axis of the embryo, with the future dorsal side developing opposite the SEP, reviewed in Jones and Smith (1999). The egg has two surface coats around its plasma membrane, an inner vitelline membrane and an outer jelly coat. After fertilization

the vitelline membrane lifts off from the egg surface, a process that allows the egg to rotate under the effects of gravity, moving the heavier yolk-laden vegetal hemisphere to the bottom. This occurs within fifteen to twenty minutes post-fertilization. Within an hour after fertilization, the embryo undergoes "cortical rotation", where a gel-like layer of actin filaments and associated materials collectively referred to as the cortex, rotates about thirty degrees towards the SEP relative to the inner cytoplasm (Vincent and Gerhart 1987) (Figure 1.2).

During cortical rotation the vegetal cortex opposite the SEP moves towards the animal pole. This region opposite the SEP becomes the future dorsal side and the SEP containing region becomes the future ventral side. The major developmental consequence of cortical rotation is the establishment of a signaling center in the vegetal region opposite the SEP. Referred to as the "Nieuwkoop Center", after the Dutch embryologist by that name, this center directs the dorso-ventral polarity of the blastula.

1.2.2 Cleavage Stages

The first cell cleavage occurs about 90 minutes after fertilization, beginning at the animal pole and dividing the cell (egg) into left and right halves. Subsequent cleavages occur at approximately 30-minute intervals. The second cleavage also begins at the animal pole and occurs at a right angle to the initial cleavage, separating the egg into dorsal and ventral halves. The third cleavage plane occurs perpendicular to the first two and separates the egg along the equatorial region into animal and vegetal halves. During these early cleavage stages, a small space forms between the animal and vegetal

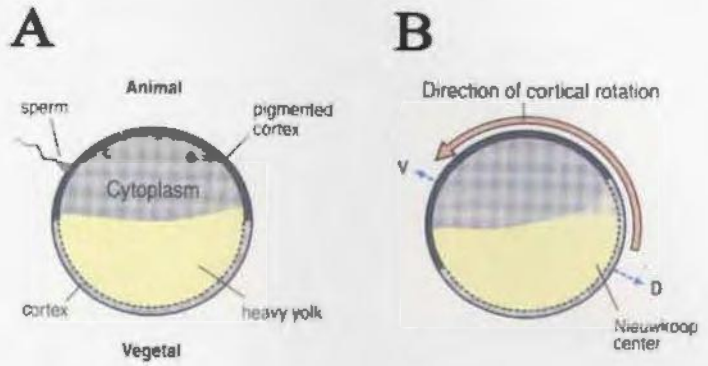

Figure 1.2: Fertilization and Cortical Rotation. (A) Fertilization indicating the sperm entry point (SEP). (B) Cortical layer rotating toward the SEP and establishing the Nieuwkoop Center. (adapted from Principles of Development, Lewis Wolpert (1998)).

hemispheres and becomes larger as cleavages continue to eventually become the blastocoel (reviewed in Jones and Smith 1999).

The period of synchronous cell division lasts for a total of 12 cleavages, which corresponds to Nieuwkoop and Faber (1967) stage 8. At this time, known as Mid-Blastula Transition (MBT), cleavage cycles become asynchronous and slow down significantly and are characterized by the onset of cell motility and zygotic transcription (Newport and Kirschner 1982; Kimelman et al. 1987).

1.2.3 Gastrulation

The blastula stage embryo next enters a period of extensive cellular rearrangement termed gastrulation. Gastrulation is first visible when some of the endodermal cells of the dorsovegetal region change shape and become known as bottle cells. These bottle cells involute to form a groove in the blastula known as the blastopore, specifically the dorsal lip of the blastopore. The layer of presumptive mesoderm and endoderm starts to move into the interior of the blastula, such that the lip forms an arc, a semi-circle and finally forms a complete circular blastopore. The first mesodermal cells to migrate are those at the dorsal side of the embryo that will give rise to head mesodermal structures. These cells migrate under the roof of the blastocoel in a single layer. It is only the leading mesodermal cells that migrate, the cells that follow undergo convergent extension. This band of presumptive mesodermal cells lie initially around the equatorial region of the embryo, they involute through the blastopore, converge into a narrow band along the dorsal midline and extend in the antero-posterior direction under the ectoderm

(Wolpert 1998). As these cells are migrating inward, the cells of the animal hemisphere, the pigmented upper half of the embryo, are undergoing epiboly, spreading/overgrowth and are converging upon the blastopore (Keller et al. 1992; Wolpert 1998). As all this cell movement and internalization proceeds, the blastopore becomes increasingly smaller until it is reduced to a slit. This closure of the blastopore is indicative of the end of gastrulation. At this point the three germ layers are appropriately positioned, the ectoderm (formerly animal hemisphere) now covers the entire external surface, the endodermal cells (formerly vegetal hemisphere) are completely internalized and the mesoderm (formerly equatorial region) forms a layer between the endoderm and ectoderm layers (reviewed in Jones and Smith 1999) (Figure 1.3). The endoderm layer will give rise to the lining of the gut and organs such as the lungs. The mesoderm will develop into notochord, muscle, heart, kidneys and blood-forming tissues. The ectoderm will give rise to epidermis and the nervous system.

1.2.4 Mesoderm Induction

Mesoderm induction is one of the first inductive interactions to occur in the developing vertebrate embryo. The early *Xenopus* embryo (pre-blastula) consists only of two cell types: presumptive ectoderm in the animal hemisphere and presumptive endoderm in the vegetal hemisphere. The formation of the third required germ layer, mesoderm, is derived from inductive interactions between the two existing cell types. Evidence for the origin of mesodermal tissues resulting from inductive interactions was achieved through the work of Nieuwkoop and colleagues (Nieuwkoop 1969; Sudarwati

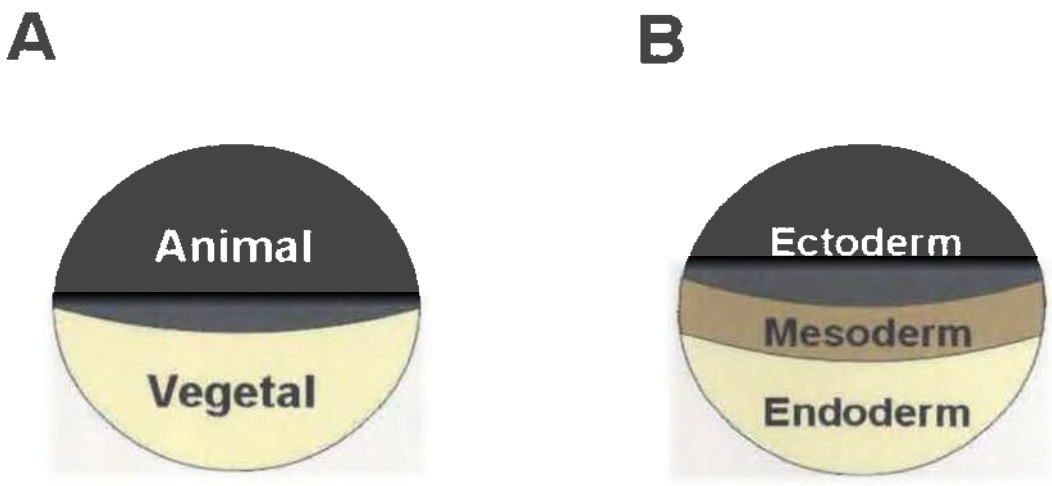

Figure 1.3: Organization of the *Xenopus laevis* early embryo. (A) Represents the maternally determined Animal and Vegetal hemispheres. (B) Represents the germ layer (ectoderm, mesoderm, and endoderm) orientation following induction of animal cells by vegetal signals.

and Nieuwkoop 1971). The work showed that when cultured independently, animal pole cells from a blastula stage embryo form epidermal derivatives and the vegetal pole cells of the same blastula stage embryo form endodermal derivatives. When the animal and vegetal pole cells of a blastula stage embryo are co-cultured, a variety of mesodermal cell types are formed (Nieuwkoop 1969; Sudarwati and Nieuwkoop 1971). Evidence that mesoderm induction is a result of secreted, diffusible molecule(s) and not direct cell-cell interactions came from Slack (Slack 1991) while re-examining the animal-vegetal pole assay of Nieuwkoop. The co-culturing of animal and vegetal pole cells was repeated with the modification of separating the two cell types using a porous membrane filter. The filter prevented direct cell-cell contacts from forming but was porous and therefore permitted soluble molecule(s) to pass through. The results obtained were identical to those determined previously by Nieuwkoop.

An additional contribution to the understanding of mesoderm induction was made in the 1970s when it was demonstrated that the type of mesoderm that forms when animal and vegetal cells are co-cultured depends on the origin of the vegetal pole cells. Boterenbrood and Nieuwkoop (1973) demonstrated, using an axolotl model, that dorsal vegetal pole cells from blastula stage embryos induce formation of dorsal mesodermal cell types (notochord and muscle) while lateral and ventral vegetal cells induce the formation of ventral mesodermal cell types (blood, mesenchyme and mesothelium). These findings were subsequently demonstrated in *Xenopus* models (Dale et al. 1985; Dale and Slack 1987).

1.2.4.1 Three-Signal Model

The previously described work led to the development of the three-signal model of mesoderm induction (Smith and Slack 1983; Slack et al. 1984) (Figure 1.4). In this model, the first signal originates from the ventral-vegetal region to induce the marginal zone cells above to specify ventral mesodermal tissue types (blood, mesenchyme and mesothelium). The second signal, emanating from the dorsal-vegetal region known as the Nieuwkoop Centre, induces the marginal zone cells overhead to specify dorsal mesodermal tissues (notochord) and results in organizer (Spemann's Organizer) activity in this region. Evidence for the first two signals was derived from the work of Boterenbrood and Nieuwkoop (1973) and evidence for the existence of the third signal (a dorsalizing signal) comes from studies by Slack and Forman (1980) and Dale and Slack (1987) (Figure 1.4). Their work demonstrated that the dorsal marginal zone tissue of an early gastrula formed notochord with some muscle and neural tissue when cultured in isolation and the ventral marginal zone tissue formed blood, mesenchyme and mesothelium. However, when co-cultured the dorsal tissue continues to form notochord while the ventral tissue forms muscle. Therefore, these results establish the presence of a third signal emanating from the newly formed dorsal mesoderm (Spemann's Organizer) and moving horizontally to exert an effect on ventral mesoderm (Slack and Forman 1980).

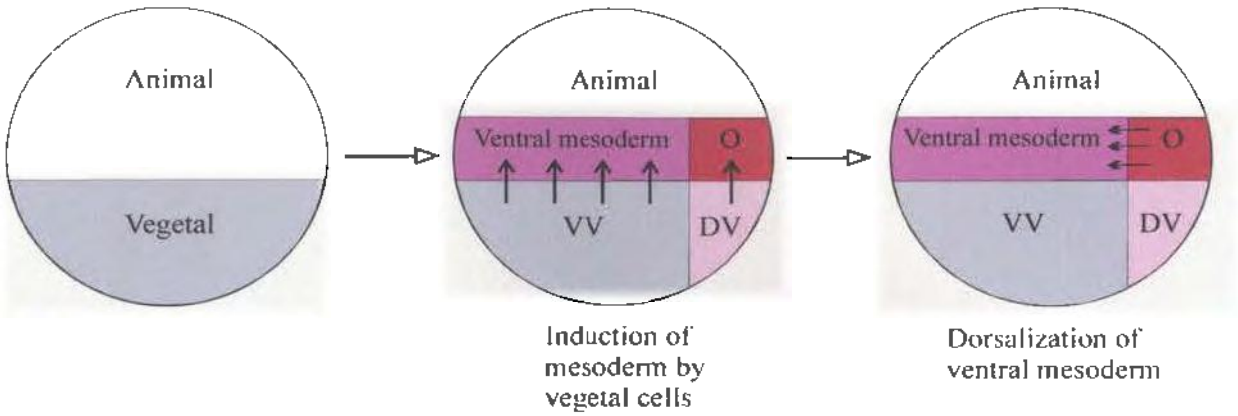

Figure 1.4: Three-signal model of mesoderm induction.
VV: ventral vegetal; DV: dorsal vegetal; O: organizer.
(as depicted in Smith et al. (1989)).

1.2.4.2 Mesoderm Inducing Factors

Mesoderm induction is the first inductive interaction in amphibian development, when cells of the marginal zone are signaled to follow different developmental pathways. While many years of developmental biology studies led to the formation of the three-signal model, i.e., that proposed mesoderm induction and subsequent patterning resulted from the action/effects of three different inducing factors, it wasn't until 1987 that progress was made in determining the chemical nature of these factors. It was at this time that Slack et al. (1987) and Kimelman and Kirschner (1987) showed that bFGF (FGF-2) displayed mesoderm-inducing activity *in vitro*. Subsequent to this, FGF induction of mesoderm was shown to be concentration dependent, such that at low concentrations ventral mesoderm (e.g. mesothelium) is induced, while at high concentrations more lateral tissues (eg. muscle) are induced (Slack et al. 1987; Slack et al. 1988). Members of the FGF family are capable of inducing all mesodermal cell types except notochord, the most dorsal mesoderm (Godsave et al. 1988), and FGF inducing activity can be greatly increased by TGF-β (Hopwood 1990; Woodland 1989). When FGF was shown to have this mesoderm inducing activity it was confidently expected that it would function similarly *in vivo*. However, while Slack's (1991) transfilter experiment suggested the factor being sought was secreted and soluble, it also suggested that bFGF (FGF-2) was not the factor released from the vegetal cells, as the inclusion of antibodies which inhibit bFGF *in vitro*, did not inhibit the natural signal *in vivo*. It may still have a role in mesoderm induction within the responding tissue, since maintenance of the early response gene *Brachyury (Xbra)* is dependent upon the expression of FGF (Isaacs et al.

1994; Schulte-Merker and Smith 1995). Pownall et al. (1996) have shown that the overexpression of eFGF causes the upregulation of the posteriorly expressed genes Xcad3 and HoxA7. The biological activity of eFGF and its expression in the posterior of the embryo suggest a potential role for it in patterning the anteroposterior axis (Pownall et al. 1996). Evidence also suggests that FGF may be required to function in conjunction with *derriere* for the formation of posterior regions (Sun et al. 1999; Zhang et al. 1998).

XTC mesoderm inducing factor (XTC-MIF) (Smith 1987; Smith et al. 1988; Rosa et al. 1988) is, as the name implies, a mesoderm-inducing factor that is secreted by the *Xenopus* XTC cell line. Smith (1987) showed that animal cap explants, when cultured in XTC-conditioned medium, differentiated into muscle and notochord tissues. Smith et al. (1990) discovered that the active molecule in the XTC-conditioned medium was a member of the TGF-β family, the *Xenopus* ortholog of Activin A (Smith et al. 1990). Although capable of inducing mesoderm *in vitro*, further work by Schulte-Merker and colleagues (1994) suggested that activin was unlikely to function as an initial mesoderm inducer *in vivo,* as the use of an activin inhibitor did not prevent the formation of mesoderm in early embryos.

The protein of Vg1 is another candidate moleeule. Vg1 is a maternal mRNA that is restricted to the vegetal hemisphere (Rebagliati et al. 1985), is a member of the TGF-β family (Weeks and Melton 1987) and shows great similarity to the deduced sequence of the *decapentaplegic (dpp)* gene product of *Drosophila*, another TGF-β family member (Padgett et al. 1987). Vg1 protein requires proteolytic cleavage to be activated. Several groups have shown that activated Vg1 protein, when injected into animal cap explants is

capable of inducing mesoderm (Kessler and Melton 1994; Forristall et al. 1995; Thomsen and Melton 1993). However, it has yet to be determined which regions of the embryo contain active Vg1 protein endogenously, if any.

VegT, is localized to the vegetal hemisphere of the mature oocyte and early embryo has been shown to be required for vegetal cells of the blastula to produce the endogenous vegetal signal(s) that cause animal caps to form mesoderm (Kofron et al. 1999; Zhang et al. 1998). As VegT is a T-box transcription factor, and as transcription of zygotic genes does not begin until after MBT and therefore mesoderm induction, a more plausible role for VegT is in determining mesodermal patterning and not as an initial mesoderm induction signal.

β-catenin was initially identified as a cell membrane associated protein in vertebrate cells (Ozawa et al. 1989) and was later shown to be a vertebrate ortholog of the *Drosophila* protein, Armadillo. It was demonstrated in *Xenopus* embryos that depletion of maternal β-catenin results in development without dorsal structures (Heasman et al. 1994). In *Xenopus* β-catenin mRNA and protein are maternally present (DeMarais and Moon 1992). Therefore β-catenin represents a potential early dorsal determinant involved in inducing organizer activity. The developmental process of cortical rotation seems to result in the cytoplasmic accumulation of β-catenin in the prospective dorsal side of the *Xenopus* embryo (Larabell et al. 1997) with subsequent nuclear accumulation in dorsal blastomeres beginning at the 16-cell stage and lasting until mid-blastula stage (Larabell et al. 1997). In the nucleus, β-catenin interacts with Tcf/Lef1 proteins to activate expression of target genes (Molenaar et al. 1996).

The molecules described above represent candidates for the initial mesoderm inducer and molecules that are potentially involved in the mesoderm induction process. To date, no single molecule or group of molecules has been confirmed as the absolute mesoderm induction signal. Taking these and additional molecules into consideration, many models have been developed and improved upon to schematically represent the process of mesoderm induction, such as that represented in the following section.

1.2.4.3 Mesoderm Induction – A Theoretical Model

A considerable amount of effort has gone into identifying molecules that are responsible for mesoderm induction *in vivo* and elucidating the model pathways through which they act. As the views on some of the potential molecules and subsequent pathways remain controversial, the model presented in Figure 1.5 (adapted from Aguis et al. 2000) is representative of a current view of mesoderm induction in *Xenopus laevis*, but is by no means the only accepted view, as the evidence remains open to interpretation.

Around stage 8 of development, the vegetally localized, maternal T-box transcription factor VegT induces the *Nodal*-related genes *Xnr1, Xnr2* and *Xnr4* (Clements et al. 1999). The nodal gene, first detected in mouse embryos, encodes a secreted protein of the TGF-β superfamily. Several nodal-related genes are expressed in *Xenopus laevis* embryos, Xnr1-6, for which maternal transcripts cannot be detected (reviewed in Tiedemann et al. 2001). The maternal TGF-β factor Vg1 may also be required for *Xnr1* and *Xnr2* expression (Agius et al. 2000). The presence of β-catenin on the dorsal side of the embryo results in higher expression of *Xnr1* and *Xnr2* on the same side (Figure 1.5). By

stage 9, these higher levels of *Xnrs*, coupled with the presence of β-catenin, result in the induction of dorsal mesoderm, whereas the lower levels in the ventral vegetal region result in the induction of ventral mesoderm. These molecules therefore fulfill the requirements as signals 1 and 2 of the three-signal model. The third signal deals with mesodermal patterning and the formation of a complete complement of mesodermal tissues initiated at approximately stage 10 of development (Figure 1.5). A current perspective on this signal is that the ventral mesoderm expresses BMP-4 (Dale and Jones 1999) and Xwnt-8 (Christian and Moon 1993; Hoppler et al. 1996) both of which ventralize mesoderm. The Spemann Organizer, as the dorsal mesoderm is known, expresses Chordin, Noggin, Follistatin (all BMP inhibitors) and Frizbee, a wnt inhibitor. The presence of these molecules in the ventral tissues and their inhibitors in the dorsal tissues results in a gradient of activity through the mesoderm, which in turn results in the formation of the entire complement of mesodermal tissue.

The current perspective on the role of FGF in mesoderm induction suggests it may be required in the animal hemisphere as a competence factor for the complete range of responses to the vegetal inducing molecules. A dominant-negative form of the *Xenopus* type 1 FGF receptor was used to show that an FGF signal is required for the full induction of mesoderm by activin, with some genes requiring higher levels of FGF signaling than others (Cornell and Kimelman 1994). Umbhauer et al. (1995) demonstrated in *Xenopus* that FGF induced activation of MAP kinases is necessary and sufficient for mesoderm formation. In 1995, Cornell *et al.* presented evidence supporting a role for maternal FGF as a competence factor at the embryonic equator, interface of the

animal and vegetal hemispheres, allowing these cells to form mesoderm in response to an activin-type signal emanating from the vegetal hemisphere. LaBonne et al. (1995) used MAP kinase phosphatase to inactivate MAP kinase and found it to prevent the induction of early and late mesodermal markers by both FGF and activin. This indicated that FGF-dependent MAP kinase activity plays an important role in establishing the responsiveness of embryonic tissues to mesoderm inducers. As reviewed in Isaacs (1997), current data suggests that maternally present FGF is required in the animal hemisphere of the early blastula to confer sub-threshold stimulation of the tyrosine kinase signal transduction pathway. This stimulation leads to the activation of *Xbra* transcription in the late blastula, Xbra then activates eFGF (FGF4) expression in the newly formed mesoderm and together these molecules establish an autocatalytic activation loop and play an important role in the formation of the mesoderm in the blastula. (Isaacs 1997) Further information about the role of FGF came from studies by Isaacs et al. (1994). These authors demonstrated that the overexpression of eFGF in *Xenopus* embryos during gastrula stages results in a phenotype of reduced head and an enlarged posterior proctodaeum. Therefore showing that FGF signaling is required for anteroposterior patterning of the mesoderm.

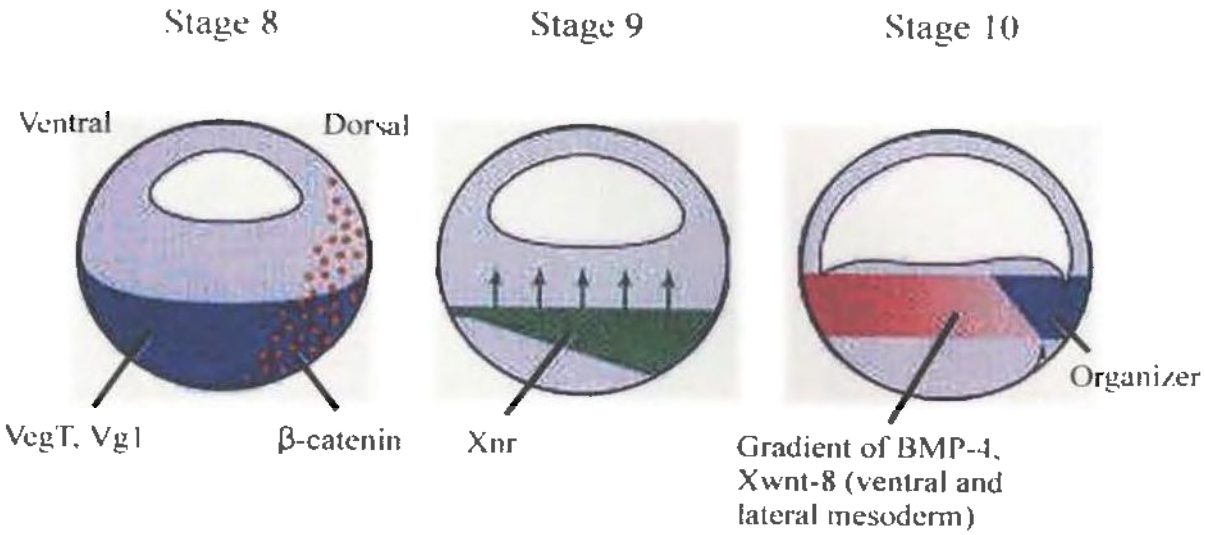

Figure 1.5: Model of mesoderm induction at the blastula stage by a dorsal to ventral gradient. (adapted from Aguis et al. 2000)

1.3 Fibroblast Growth Factors

Research in the laboratory of Drs. Laura Gillespie and Gary Paterno has focused on the molecular role of FGF in regulating cell growth and differentiation. The following sections provide information about fibroblast growth factors and components of their signal transduction pathway, primarily the FGF cell surface receptor (FGFR).

To date, fibroblast growth factors (FGFs) constitute a family of twenty-three structurally related proteins, FGF1-23, in mammals. The name Fibroblast Growth Factor is misleading. While some FGFs do indeed stimulate fibroblast proliferation, they induce proliferation of many other cells as well, and their actions are more general than proliferation. They are a family because they are structurally, but not necessarily biologically related. FGF was initially identified as an activity that stimulates the proliferation of NIH3T3 cells (Gospodarwicz 1974). FGFs have since been shown to be involved in numerous processes including: developmental induction and differentiation; cell growth and migration; bone growth and development; neuronal differentiation; angiogenesis; wound healing; tumorigenesis (reviewed in Basilico and Moscatelli 1992; Burgess and Maciag 1989). Defining features of the FGF family include a strong affinity for heparin and heparin-like glycosaminoglycans (HLGAG) (Burgess and Maciag 1989) and a central core of 140 amino acids that forms a compact cylindrical barrel of twelve antiparallel β-strands (Zhang et al. 1991). Historical nomenclature was based on biological activity, however the current convention is to describe them as "FGFs" followed by a numerical designation (Baird and Klagsbrun 1991). Table 1.1 provides a

complete list of mammalian fibroblast growth factors and Table 1.2 provides a list of the identified *Xenopus* fibroblast growth factors.

FGF-1 (acidic FGF) was initially isolated from bovine pituitary extract by Gospodarowicz (1975) by its ability to cause proliferation and delayed differentiation of myoblasts. It was later rediscovered by its ability to stimulate endothelial cell proliferation (reviewed in Gospodarowicz *et al.*, 1987). FGF-1 does not have a signal sequence for targeting to the secretory pathway (Jaye et al. 1986), although it does contain a nuclear localization motif (Imamura et al. 1990), which appears to be important in FGF-1 induced mitogenesis.

FGF-2 (basic FGF) was first identified in 1974 (Gospodarwicz 1974) for its ability to cause proliferation and transformation of BALB/c 3T3 cells. FGF-2 maintains 55% sequence identity with FGF-1, and as with FGF-1, FGF-2 does not contain a signal sequence for secretion.

Table 1.1: Mammalian Fibroblast Growth Factor family members.

Current Nomenclature	Historical Name	Reference
FGF-1	Acidic FGF (aFGF)	Gospodarowicz et al. 1975
FGF-2	Basic FGF (bFGF)	Gospodarowicz et al. 1974
FGF-3	INT-2	Dickson et al. 1984
FGF-4	HST-1/kFGF	Sakamoto et al. 1986
FGF-5	---	Zhan et al. 1988
FGF-6	HST-2	Marics et al. 1989
FGF-7	KGF	Rubin et al. 1989
FGF-8	AIGF	Tanaka et al. 1992
FGF-9	GAF	Miyamoto et al. 1993
FGF-10	---	Yamasaki et al. 1996
FGF-11	FGF homologous factor –1	Smallwood et al. 1996
FGF-12	FGF homologous factor –2	Smallwood et al. 1996
FGF-13	FGF homologous factor –3	Smallwood et al. 1996
FGF-14	FGF homologous factor –4	Smallwood et al. 1996
FGF-15	---	McWhirter et al. 1997
FGF-16	---	Miyake et al. 1998
FGF-17	---	Hoshikawa et al. 1998
FGF-18	---	Ohbayashi et al. 1998
FGF-19	---	Xie et al. 1999
FGF-20	---	Ohmachi et al. 2000
FGF-21	---	Nishimura et al. 2000
FGF-22	---	Nakatake et al. 2001
FGF-23	---	Yamashita et al. 2000

Table 1.2: *Xenopus laevis* Fibroblast Growth Factor family members.

Current Nomenclature	Reference
XFGF-2	Kimelman et al. 1988; Kimelman and Kirschner 1987
XFGF-3	Tannahill et al. 1992
XFGF-4	Isaacs et al. 1992
XFGF-8	Christian and Slack 1997
XFGF-9	Song and Slack 1996
XFGF-20	Koga et al. 1999

1.4 Fibroblast Growth Factor Receptors

The search for molecules involved in fibroblast growth factor signaling uncovered both low and high affinity FGF binding sites on the plasma membrane of cells. Fibroblast growth factors bind specifically and with nanomolar affinity (K_D=2nM) to heparin sulfate proteoglycans and therefore constitute the low affinity binding site (Moscatelli 1987; Burgess and Maciag 1989). A group of receptor tyrosine kinases were shown to bind FGFs with picomolar affinity (K_D=20pM) and therefore constitute the high affinity site for FGFs on the cell surface (Moscatelli 1987; Burgess and Maciag 1989).

1.4.1 Receptor Tyrosine Kinases – The High-Affinity Fibroblast Growth Factor Receptors

There are presently more than 50 Receptor Tyrosine Kinases (RTKs) that belong to at least 13 different receptor families (Fedi and Aaronson 2001). The structural characteristics of RTKs include a glycosylated extracellular ligand-binding domain, a single hydrophobic transmembrane region and a cytoplasmic region with a conserved tyrosine kinase catalytic domain (Fedi and Aaronson 2001; Ullrich and Schlessinger

1990; Wilks 1993). Included in this broad category of receptors are the four high-affinity Fibroblast Growth Factor Receptors, FGFR1-4.

There are four known mammalian genes that encode receptor tyrosine kinase FGF receptors, referred to as *fgfr 1-4* (refer Table 1.2). The gene for FGFR-1 was initially described as an fms-like gene (flg) by Ruta et al. (1988) when it was isolated by low stringency hybridization using a cDNA probe corresponding to the tyrosine kinase domain of the CSF-1 (colony-stimulating factor 1) receptor. It was described as a FGF-2 receptor when the chicken form of the protein was isolated by FGF-2 affinity chromatography (Lee et al. 1989), it has since been shown to bind with high-affinity to FGF-1 and FGF-2 (Ruta et al. 1989). The FGFR-2 gene was initially described as bacterially expressed kinase (bek), for which a partial cDNA was first isolated by phosphotyrosine antibody screening of a mouse liver expression library (Kornbluth et al. 1988). Full-length cDNA for human and chicken bek were later described (Dionne et al. 1990; Pasquale 1990; Houssaint et al. 1990) and shown to bind with high-affinity to FGF-1 and –2 (Houssaint et al. 1990; Dionne et al. 1990; Mathieu et al. 1995). The third known FGFR (FGFR-3) was originally named chicken embryo kinase-2 (CEK-2) as it was isolated by phosphotyrosine antibody screening of a chicken embryo expression library (Pasquale 1990; Pasquale and Singer 1989) and has been shown to bind both FGF-1 and FGF-2 with high-affinity (Mathieu et al. 1995). The most recently identified receptor, FGFR-4, was cloned from human erythroleukemia cells (Partanen et al. 1991) and was shown to bind FGF-1 with high affinity but not FGF-2 (Partanen et al. 1991). cDNA encoding *Xenopus* orthologs of fibroblast growth factor receptor-1, -2 and –4 have

been cloned (Musci et al. 1990; Friesel and Brown 1992; Shiozaki et al. 1995). The interactions of the numerous FGFs and the multiple forms of the FGFRs are being widely studied, but an in-depth description of the multitude of interactions is beyond the scope of this project's research and will not be discussed in this thesis.

Table 1.3: Fibroblast Growth Factor Receptors

Numerical Designation	Historical Names	References
FGFR-1	Mammalian flg	Ruta et al. 1988
	Chicken cek-1	Pasquale 1990
FGFR-2	murine and human bek	Kornbluth et al. 1988 Dionne et al. 1990
	Chicken cek-3	Pasquale 1990
FGFR-3	murine flg-2	Avivi et al. 1991
	chicken cek-2	Pasquale 1990
FGFR-4	---	Partanen et al. 1991

1.4.2 Fibroblast growth factor receptor structure

The high affinity FGFR is a monomeric molecule characterized by the presence of an extracellular ligand-binding domain composed of three immunoglobulin-like domains (Ig-loops), an acidic box domain between Ig-loops I and II, a transmembrane segment that functions to anchor the receptor in the cell membrane, a juxtamembrane region, and a split tyrosine kinase domain (Figure 1.6). The tyrosine kinase domain is the most highly conserved region of the receptor molecule. The insert sequence that splits the kinase domain is highly conserved between species for specific receptors and is believed to

regulate interactions between the receptor and cellular substrate proteins. (Reviewed in Ullrich and Schlessinger (1990)).

1.4.3 Multiple forms of FGFR

Generally speaking, each of the four fibroblast growth factor receptors is capable of binding and subsequently being activated by more than one fibroblast growth factor. To further enhance and diversify the FGF-FGFR system, each of the four FGFR genes can be alternatively spliced to present a number of variant isoforms. One of the well-documented splice variants includes those that exclude the first of the three Ig-like domains (Figure 1.7A). As mentioned, the primary structure for the FGFR contains an extracellular domain with three Ig-like loops. It has been shown that an alternative-splicing event occurs in both FGFR-1 and –2 that results in receptors with truncated extracellular domains (Johnson et al. 1990; Eisemann et al. 1991; Friesel and Dawid 1991; Musci et al. 1990). These truncated receptors lack the amino-terminal Ig-like loop (loop I) leading to the formation of a 2 Ig-like domain FGFR (Figure 1.7). The three and two Ig loop receptor forms have been termed α and β respectively. The functional significance of the exclusion of the first Ig loop is uncertain as the truncation does not prohibit ligand binding and the receptor appears to function in a normal capacity (Chellaiah et al. 1999; Duan et al. 1992; Wang et al. 1995a), however it does appear to modulate ligand-binding affinity (Coutts and Gallagher 1995; Wang et al. 1995b). Another known splicing event occurs in the carboxy-terminus of the third Ig-like domain which is encoded by three exons, of which two are alternatively spliced (Johnson and

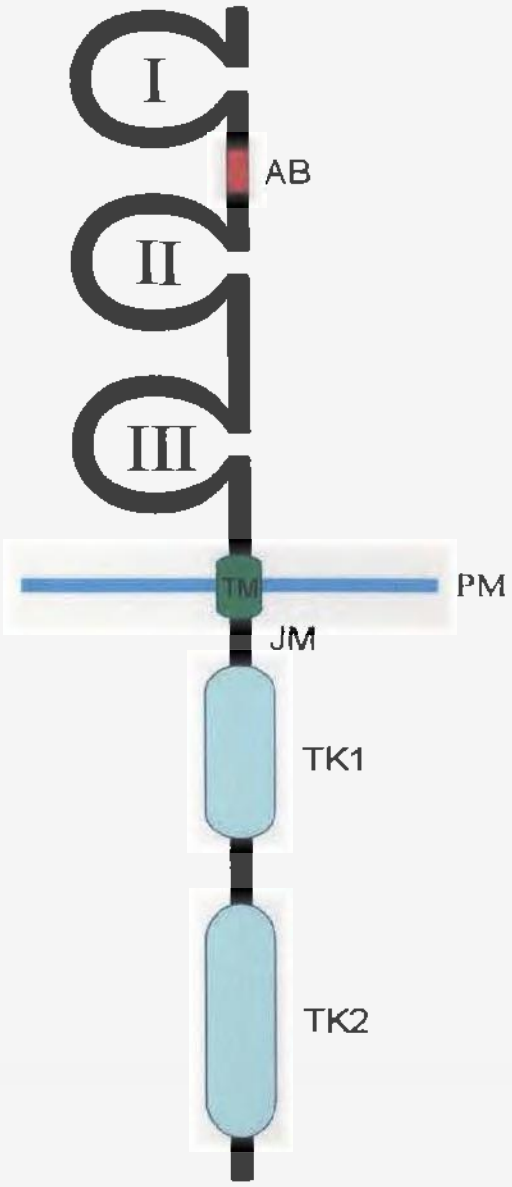

Figure 1.6: General structure of type 1 fibroblast growth factor receptor. Depicted here are the three extracellular immunoglobulin-like domains (I, II, III), the acidic box (AB), the transmembrane domain (TM) and the intracellular split tyrosine kinase domain (TK1 and TK2). The transmembrane domain passes through the plasma membrane (PM), with the Juxtamembrane (JM) region located just inside the PM.

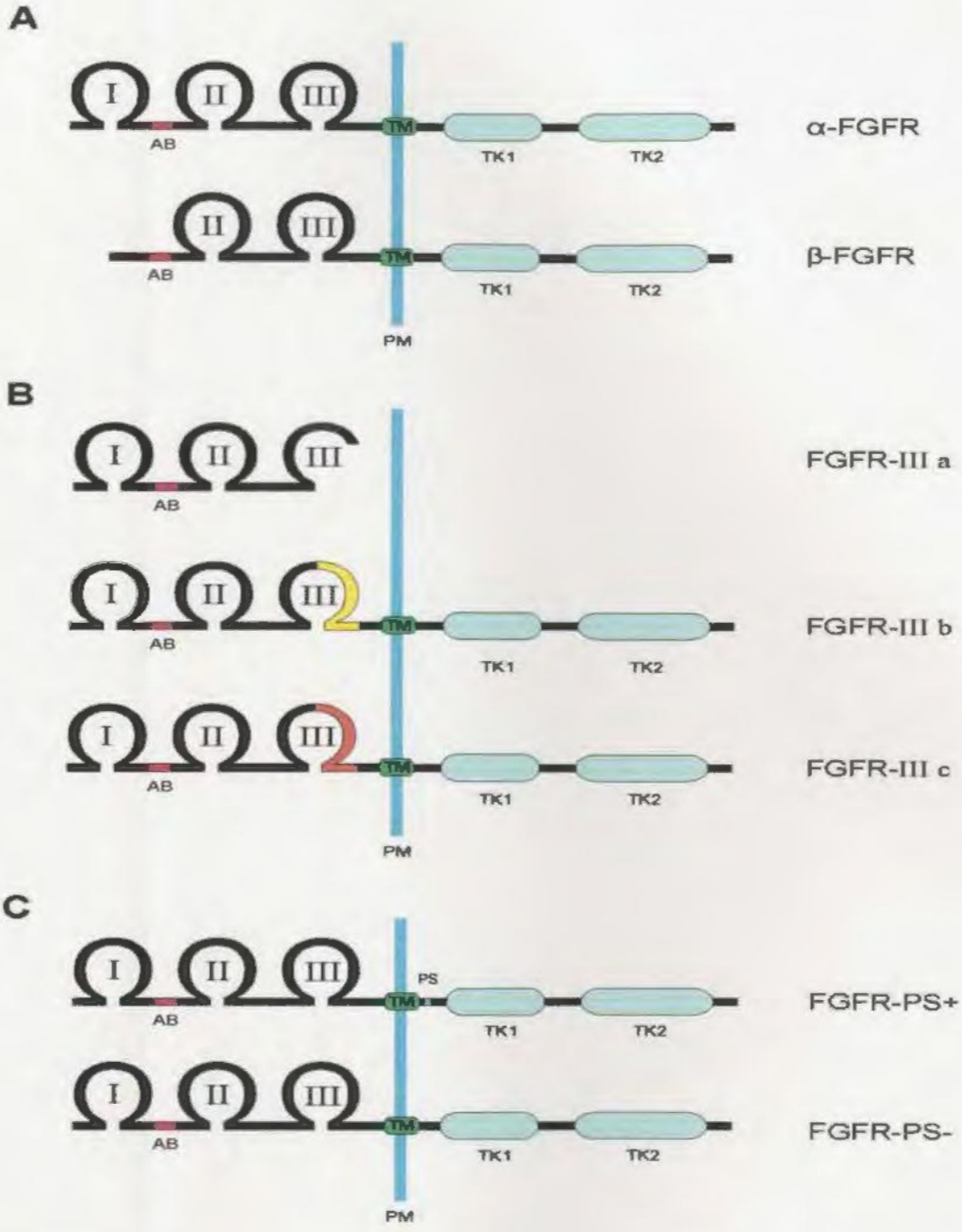

Figure 1.7: Variant forms of FGFR1. (A) α-FGFR, 3 Ig form of the receptor; β-FGFR, 2 Ig form of the receptor. (B) FGFR-IIIa, truncated, soluble form of the receptor; FGFR-IIIb and FGFR-IIIc, fully functional receptors with differing FGF binding affinities. (C) FGFR-PS+ and FGFR-PS-, differing only by the inclusion or exclusion of Proline^{442}-Serine^{443} dipeptide.

Williams 1993). The variants that differ in the second half of their third Ig loop have been termed IIIa, IIIb and IIIc respectively and have been shown to differ in their ligand binding affinities (Figure 1.7). The FGFR IIIa variant is a truncated soluble form of the receptor that cannot transduce an intracellular signal. However, the IIIa receptor variant has been demonstrated to bind FGF-2 with a higher affinity than FGF-1, which may suggest it functions to sequester released FGFs (Beer et al. 2000). The IIIb and IIIc variants have been shown to dramatically alter the FGF affinity of a given receptor. These variants have been described for FGFR 1, 2 and 3. In studies utilizing FGFR2-IIIb and -IIIc, the IIIc variant binds aFGF and bFGF with equal affinity, however the IIIb variant binds bFGF with 1000-fold less affinity, aFGF is still bound and it also binds KGF (FGF-7) (Dell and Williams 1992; Yayon et al. 1992; Ornitz et al. 1996; Beer et al. 2000).

1.4.4 FGF-FGFR Interactions/Signaling

Fibroblast growth factors exert their effects on cells through the binding of the high-affinity transmembrane receptors that initiates an intracellular signaling cascade. The generalized sequence of events involved in the FGF-FGFR signal activation is outlined here in Figure 1.8. The FGF binds to its high-affinity receptor and results in receptor dimerization. The cytoplasmic domains are brought into close proximity due to the dimerization and subsequently autophosphorylate each other's cytoplasmic domains at distinct tyrosines. This state of autophosphorylation results in activation of the receptor dimer to phosphorylate cytoplasmic substrates and initiate intracellular signaling

pathways. (Reviewed in Jaye et al. 1992; van der Geer et al. 1994) (Figure 1.8). These pathways include phospholipase C-gamma (PLC-γ), Ras and the less well understood phosphotidylinositol 3-kinase (PI3K) pathways.

When PLC-γ is activated, it cleaves phosphatidyl-inositol-4,5-bisphosphate (PIP_2) into inositol triphosphate (IP_3) and diacylglycerol (DAG). The IP_3 facilitates the release of calcium from intracellular stores that in combination with DAG activates protein kinase C (PKC) (Powers et al. 2000), these molecules then activate additional molecules and thereby bring about the desired processes such as transcription.

The Ras pathway is activated by receptor dimerization and autophosphorylation. Growth factor receptor binding protein 2 (Grb2) forms a complex with the cytoplasmic molecule son of sevenless (SOS), this complex then binds to the phosphotyrosine of the receptor through the SH2 domain of Grb2. The receptor Grb2-SOS combination then activates Ras. Ras activation then takes the pathway through the subsequent activation of Raf, MEK and MAP kinases. The signal has then traveled to the nucleus where MAP kinase activates transcription factors via phosphorylation. (Gilbert 1997; Lewin 2000)

The enzyme PI3K is thought to interact with the phosphotyrosine of an active receptor dimer via the p85 subunit of PI3K. PI3K is also shown to act in the FGF signaling pathway downstream of Ras and in parallel to the MAP kinase signaling (Carballada et al. 2001). In general, interaction with the receptor brings PI3K into close proximity with various membrane phosphoinositols which in turn activate particular proteins. Some of the proteins activated by this pathway include: a Ser/Thr kinase, Akt (PKB), which is known to activate GSK3; $p70^{S6k}$ (p 70 ribosomal S6 kinase) that

phosphorylates the S6 protein component of the 40S ribosomal subunit during mitogenic responses and may contribute to the regulation of other cellular processes; PKC and PRK (PKC-related kinases). (Vanhaesebroeck et al. 1997)

1.4.5 *Xenopus* FGFRs

Three RTK FGFR genes have been cloned in *Xenopus*, the FGFR-1 gene is expressed throughout early *Xenopus* development (Musci et al. 1990), the FGFR-2 is first detected during gastrulation (Friesel and Brown 1992) and FGFR-4 is expressed throughout development but in a manner that differs from FGFR-1 and FGFR-2 (Shiozaki et al. 1995). Two previously cloned isoforms of XFGFR1 in *Xenopus* include a three Ig domain XFGFR-A1 (Musci et al. 1990) cloned from an oocyte library and a two Ig domain XFGFR-A2 (Friesel and Dawid 1991) cloned from a *Xenopus* cell line. A dominant negative mutant of XFGFR was also produced for *Xenopus* from Musci's XFGFR1. The mutant, known as XFD contains only intact extracellular and transmembrane domains and has been shown to successfully inhibit FGF signaling in the *Xenopus* oocyte (Amaya et al. 1991). Amaya et al. used this dominant negative receptor to examine the role of FGF in early *Xenopus* development. The studies went on to show that explants from embryos expressing XFD failed to form mesoderm in response to FGF and in whole embryos XFD resulted in gastrulation and posterior development defects.

Figure 1.8: The signal transduction pathways activated by the binding of two FGFs to the FGF receptors. The ras G protein signals the transcription of new mRNAs, phospholipase C- gamma (PLC-γ) is activated to cleave PIP_2 into IP_3 and DAG, and PI3K signals cellular regulatory molecules. (adapted from Developmental Biology, 6^{th} Ed, Scott F Gilbert)

While undertaking studies to investigate the molecular mechanisms involved in mesoderm induction, through the initial determination of which FGFR genes are involved and how FGFR signaling is regulated, the research group of Drs. Laura Gillespie and Gary Paterno isolated a cDNA clone that encoded a variant form of XFGFR, named FGFR-VT- (Gillespie et al. 1995).

1.4.6 Review of FGFR-VT-

Compared structurally to the two previously cloned *Xenopus* type 1 FGFR, XFGFR-A1 and XFGFR-A2, FGFR-VT- contained a deletion of Val^{423}-Thr^{424} (VT) in the juxtamembrane region. Through sequencing of the genomic fragment containing the VT region and subsequent analysis, it was concluded that the most likely mechanism for the production of the two isoforms is the use of alternative 5' splice donors (Gillespie et al. 1995). Potential for amino acid position 424 as a phosphorylation site was investigated by *in vitro* kinase assays using PKA and PKC. Short peptides for both FGFR-VT- (AA 417-428) and FGFR-VT+ (AA 417-430) were constructed and an *in vitro* assay revealed that neither peptide was phosphorylated by PKA and that the FGFR-VT+ (AA 417-430) peptide was phosphorylated by PKC (Gillespie et al. 1995). For comparison, a full-length FGFR1 was constructed that contains 3 Ig-like domains and Val^{423}-Thr^{424} and thus differs from FGFR-VT- only by the presence of Val^{423}-Thr^{424}, referred to as FGFR-VT+ (Figure 1.9). Full-length proteins were both phosphorylated by PKC, but the VT+ form displayed twice the level of incorporation of VT- (Gillespie et al. 1995). The spatial and temporal expression patterns of VT+ and VT- were examined in embryos at stages when

mesoderm induction was known to take place. VT- expressed predominantly in the marginal zone (presumptive mesoderm) and VT+ expressed throughout the embryo as determined by RNase protection assay (Paterno et al. 2000). At 4.5 hours post fertilization VT+ is the major isoform, this switches at 5 hours post fertilization when VT- becomes the predominant form, then at 5.5 hours post fertilization and all subsequent times studied, VT+ returns as the predominant form as determined by RT-PCR. The effect of overexpressing each receptor isoform in *Xenopus* embryos was studied. Control embryos and those overexpressing FGFR-VT- developed normally, while less than 10% of those embryos overexpressing FGFR-VT+ developed normally (Paterno et al. 2000). The abnormal phenotype, a severe posterior truncation, was similar to that resulting from the overexpression of a dominant negative FGFR1, XFD, that consists of an extracellular domain, transmembrane domain and the first 7 amino acids of the intracellular domain (Figure 1.9) and when overexpressed in embryos, inhibits endogenous FGFR (Amaya et al. 1991). Those abnormalities were shown to be the result of a reduction in posterior mesoderm development. The effect of VT+ and VT- overexpression on mesoderm formation *in vitro* was investigated. FGF-2 dose-response was measured in explants from embryos overexpressing either VT+ or VT- and compared to normal embryos. It was deduced that VT+ overexpressing explants required a 2-fold higher concentration of FGF-2, while VT- overexpressing explants required a 5-fold lower concentration of FGF-2, than control explants to achieve 50% mesoderm induction (Paterno et al. 2000). Overexpression of VT+ decreased sensitivity to FGF, while overexpression of VT- greatly increased sensitivity, and further examination revealed that

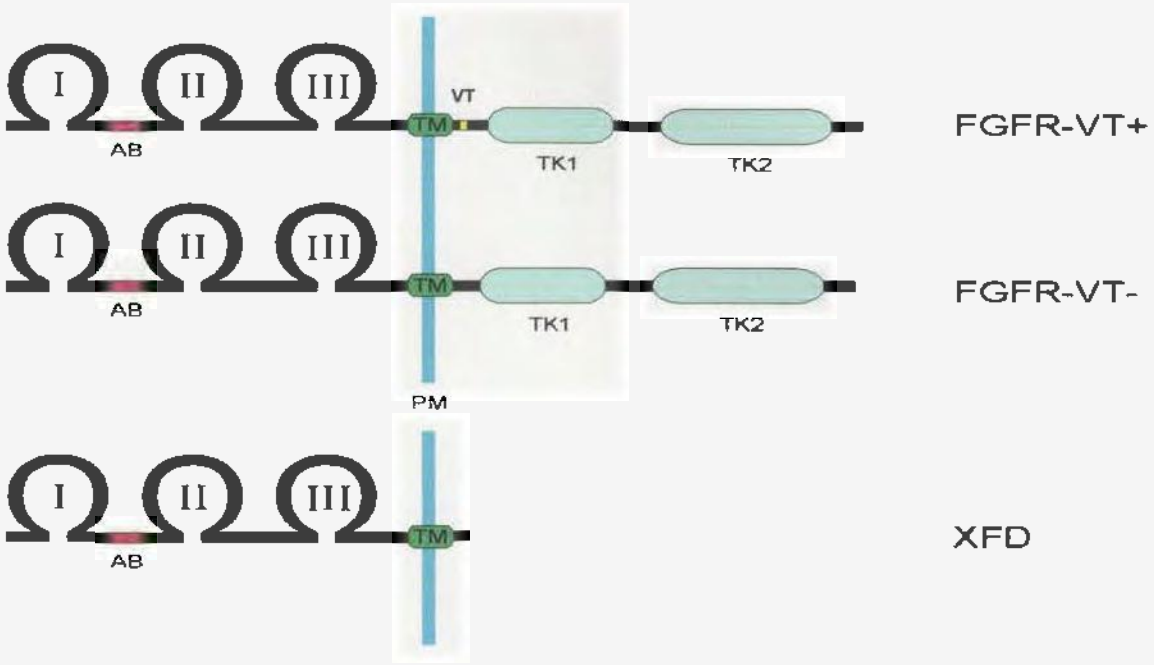

Figure 1.9: Structure of the fibroblast growth factor receptor isoforms FGFR-VT+ and FGFR-VT- and the dominant-negative FGF receptor XFD.

the sensitivity to FGF was directly correlated with the relative expression levels of the two isoforms. Thereby demonstrating that VT+ can function to negatively regulate mesoderm formation and therefore the abnormal phenotype that resulted may have been the consequence of a deficiency in mesoderm formation (Paterno et al. 2000).

1.5 Target Genes of FGF Induction

The initial response to mesoderm induction is rapid changes in levels of gene expression, in particular, genes that encode classes of proteins that are likely to be involved in mesodermal differentiation, such as transcription factors and growth factors. Immediate early response genes represent the first genes to be transcribed after a cell or population of cells has been stimulated by a growth factor. RNA expression analysis of cells that have been treated with growth factor alone or growth factor in the presence of protein synthesis inhibitor, such as cycloheximide, is normally performed to confirm an immediate early gene. Expression of an immediate early target will be induced by growth factor in both the absence and presence of cycloheximide, as was shown to be the case for *Xbra*, an immediate early target of FGF signaling (Smith et al. 1991). The genes that become expressed in response to mesoderm induction therefore double as markers or indicators of induction.

The abnormal phenotype observed for the embryos overexpressing FGFR-VT+ is a posterior truncation with normal head development and is the result of a reduction in posterior mesoderm. Therefore, part of this project studied the effect of overexpressing FGFR-VT+ on the expression patterns of genes expressed in these affected regions. As

there are many genes known to be expressed at this time, I started with markers known to be affected by XFD, as the VT+ phenotype is similar to that produced by overexpression of XFD (Paterno et al. 2000).

Brachyury is a T-box gene required for formation of mesoderm and notochord in mouse, the *Xenopus* ortholog is known as *Xbra* (Herrmann et al. 1990; Wilkinson et al. 1990). Through molecular analysis it was revealed that *Xbra* is an immediate early response gene to Activin and FGF (Smith et al. 1991) and is maintained by a feedback loop with FGF (Isaacs et al. 1994; reviewed in Technau 2001). *Xbra* is considered an excellent marker of early mesoderm as transcripts first appear at MBT, with highest levels of expression observed during gastrulation in the presumptive mesodermal cells around the blastopore lip (Smith et al. 1991). Overexpression of the dominant-negative *Xenopus* type 1 FGF receptor, XFD, is shown to inhibit expression of *brachyury* (Amaya et al. 1993). Therefore we anticipated seeing a decrease in *Xbra* expression in our analysis.

Xwnt-8 is a *Xenopus Wnt*-1-related gene that is expressed in the ventral-lateral marginal zone after MBT and is involved in a *Wnt* pathway required for patterning of the mesoderm (Christian and Moon 1993; Christian et al. 1991; Hoppler et al. 1996). This gene is expressed in the region of the embryo missing or truncated by VT+ overexpression, we anticipated a reduction in its expression.

Bone morphogenetic proteins (BMP) are maternally expressed in *Xenopus* embryos (Nishimatsu et al. 1992; Dale et al. 1992). BMP-4 has been shown to induce ventral mesodermal tissues in a standard mesoderm induction assay (Dale et al. 1992; Jones et al.

1992). Evidence suggests that BMP signaling is not essential for initial mesoderm induction, but is involved in the dorsoventral organization of mesoderm (Graff et al. 1994). Therefore this gene is involved in patterning the region of the embryo missing or truncated by VT+ overexpression and we anticipated a reduction in its expression.

Zygotic expression of *noggin* occurs at the correct place and time for it to have a role in the functions of the Spemann Organizer, which among other things dorsalizes ventral mesoderm (Smith and Harland 1992). Noggin protein has been shown to function by antagonizing BMP signaling by direct binding to BMP molecules (Smith et al. 1993). This gene is expressed in the apparently normally developing region of the VT+ overexpressing embryos, we anticipated no change or a possible increase in its expression.

Goosecoid (gsc) is a homeobox gene shown to encode a DNA-binding protein. The *gsc* gene is expressed in the Spemann organizer of *Xenopus* embryos as a primary response to mesoderm inducing factors (Cho et al. 1991). Goosecoid is expressed at the right time and place for mesoderm specification and can pattern mesodermal differentiation through a concentration gradient (Niehrs et al. 1994). Overexpression of the dominant-negative receptor XFD has been shown to have no effect on *goosecoid* expression in *Xenopus* (Amaya et al. 1993). As the XFD receptor was shown to have no effect, we expected a similar result from overexpressing our receptor.

Mesoderm induced homeobox 1 (Mix.1) behaves as an immediate early response to induction and the gene encodes a transcription factor (Rosa 1989; Lemaire et al. 1998). It has been shown that *Mix.1* mediates the ventralization effect of BMP-4 during mesoderm

formation (Mead et al. 1996). As this gene is shown to be linked to BMP-4, we anticipated seeing a decrease in its expression.

Xenopus posterior (Xpo) is an immediate early marker of ventral and lateral mesoderm that is activated at or shortly after MBT (Sato and Sargent 1991; Amaya et al. 1993). It has been demonstrated that overexpression of the dominant-negative receptor XFD, in *Xenopus*, results in an inhibition of *Xpo* expression (Amaya et al. 1993). As XFD was shown to inhibit expression of this gene, we expected a similar result from the overexpression of our receptor.

1.6 Hypotheses and Objectives

Previous findings demonstrated that FGFR-VT+ negatively regulates mesoderm formation when overexpressed in *Xenopus* embryos and results in severe reductions in trunk and tail structures. The primary objective of my project was to investigate the molecular basis of the abnormal pattern of development observed in the *Xenopus* embryos overexpressing FGFR-VT+. Based on the abnormalities observed in the VT+ overexpressing embryos, it was hypothesized that distinct misexpression of molecular marker(s) known to be required for, or a consequence of, normal mesoderm formation would be observed.

A second objective for this project was to investigate the expression patterns of other known FGFR1 isoforms and was based on the hypothesis that FGFR isoforms have distinct function and therefore would be differentially expressed during embryonic development. We examined the temporal and spatial expression of two additional

receptor variants. One of these variants differed from the reported sequence by the deletion of Proline^{442}-Serine^{443} (Figure 1.7). We felt this might be of interest as the serine residue represents a potential phosphorylation site that may regulate receptor function. The other FGF receptor variant involves the extracellular immunoglobulin-like (Ig) domains. These variants represent the α-form (3 Ig-like domains) and the β-form (2 Ig-like domains) of the fibroblast growth factor receptors that differ by the inclusion or exclusion of the first of the three Ig domains. These variants are of interest because they may have different ligand binding specificities and affinities.

Chapter 2
Materials and Methods

2.1 *Xenopus laevis*: artificially-induced ovulation and *in vitro* fertilization

Materials: *Xenopus laevis* were purchased from Nasco, Fort Atkinson, Wisconsin.

Methods: Approximately 16 hours prior to the time the eggs were required, female *Xenopus laevis* were given a subcutaneous injection of 750 I.U. of Human Chorionic Gonadotrophin (Sigma) into the hind leg, just above the cloaca, and held in tanks at room temperature. Within 12-18 hours, the females began to lay eggs in their holding tanks. During this time period, females were manually stripped of their eggs. These recovered eggs were then fertilized in a petri dish using a macerated piece of testes from a sacrificed male *Xenopus laeivs*. The fertilized embryos were chemically dejellied using 2.3% L-cysteine hydrochloride (pH 7.8-8.1), washed with deionized-distilled water and transferred to a petri dish containing NAM/20 *Xenopus* culture medium (Tables 2.1 and 2.2). The embryos are then cultured at room temperature.

Table 2.1: Composition of 10x Normal Amphibian Medium (NAM) Stock

Salt	Per liter of stock
NaCl	65 g
KCl	1.5 g
$Ca(NO_3)_2 \cdot 4H_2O$	2.4 g
$MgSO_4 \cdot 7H_2O$	2.5 g
0.5M EDTA (pH 8.0)	2 ml
1M Hepes (pH7.5)	100 ml

Table 2.2: *Xenopus* Embryo Culture Mediums

per 100 ml final volume	*NAM*	*NAM/2*	*NAM/20*
10x NAM salts	10 ml	5 ml	0.5 ml
0.1M NaBicarb	1 ml	1 ml	1 ml
Gentamycin (10mg/ml)	0.25 ml	0.25 ml	0.25 ml
Sterile dH_2O	up to 100 ml	up to 100 ml	Up to 100 ml

2.2 Synthesis of VT+ and VT- cRNA

Materials: Ribomax™ Large Scale RNA Production System – SP6 was purchased from Promega Corporation, Madison, Wisconsin.

Method: *In vitro* transcription reactions were performed as described in the Ribomax™ kit insert.

Template Linearization. The DNA templates (SP64T-VT- and SP64T-VT+) were linearized in a reaction using restriction enzyme XbaI. A 50 µl digestion reaction was setup in a 1.7 ml eppendorf tube (containing 5 µl 10X REact 2 digestion buffer; 3 µl XbaI (10U/µl); 30 µl DNA template (0.5 µg/µl); 12 µl DEPC-treated water) and was incubated at 37°C for 2 hours. 1 µl of digested template was then run on a 0.7% agarose gel to ensure complete linearization. 200 µl DEPC-treated water was then added to each of the digestion reaction tubes. This was followed by extraction with equal volume of Phenol/Chloroform/IAA (Invitrogen). The aqueous phase was transferred to a new 1.7 ml eppendorf tube and the linear DNA template was precipitated with 2X the volume of ethanol and $^1/_{10}$ the volume of 3M NaOAc at -20°C overnight. The linear DNA template was then collected by centrifugation, washed with cold 70% ethanol, dried under vacuum and resuspended in 150 µl DEPC-treated water.

In vitro Transcription. Transcription reactions were carried out in 100 µl volumes. For each DNA template, a master mix was prepared in a 1.7 ml eppendorf tube that contained the following: 20 µl SP6 Transcription 5X buffer; 27.5 µl rNTP mix (5 µl each 100mM rATP, 100 mM rCTP, 100mM rUTP, 2.5 µl 100mM rGTP and 10 µl 30mM CAP analogue); 10 µl Enzyme Mix, SP6 RNA Polymerase. To this mix 15 µl linear DNA template was added and the volume made up to 100 µl with DEPC-treated water. The reaction mixture was gently pipetted to mix and then incubated at 37°C for 3 hours. At the end of the incubation, the DNA template was removed by digestion with RQ1 RNase-free DNase. RQ1 was added to the reaction tube to a concentration of 1 U per 1 µg of initial DNA template and incubated at 37°C for 15 minutes. After incubating, 150 µl of DEPC-treated water is added to each tube. This is followed by extraction with equal volume of Phenol/Chloroform/IAA. The aqueous phase was transferred to a new 1.7 ml eppendorf tube and the linear DNA template was precipitated with 2.5X the volume of ice cold 100% ethanol and $^1/_{10}$ the volume of 3M NaOAc at -20°C for 30 minutes. The RNA was then collected by centrifugation, washed with cold 70% ethanol, dried under vacuum and resuspended in 100 µl DEPC-treated water.

Spectrophotometric Quantitation. The final concentration of the resuspended cRNA was determined through spectrophotometric quantitation. Readings for 300 and 600 fold dilutions of cRNA were prepared and the absorbance read at 260 nm and 280 nm wavelengths (A_{260} and A_{280}). One A_{260} unit equals 40 µg/ml of RNA and the ratio of A_{260} and A_{280} readings should equal 2.0 barring the presence of contaminating protein or phenol.

2.3 *In Vitro* Coupled Transcription-Translation

Materials: TNT™ SP6 Coupled Reticulocyte Lysate System was purchased from Promega Corporation. 2X SSB contains 5ml stacking gel buffer (0.5M Tris, pH 6.8), 5ml 20%SDS, 2.5 ml β-mercaptoethanol (BDH Inc., Toronto, Ontario), 5 ml glycerol, 5 ml dH_2O and a few bromophenol blue crystals.

Method: The *in vitro* transcription-translation reaction mixture contained 12.5 µl TNT™ Rabbit Reticulocyte Lysate, 1 µl TNT™ Reaction Buffer, 0.5 µl 1mM Amino Acid Mixture minus Methionine, 0.5 µl RNAguard, 1 µg FGFR cRNA, 2 µl ^{35}S-methionine (PerkinElmer Canada Inc., Woodbridge, Ontario) and DEPC-treated water to a final volume of 25 µl. TNT™ SP6 RNA Polymerase was omitted from this reaction since the starting material was an RNA sample and therefore the transcription step was not required. The reaction mixture was incubated at 30°C for 90 minutes. Determination of percent incorporation of the radioactive label analysis and sodium dodecyl sulfate-polyacrylamide gel electrophoresis (SDS-PAGE) analysis of the translation products were conducted.

2.3.1 Determination of Incorporation of Radioactive Label

Method: 2 µl of the above translation products and 98 µl of 1N NaOH/ 2% H_2O_2 (100 µl 10N NaOH, 67 µl 30% H_2O_2 and sterile dH_2O to 1000 µl final volume) were mixed by vortexing and incubated at 37°C for 10 minutes. Following the incubation 900 µl of ice cold 25%TCA/ 2% Casamino acids were added to precipitate the translation product, this mixture was incubated on ice for 30 minutes. The precipitated translation product was

then collected on Whatman GF/A glass fiber filters under vacuum and washed 3X with 1ml ice cold 5%TCA followed by 1 ml ice cold 100% ethanol. The filter was allowed to dry under vacuum. For determination of ^{35}S incorporation, the filter was placed in 3 ml of scintillation fluid in a glass scintillation vial and counted in a Beckman LS 3801 liquid scintillation counter.

2.3.2 SDS-Polyacrylamide Gel Electrophoresis (SDS-PAGE)

Method: 5 µl of the above translation products and 30 µl of 1.5X SSB (sample buffer) (3 parts 2X SSB and 1 part dH_2O) were mixed. An 8% SDS-Polyacrylamide gel (Table 2.4) is topped with a Stacking gel (Table 2.5) and set with a comb to form the wells into which the samples are loaded. Samples were denatured for 5 minutes in a boiling water bath and then loaded onto the gel. Electrophoresis was performed for 1.5 hours at a constant current of 30mA supplied by BIO-RAD Model 1000/500 Power Supply until the blue dye front migrated to the bottom edge of the gel. The gel was then fixed (Table 2.6) for 15 minutes, destained (Table 2.6) for additional 15 minutes and finally soaked in Amplify (Amersham) for 30 minutes. The gel was then transferred to a small piece of Whatman 3mm Chromatography paper and dried at 80°C under vacuum for 1.5 hours. The dried gel was exposed to X-ray film (Kodak X-AR film), overnight at room temperature in a Fisher Biotech Electrophoresis Systems FBAC 810 autoradiography cassette (Fisher Scientific). Exposed films were developed using a Kodak RP X-OMAT Processor in the Radiology Department of the Health Sciences Centre, MUN, St. John's, NF.

Table 2.3: Composition of SDS-PAGE Running Gel.

Per 10 ml final volume	**8%**	**10%**	**12%**	**15%**
30% Acrylamide	2.67 ml	3.33 ml	4.0 ml	5.0 ml
Running Gel Buffer	2.5 ml	2.5 ml	2.5 ml	2.5 ml
20% SDS	40 µl	40 µl	40 µl	40 µl
Sterile dH_2O	4.72 ml	4.06 ml	3.39 ml	2.39 ml
10% AP	66 µl	66 µl	66 µl	66 µl
TEMED	4 µl	4 µl	4 µl	4 µl

Table 2.4: Composition of SDS-PAGE Stacking Gel

per 5 ml final volume	
30% Acrylamide	0.66 ml
Stacking Gel Buffer	1.25 ml
20% SDS	25 µl
Sterile dH_2O	3.03 ml
10% AP	33 µl
TEMED	4 µl

Table 2.5: Composition of SDS-PAGE gel Fix and Destain Solutions

Fix	**per 100 ml final volume**	**Destain**
45 ml	*100% Methanol*	20 ml
10 ml	*Glacial Acetic Acid*	6 ml
45 ml	*dH_2O*	74 ml

2.4 Microinjection of *Xenopus* embryos.

Materials: Microinjection apparatus was a Drummond Nanoject II Microinjector from Fisher Scientific, Nepean, Ontario. Microinjection needles were prepared by pulling 3.5 inch Drummond Glass Capillary tubes (Fisher Scientific) vertically using a Narishige Model PB-7 micropipette puller. Needle tips were beveled at a 20° angle with a Narishige EG-40 grinder. An injection plate that was fashioned using chloroform to

adhere a small section of fine plastic mesh to the bottom of a 60 x 15 mm Fisher brand disposable petri dish was used to hold embryos in the correct orientation during injections. The cRNA of fibroblast growth factor receptor variants VT+ and VT- were produced in the lab of Drs. Gillespie and Paterno, as previously described.

Method: Synthetic VT+ and VT- cRNAs were injected into the animal pole of *Xenopus laevis* embryos at stage 1, pre-first cleavage (Figure 2.1). Through an injection volume of 4.6 nl, each embryo received DEPC-treated water or 10 ng of VT+ cRNA, VT- cRNA. Embryos were placed in NAM/2 (Table 2.2) + 4% Ficoll PM400 (Amersham Pharmacia Biotech) for injections and subsequent culture. The embryos were left to develop at room temperature until they reached the desired stage of development.

2.5 Total RNA extraction from whole *Xenopus* embryos

Materials: TRI Reagent™ - RNA/DNA/Protein Isolation Reagent was purchased from Invitrogen, Carlsbad, California.

Metbod: Total RNA was extracted from whole embryos as described in the TRI Reagent package insert. Briefly, five *Xenopus* embryos at the same stage of development were transferred to a 1.7 ml eppendorf tube and homogenized in 1ml TRI Reagent by pipeting up and down and then stored at –70°C. Phases were separated by addition of 0.2ml chloroform per 1ml TRI Reagent, vortexing for 15 seconds and then the tube was left at room temperature for 2-15 minutes. Tubes were then centrifuged at 4°C, 12,000 rpm for 15 minutes. After centrifugation the aqueous, RNA containing phase was recovered and pipetted into a new 1.7 ml eppendorf tube. The total RNA was then precipitated out of

solution by adding 0.5 ml isopropanol per 1ml of initial TRI Reagent volume and incubating the tube at room temperature for 5-10 minutes. Tubes were then centrifuged at 4°C, 12,000 rpm for 20-25 minutes. The total RNA precipitate formed a gel like pellet on the side and bottom of the tube. The supernatant was decanted and the total RNA was washed once with cold 75% ethanol by vortexing the tube and then centrifuging at 4°C, 12,000 rpm for 10-15 minutes. The ethanol was decanted off and the washed RNA pellet was dried briefly under vacuum (3-5 minutes maximun) then resuspended by pipetting up and down in 50 µl of DEPC-treated water. The solubilized RNA was then treated with RNase-free DNase RQ1 (Promega) at 37 °C for 15-20 minutes. This was followed by extraction with an equal volume of Phenol/Chloroform/IAA. The aqueous phase was transferred to a new 1.7 ml eppendorf tube and re-extracted with an equal volume of Chloroform/IAA. The aqueous layer was transferred to a new 1.7 ml eppendorf tube and total RNA was precipitated with 2 times the volume of ethanol and $^1/_{10}$ the volume of 3M NaOAc at -20°C overnight. The total RNA was then collected by centrifugation, washed with cold 70% ethanol, dried under vacuum and resuspended in 30 µl DEPC-treated water. 1 µl RNAguard™ RNase Inhibitor (Amersham Pharmacia Biotech) was added to the resuspended RNA and stored at -70 °C.

2.6 Reverse transcription of mRNA from *Xenopus laevis* embryos

Materials: Random primer oligonucleotide (mostly hexamers - $d(N)_6$), 5X First Strand Buffer and Moloney Murine Leukemia Virus Reverse Transcriptase (M-MLV-RT), were

all purchased from Invitrogen. Dithiothreitol (DTT) was purchased from Sigma-Aldrich Canada Ltd., Oakville, Ontario.

Method: 2 µl of $d(N)_6$ Random Primer (100ng/µl) was added to 15 µl of the resuspended total RNA (2 µl total RNA + 13 µl DEPC-treated water). This mixture was heated to 70°C for 10 minutes and then quicked cooled in an ice-water bath for a minimum of 2 minutes. This was followed by the addition of 8 µl 5X first strand buffer, 2 µl each 10mM dNTPs, 4 µl 100mM DTT, 1 µl RNAguard™ RNase Inhibitor and 2 µl M-MLV reverse transcriptase. This mixture was allowed to incubate at 37°C for 60 minutes. The reverse transcription products were used directly in PCR reactions.

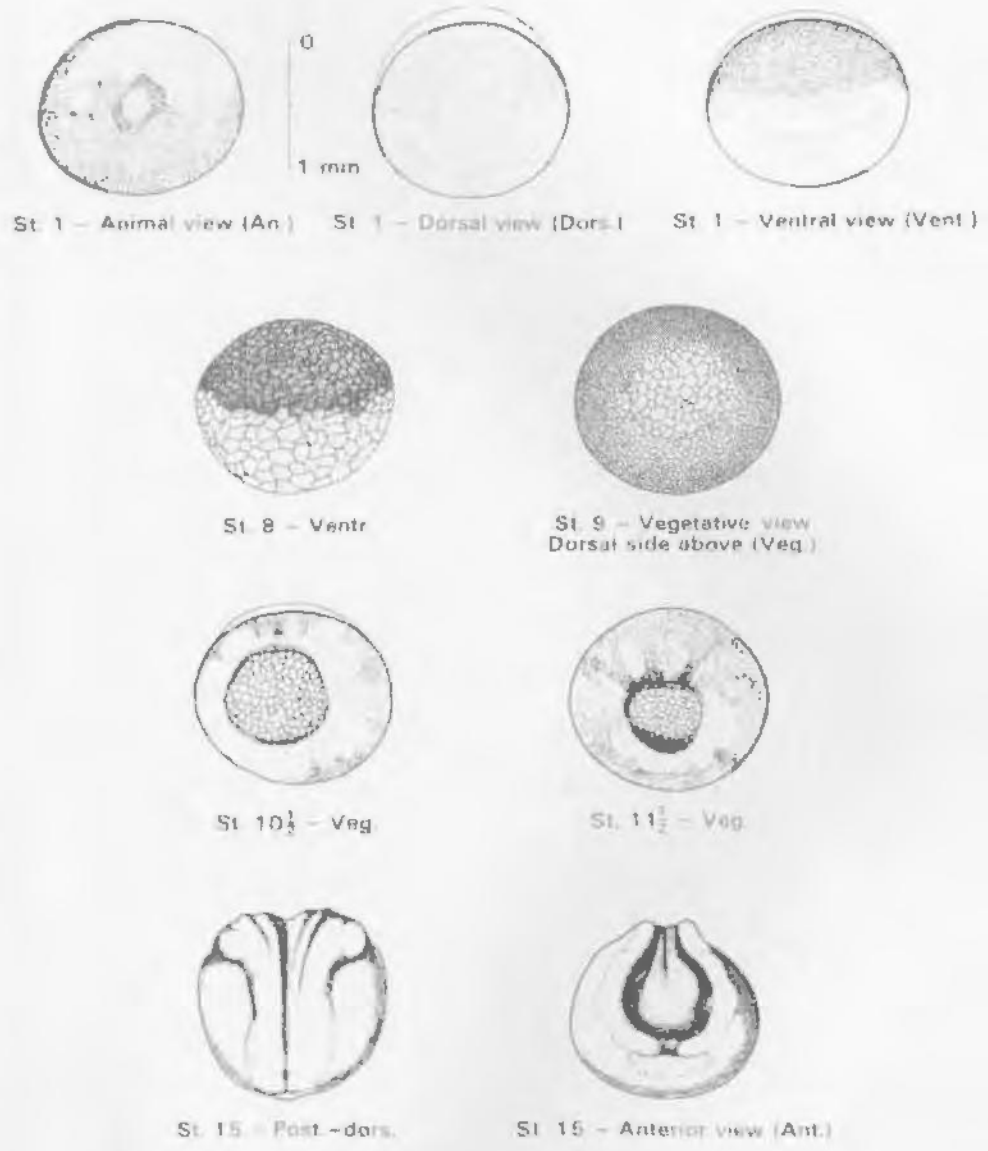

Figure 2.1: Stages of *Xenopus laevis* embryonic development that were injected (Stage 1) and from which total RNA was collected for the RT-PCR experiments described (Stages 8.5, 10.5, 11.5 & 15).
Stage 1: Age 0 hr; length 1.4-1.5 mm; one cell stage
Stage 8: Age 5 hr; length 1.4-1.5mm; medium cell blastula stage
Stage 9: Age 7 hr; length 1.4-1.5 mm; fine cell blastula stage
Stage 10.5: Age 11 hr; length 1.4-1.5 mm; crescent-shaped blastopore stage
Stage 11.5: Age 12.5 hr; length 1.4-1.5 mm; large yolk-plug stage
Stage 15: Age 17.5 hr; length 1.5-1.6 mm; early neural fold stage
(adapted from Nieuwkoop and Faber, 1967.)

2.7 PCR of reverse transcribed *Xenopus* embryo mRNA for known molecular markers.

Materials: The PCR machine used was the Hybaid PCR Express from VWR Canlab, Mississauga, Ontario. 10X PCR buffer, 50mM $MgCl_2$ and Platinum Taq polymerase were all purchased from Invitrogen. 100mM dATP, 100mM dCTP, 100mM dGTP, and 100mM dTTP were purchased from Invitrogen. Primers used are presented in Table 2.3. Deionized formamide was prepared by mixing 50 ml formamide and 5 g Mixed Bed Resin (Bio-Rad Laboratories (Canada) Ltd., Mississauga, Ontario) and gently stirring for 30 minutes at 4°C, after which it was filtered twice through Whatman No. 1 filter paper. The finished product was stored in a foil wrapped 50ml Falcon tube at -20°C. 10X Tris-Borate/EDTA electrophoresis buffer (10X TBE) in 1 L final volume contains 108 g Tris-HCl, 55 g Boric acid, 40ml 0.5M EDTA (pH 8.0) and sterile dH_2O.

Method: PCR reactions were carried out in 50 µl volumes at cycling parameters outlined in Figure 2.2. For each molecular marker examined a PCR Master Mix was prepared that contained the following: 100 µl 10X PCR buffer; 30 µl 50mM $MgCl_2$; 80 µl 2.5mM dNTPs (25 µl each 100mM dATP, 100mM dCTP, 100mM dGTP, and 100mM dTTP plus 900 µl sterile DEPC-H_2O); 5 µl Platinum Taq polymerase; 740 µl sterile dH_2O; 5 µl α-^{32}P-dATP (PerkinElmer); 20 µl 100ng/µl primer 1; 20 µl 100ng/µl primer 2. For each 50 µl PCR reaction, 48 µl of this Master Mix was added to a thin walled PCR tube containing 2 ul of Reverse Transcription products that were described previously. After cycling was completed, PCR reactions were inactivated by the addition of 50µl STOP buffer (in final volume 10 ml, 400 µl 0.5M EDTA; 9.6 ml deionized formamide; 5 mg

Xylene Cyanol (BIO-RAD); 5 mg Bromophenol blue (BDH)). The PCR products were separated by electrophoresis on 6% acrylamide DNA sequencing gels.

2.7.1 Electrophoretic Separation of the PCR products

The PCR reaction/STOP buffer mixture was denatured at 80°C-90°C for a minimum of 3 minutes. 4 µl was then loaded onto a 6% acrylamide DNA sequencing gel (in 100ml final volume, 6% sequencing mix contains 48 g Urea, 15 ml 40% 19:1 acrylamide/bis-acrylamide (BIO-RAD), 10 ml 10X TBE and up to final volume with sterile dH_2O). 70-80 ml of sequencing gel mix was polymerized with 44 µl TEMED (N, N, N', N'-tetramethylethylenediamine) and 440 µl 10% electrophoresis grade ammonium persulfate (0.1 g dry weigh in 1ml sterile dH_2O). This mix was poured into a BIO-RAD 38x30 Sequi-Gen® Cell and allowed to polymerize. Electrophoresis was performed for 1.5 hours at 70W constant power, supplied by a BIO-RAD Model 3000Xi Computer Controlled Electrophoresis Power Supply. When electrophoresis was completed the gel was fixed (1 L final volume of 10% Glacial Acetic Acid, 10% Methanol), transferred to filter paper (Whatman 3mm Chromatography paper, 46x57 cm) and dried under vacuum at 80°C for 1.5-2 hours. The dried gel was exposed to X-ray film (Kodak X-AR film), overnight at -70°C in Fisher Biotech Electrophoresis Systems FBAC 1417 autoradiography cassette with a Fisher Biotech L-Plus intensifying screen (Fisher Scientific). Exposed films were developed using a Kodak RP X-OMAT Processor in the Radiology Department of the Health Sciences Centre, MUN, St. John's, NF.

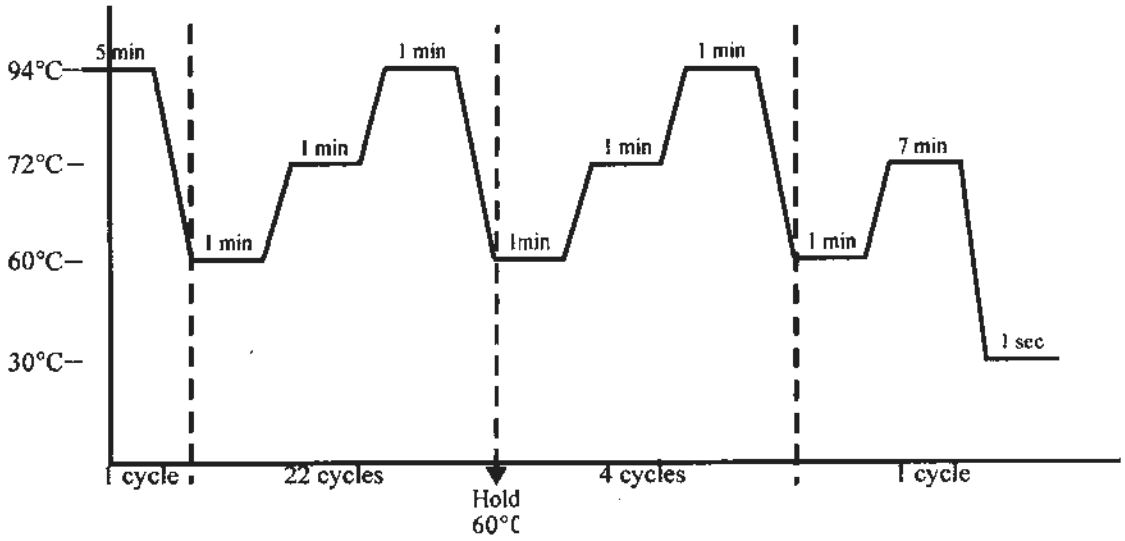

Figure 2.2: PCR cycling parameters. PCR reactions consisted of 1 cycle of 94°C for 5 minutes; 22 cycles of 60°C for 1 minute, 72°C for 1 minute, and 94°C for 1 minute (for the Histone (H4) positive control); hold at 60°C until H4 samples removed and cycling program resumed; 4 cycles of 60°C for 1 minute, 72°C for 1 minute, and 94°C for 1 minute (additional cycles for Molecular marker PCR products); 1 cycle of 60°C for 1 minute, 72°C for 7 minutes, and 30°C for 1 second.

Table 2.6: Sequences of upstream and downstream oligonucleotide primer pairs used in RT-PCR.

Name	Sequence	References
H4-1	5' – CGG GAT AAC ATT CAG GGT ATC ACT – 3'	Turner & Woodland (1982)
H4-2	5' – ATC CAT GGC GGT AAC TGT CTT CCT – 3'	
BMP-4U	5' – GCA TGT AAG GAT AAG TCG ATC – 3'	Koster *et al.* (1991)
BMP-4D	5' – GAT CTC AGA CTC AAC GGC AC – 3'	
Gsc-U	5'– GAG CAA AGT GGA GGA GGC AG – 3'	Blumberg *et al.* (1991)
Gsc-D	5'– CCC ACA TCG TGG CAC TGC TG – 3'	
Mix1-1	5' – ATG TCT CAA GGC AGA GGT – 3'	Rosa (1989)
Mix1-2	5' – CAC TGA CAC CAG AAT CTG – 3'	
Nog-1	5' – AGT TGC AGA TGT GGC TCT – 3'	Smith & Harland (1992)
Nog-2	5' – AGT CCA AGA GTC TGA GCA – 3'	
Xbra-1	5' – CAA GGA TCG TTA TCA CCT CTG – 3'	Smith *et al.* (1991)
Xbra-2	5' – TGT GTA GTC TGT AGC AGC AG – 3'	
XFkh1-1	5' – GCA GCT CTA TTA CCG ACA AG – 3'	Dirksen & Jamrich (1992)
XFkh1-2	5' – GCA AAA GTC TGC TCC ATT GT – 3'	
Xpo-1	5' – CAC TTA GGG ATT GGT CTC AGG AGT C – 3	Sato & Sargent (1991)
Xpo-2	5' – TGA GGG AGG GCT ATG GTC TAG G – 3'	
Xwnt-8U	5' – CGA GAG TGC CTG CAA AGT GG – 3'	Christian *et al.* (1991)
Xwnt-8D	5' – TCC GGT GGC CTC TGT TCT TC – 3'	
$T_{3\text{-}5}$	5' – GGG CTG CTT TTG TGT CCG CAA T – 3'	Gillespie *et al.* (1995)
VT3'	5' – CAT TGA TGA GCT GGA GTC CCC TG – 3'	
$T_{3\text{-}1}(T_{301})$	5' – TAG CCA ACT TGG GAT GTT CTC C – 3'	Gillespie *et al.* (1995)
$XFGFR_{733\text{-}754}$	5' – TGC CAT TCT TCA GCC AGG GAA G – 3'	
FRPS-5'-02	5' – CAG CTC ATC AAT GAA CTC TGG AG – 3'	Gillespie *et al.* (1995)
FRPS-3'	5' – CAG TCT GTC CCT TGC CAC TTC C – 3'	

Chapter 3
Results

3.1 Overexpression of FGFR-VT+ and FGFR-VT-

It has been demonstrated previously that the microinjection of 650 pg/nl FGFR-VT+ cRNA into stage 1 *Xenopus* embryos resulted in > 90% developing into abnormal tadpoles, while controls injected with 650 pg/nl FGFR-VT- cRNA or DEPC-treated H_2O developed normally (Paterno et al. 2000). The abnormal phenotype presented itself at 10-12 hours post-injection as incomplete gastrulation resulting in an enlarged blastopore with a protruding yolk plug (Paterno et al. 2000). The embryos continued to develop with clear reductions in trunk and tail structures in the resulting tadpoles (Paterno et al. 2000). *Xbra* expression had been observed, by *in situ* hybridization, to be undetectable or only very faintly detectable in embryo samples overexpressing FGFR-VT+, when compared to controls (Paterno et al. 2000). The primary objective of my research was to investigate the molecular basis of the abnormal pattern of development observed in the *Xenopus* embryos overexpressing FGFR-VT+. To accomplish this, FGFR-VT+ and FGFR-VT- injected embryos were analyzed by comparing the expression patterns of known molecular markers of mesoderm induction.

The first step in conducting these experiments was to characterize the stocks of FGFR1 cRNAs to ensure that they were equally well translated. To confirm the translational efficiency of the cRNA stock samples, microinjection experiments and TNT™ *in vitro* translation experiments were conducted. Figure 3.1 shows that when the cRNA samples are translated using the TNT™ Reticulocyte Lysate system, ^{35}S-

methionine incorporation are similar for VT+ and VT- samples. Figure 3.1A shows SDS-PAGE results for the translation products and no significant visual discrepancy is observed. Figure 3.1B displays the scintillation data of the radioactive label (^{35}S-methionine) incorporation levels into each sample. FGFR-VT+ incorporation of ^{35}S-methionine measured at an average of 71499 cpm and incorporation into FGFR-VT- averaged 76394 cpm over 6 repeated translation reactions from the stock VT+ and VT- cRNA samples. These levels are not statistically different (p-value of 0.8799).

Subsequently I verified that I could reproduce the reported abnormalities by microinjecting stage 1 embryos with 4.6 nl DEPC-H_2O or 2.17 ng/ul FGFR-VT+ cRNA or 2.17 ng/ul FGFR-VT- cRNA. Figure 3.2 is a graphical representation of the phenotype data obtained. It reveals that 81.5% and 76.7% of the DEPC-H_2O injected and FGFR-VT- overexpressing embryos developed normally, respectively, while it was observed that only 7.3% of the embryos overexpressing FGFR-VT+ form of the receptor developed into normal tadpoles.

Sample embryos, representative of the developmental phenotype observed after microinjection with the various receptor isoform cRNAs are presented in Figure 3.3. Both the DEPC H_2O control (Figure 3.3 A) embryos and the FGFR-VT- injected (Figure 3.3 B) embryos display normal patterns of development. The embryos injected with FGFR-VT+ cRNA display a range of abnormal development in the posterior portion of the embryo. Figures 3.3 C and D display less severe posterior truncation and splitting while Figures 3.3 E and F represent the more severe abnormalities observed in that the entire embryo posterior to the head has been truncated and twisted into an

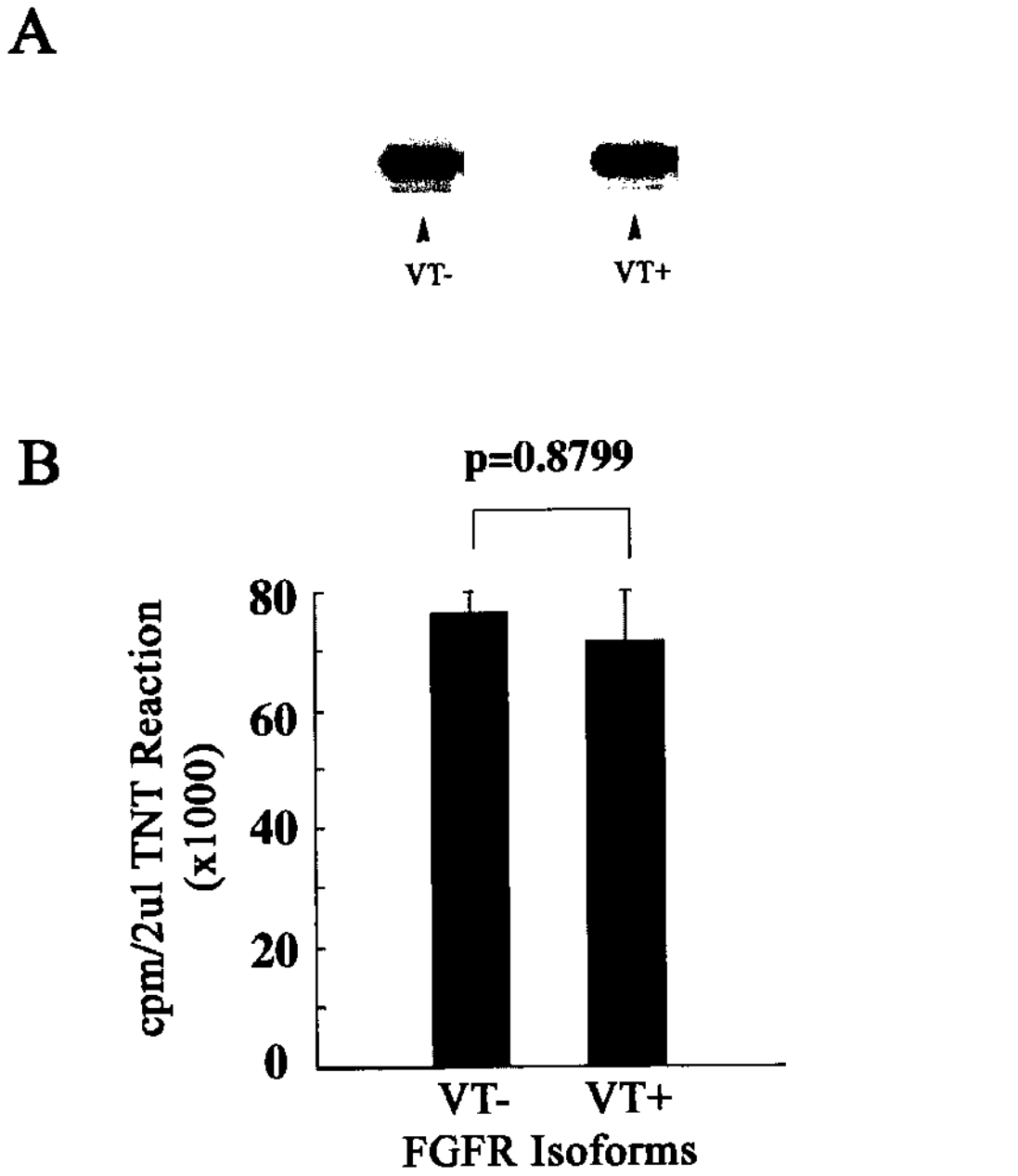

Figure 3.1: *In vitro* translation of synthetic FGFR-VT+ and FGFR-VT- RNA.

A. Representative electrophoretic gel of level of ^{35}S-methionine incorporation in 5 µg of FGFR-VT+ (VT+) and FGFR-VT- (VT-) stock cRNA *in vitro* translated.

B. Scintillation data of ^{35}S-methionine incorporation into each of the two FGFR isoforms. Values represent the average of 6 repeated translation reactions from stock cRNA samples.

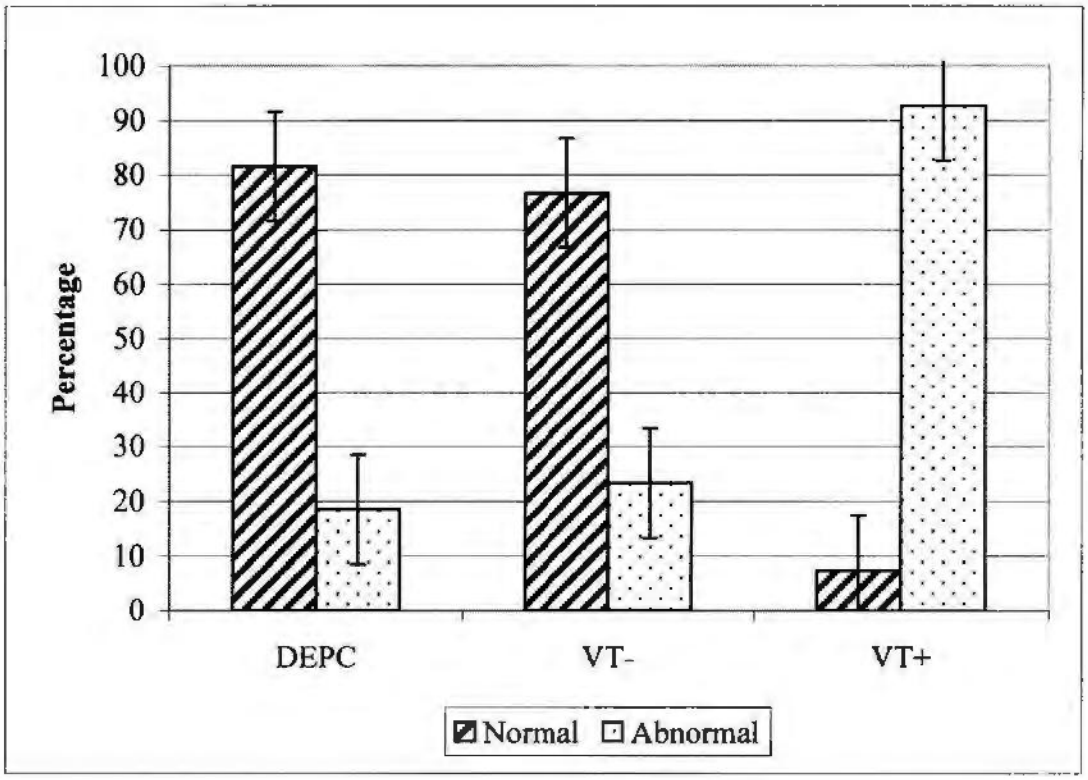

Figure 3.2: Graphical representation of the phenotype expression in *Xenopus* embryos overexpressing FGFR-VT+ (VT+) and FGFR-VT- (VT-) and that of the DEPC-H_2O (DEPC) control group. A total of 135 embryos (45 VT+, 45 VT- and 45 DEPC) were used for each experiment, and averages and standard deviation (error bars) values of 7 individual experiments are shown. *Xenopus* embryos at Nieuwkoop and Faber stage 40 of development.

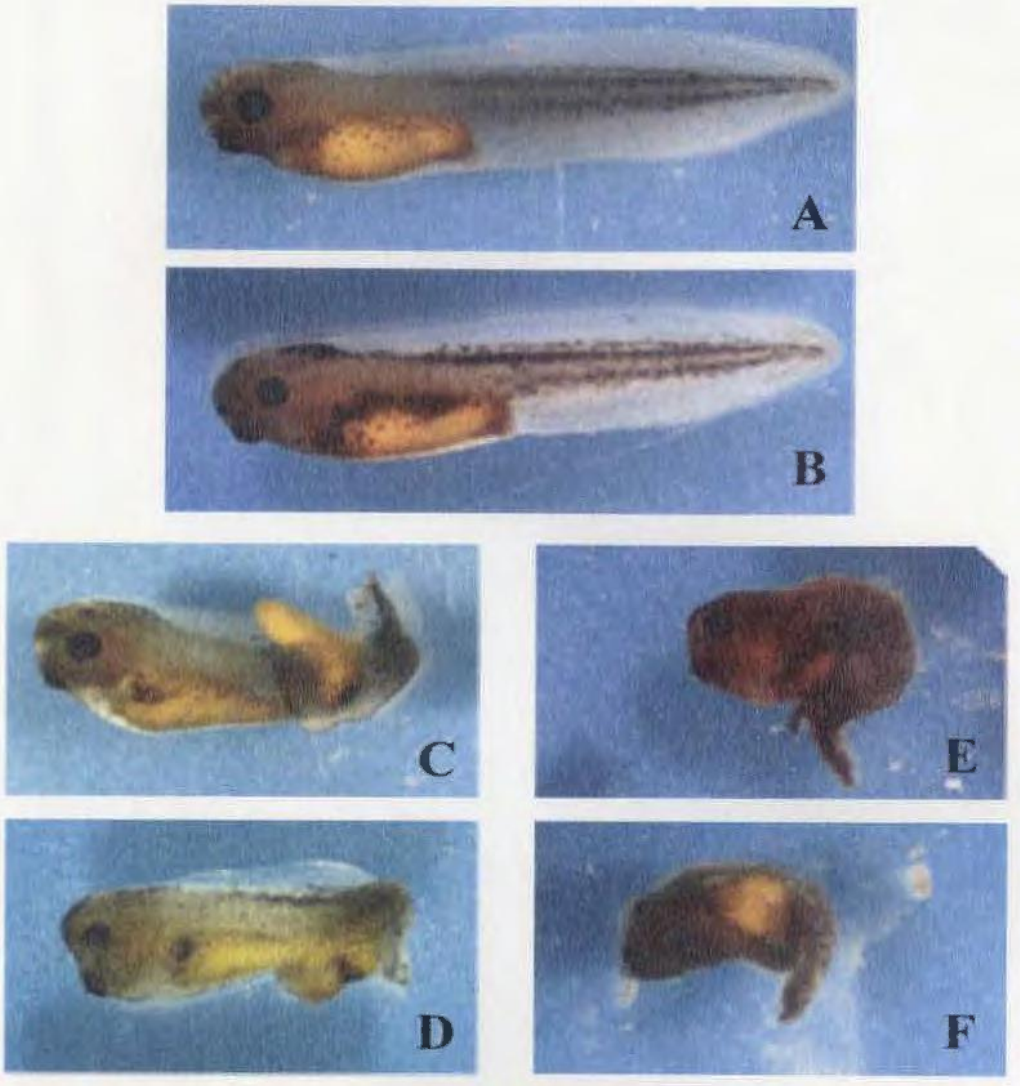

Figure 3.3: Embryos representative of the developmental phenotype observed after microinjection with either of the receptor isoform cRNAs or the control injection. **A.** DEPC H_2O control injection – normal phenotype. **B.** FGFR-VT- injection – normal phenotype. **C – F.** FGFR-VT+ injection – various degrees of posterior truncation observed. *Xenopus* embryos at Nieuwkoop and Faber stage 40 of development.

undistinguishable mass of tissues. The majority of embryos injected with FGFR-VT+ display severe reductions in trunk and tail structures. These results are in agreement with those reported previously by Paterno et al. (2000).

3.2 Molecular Marker Analysis

The primary objective of this project was to investigate the molecular basis of the abnormal pattern of development observed in the *Xenopus* embryos overexpressing FGFR-VT+. Total RNA samples were isolated from batches of embryos injected with FGFR-VT-, FGFR-VT+ cRNAs or DEPC H_2O (Control) at developmental stages 8.5, 10.5, 11.5 and 15 as described in Chapter 2: Materials and Methods (page 40). The embryos selected for these samples consisted of normally developing embryos from the controls, DEPC H_2O and FGFR-VT-, and abnormally developing embryos from the FGFR-VT+ injection set. Embryos were sampled in this manner because we were investigating the possibility of gene expression differences between the abnormal and normal embryos that are overexpressing these two FGFR isoforms. The total RNA samples were reverse-transcribed into cDNA and then used for RT-PCR analysis. A series of *Xenopus* molecular markers known to have differential expression in the affected regions were chosen for analysis in an effort to elucidate a molecular basis for the observed abnormal phenotype. The amount of cDNA added to each PCR reaction was normalized using Histone 4 (H4). Equivalent H4 levels indicate equivalent cDNA input concentrations. This allowed for the comparison of samples within each marker primer set. With the input normalized, differences that appear in the PCR product levels

between samples represent differences in expression of the molecular markers, not differences in the overall cDNA input. This holds true provided that the PCR reaction has not reached a point of saturation. The PCR amplification reaction is not unlimited; the amplification target will gradually stop accumulating exponentially and it will enter a level phase known as the "plateau" (Innis and Gelfand 1990; Saiki 1989). If reactions have reached saturation, due to incorrect reaction parameters, then differences between product bands may be decreased or less obvious.

Prior to commencing radiolabeled PCR reactions, every total RNA sample collected and subsequently reverse transcribed was assayed initially for histone-4 (H4) expression. As an input control, it was empirically determined that 26 cycles produced a sufficient level of H4 for detection using a standard unlabeled PCR reaction. It was subsequently empirically determined that for radiolabeled PCR reactions, 22 cycles would produce sufficient levels for H4 detection and 26 cycles would produce sufficient levels of the molecular markers for detection. Every marker analyzed was examined in duplicate along with H4 input control using the labeled PCR protocol. The PCR product bands were analyzed by densitometry using AlphaEase™ Stand Alone Software Version 3.2 on the ChemiImager 4000 Digital Imaging and Analysis System (Alpha Innotech Corporation) to quantify expression levels.

BMP-4 expression levels are shown in Figure 3.4A and densitometric analysis results are graphically represented in Figure 3.4B. It is shown that only subtle differences in expression levels were detected for BMP-4 within each stage of development for all three of the sample conditions. The pattern of expression between the DEPC H_2O (Control)

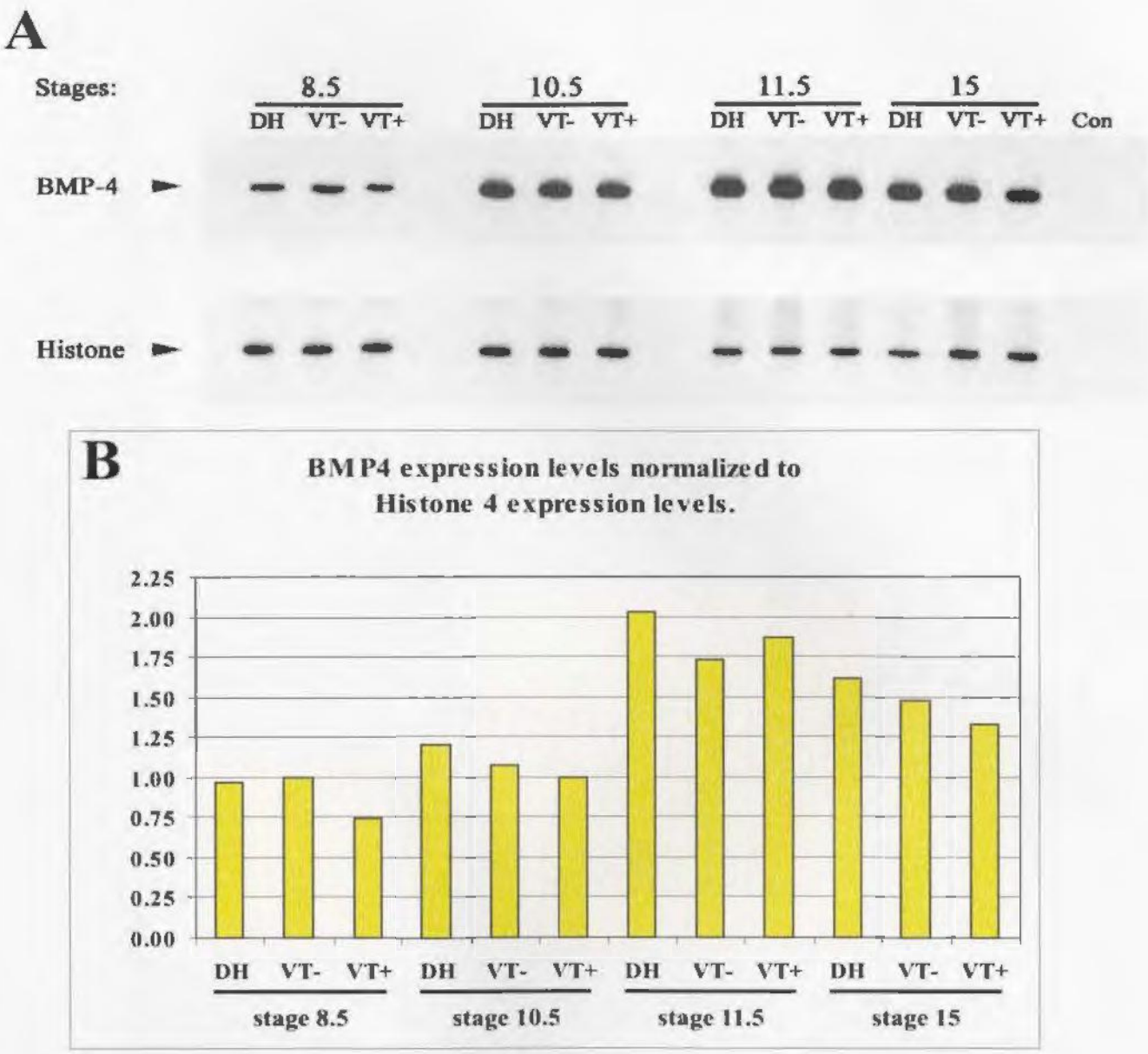

Figure 3.4: **A.** RT-PCR analysis of BMP-4 expression in stage 8.5, 10.5, 11.5 and 15 *Xenopus* embryos injected with DEPC-H_2O (DH) or overexpressing FGFR-VT+ (VT+) or FGFR-VT- (VT-). Total RNA was extracted and analyzed from five embryos for each injection set at each stage indicated. Histone (H4) levels were used to normalize the cDNA input for each PCR reaction. PCR cycles: 22 Histone; 26 BMP-4. (Con) represents a negative control, PCR reaction without cDNA. **B.** Densitometric analysis of the expression level of BMP-4 normalized to H4 for each sample presented in Figure 3.4A. Duplicate PCR analysis was performed on two separate injection experiments and a representative gel is shown above.

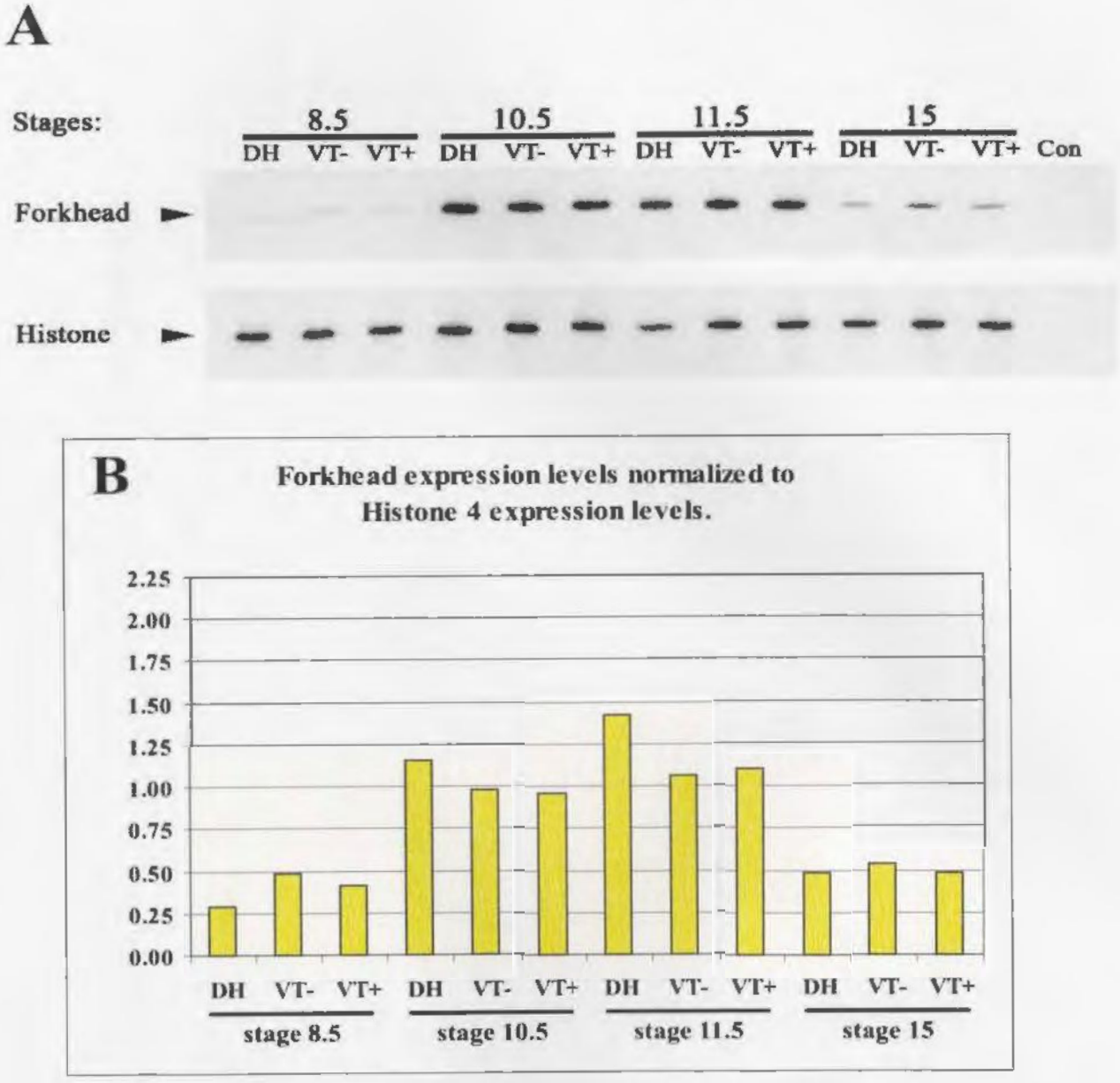

Figure 3.5: **A.** RT-PCR analysis of Forkhead expression in stage 8.5, 10.5, 11.5 and 15 *Xenopus* embryos injected with DEPC-H_2O (DH) or overexpressing FGFR-VT+ (VT+) or FGFR-VT- (VT-). Total RNA was extracted and analyzed from five embryos for each injection set at each stage indicated. Histone (H4) levels were used to normalize the cDNA input for each PCR reaction. PCR cycles: 22 Histone; 26 Forkhead. (Con) represents a negative control, PCR reaction without cDNA. **B.** Densitometric analysis of the expression level of Forkhead normalized to H4 for each sample presented in Figure 3.5A. Duplicate PCR analysis was performed on two separate injection experiments and a representative gel is shown above.

samples of the four stages examined followed the normal pattern of expression reported in the literature (Nishimatsu et al. 1992; Dale et al. 1992), i.e. BMP-4 gene expression begins around MBT stage 8.5, peaks during gastrulation and declines in level after that, however transcripts persist into early tadpole stages (stage 34).

Xenopus Forkhead expression levels are presented in Figure 3.5A, with graphical representation provided in Figure 3.5B. No difference in Xenopus forkhead expression level was detected for any of the sample conditions within each stage examined. The pattern of expression between the DEPC H_2O (Control) samples for the stages examined followed the normal pattern of expression reported in the literature (Dirksen and Jamrich 1992), i.e. gene expression commences at MBT, represented by stage 8.5, peaks between stages 10 and 12, and transcripts decrease from then on.

Goosecoid expression levels are shown in Figure 3.6A, while Figure 3.6B provides graphical representation of the densitometry data. Goosecoid expression is barely detectable at stage 8.5 for all three injection samples; by stage 10.5 the expression level had peaked and was similar for all three samples within the stage. By visual evaluation of Figure 3.6A, Goosecoid levels at stage 11.5 appear to be elevated in the FGFR-VT- injected sample when compared to FGFR-VT+ and DEPC H_2O (Control) samples at the same stage. Densitometric analysis of this sample (Figure 3.6B) revealed that the difference is subtle and is comparable to that observed at stage 10.5. By stage 15, the levels of expression are reduced, but the DEPC H_2O (Control) sample maintains slightly higher expression than either FGFR-VT- or FGFR-VT+ (Figures 3.6A & B). The pattern of

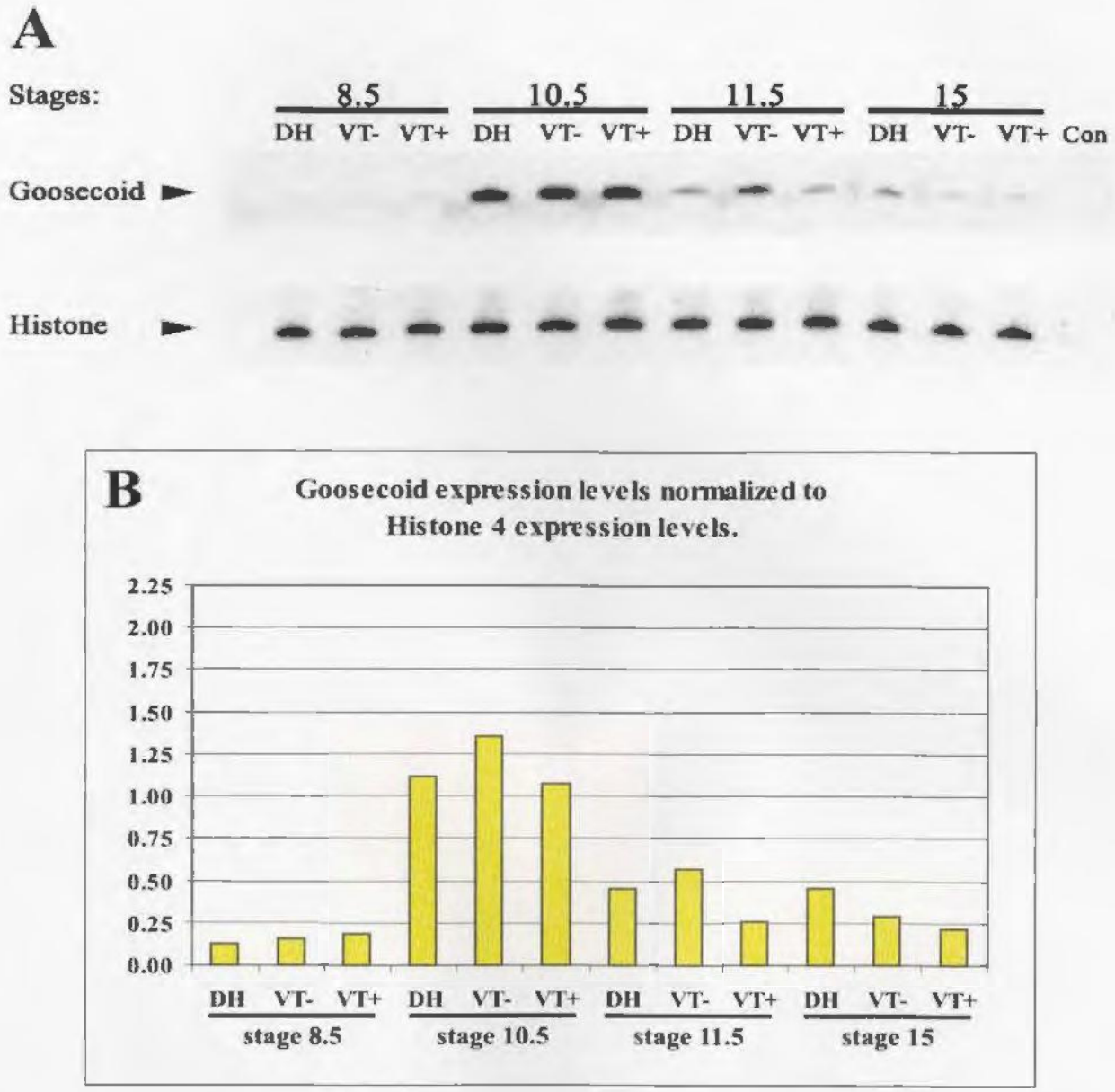

Figure 3.6: **A.** RT-PCR analysis of Goosecoid expression in stage 8.5, 10.5, 11.5 and 15 *Xenopus* embryos injected with DEPC-H_2O (DH) or overexpressing FGFR-VT+ (VT+) or FGFR-VT- (VT-). Total RNA was extracted and analyzed from five embryos for each injection set at each stage indicated. Histone (H4) levels were used to normalize the cDNA input for each PCR reaction. PCR cycles: 22 Histone; 26 Goosecoid. (Con) represents a negative control, PCR reaction without cDNA. **B.** Densitometric analysis of the expression level of Goosecoid normalized to H4 for each sample presented in Figure 3.6A. Duplicate PCR analysis was performed on two separate injection experiments and a representative gel is shown above.

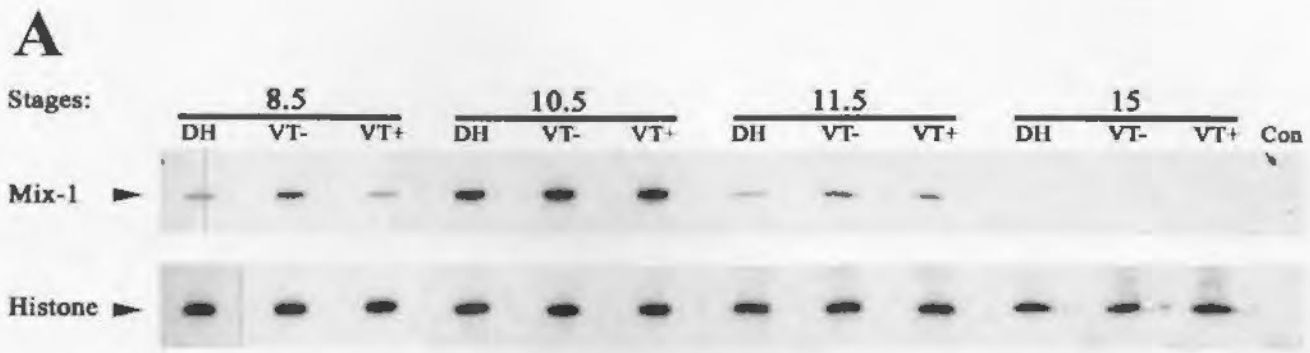

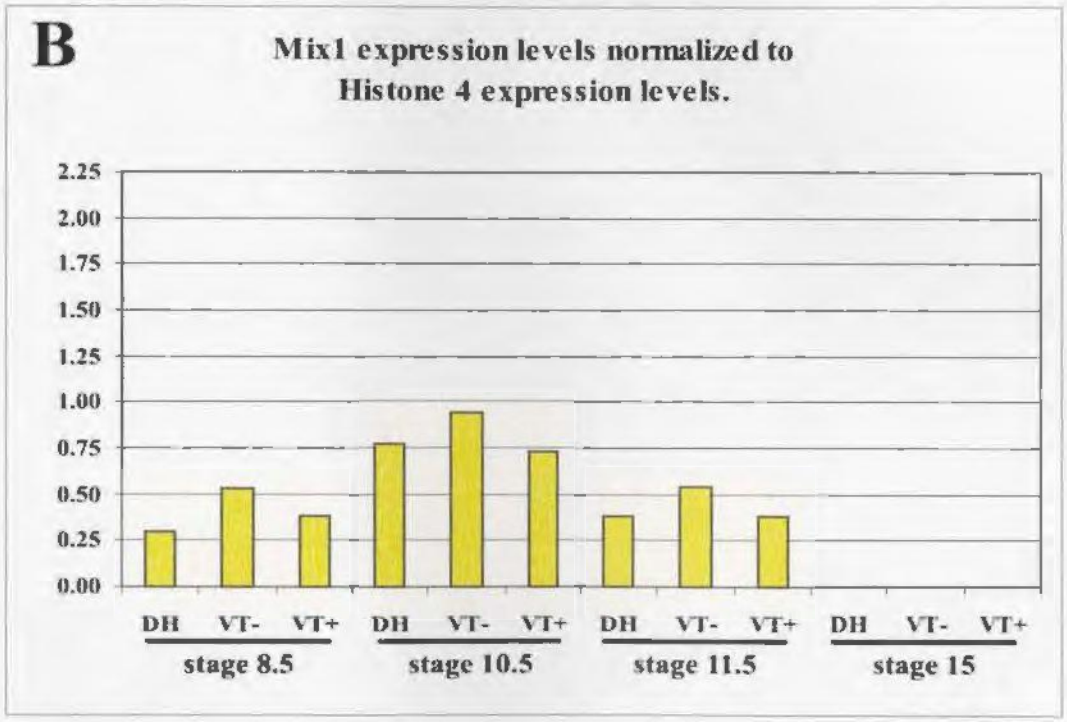

Figure 3.7: **A.** RT-PCR analysis of Mix-1 expression in stage 8.5, 10.5, 11.5 and 15 *Xenopus* embryos injected with DEPC-H_2O (DH) or overexpressing FGFR-VT+ (VT+) or FGFR-VT- (VT-). Total RNA was extracted and analyzed from five embryos for each injection set at each stage indicated. Histone (H4) levels were used to normalize the cDNA input for each PCR reaction. PCR cycles: 22 Histone; 26 Mix-1. (Con) represents a negative control, PCR reaction without cDNA. **B.** Densitometric analysis of the expression level of Mix-1 normalized to H4 for each sample presented in Figure 3.7A. Duplicate PCR analysis was performed on two separate injection experiments and a representative gel is shown above.

expression in the DEPC H_2O (Control) samples of the four stages examined followed the normal pattern of expression reported in the literature (Cho et al. 1991).

Mix-1 expression levels are presented in Figure 3.7A and graphically represented in Figure 3.7B. It is shown that only subtle differences in expression levels were detected for Mix-1 within each of stages 8.5, 10.5 and 11.5 for all three of the sample conditions and Mix-1 expression was not detected for any of the stage 15 samples. The observed expression pattern in the DEPC H_2O (Control) samples for the stages examined corresponds with that reported in the literature for Mix-1, initially detected shortly after MBT (St. 8.5), peak expression at St. 10 and decays gradually to be undetectable by neurulation (Rosa 1989).

Noggin expression levels are presented in Figure 3.8A and graphically represented in Figure 3.8B. Noggin expression levels were similar for all three experimental conditions within each stage of development. The observed expression pattern in the DEPC H_2O (Control) samples for the four stages examined is consistent with that reported in the literature: low levels of expression in the oocytes (maternal transcripts) and higher expression by stage 11 due to zygotic transcription (Smith and Harland 1992).

Xenopus Brachyury (Xbra) expression levels are shown in Figure 3.9A and graphical representation of the densitometric analysis is provided in Figure 3.9B. It is shown that no differences are detected in Xbra expression levels within each stage of development for all three of the sample conditions. The expression pattern observed in the DEPC H_2O (Control) samples for the stages examined is consistent with that reported in the literature for Xbra, with it being initially detected at MBT (Stage 8.5), highest

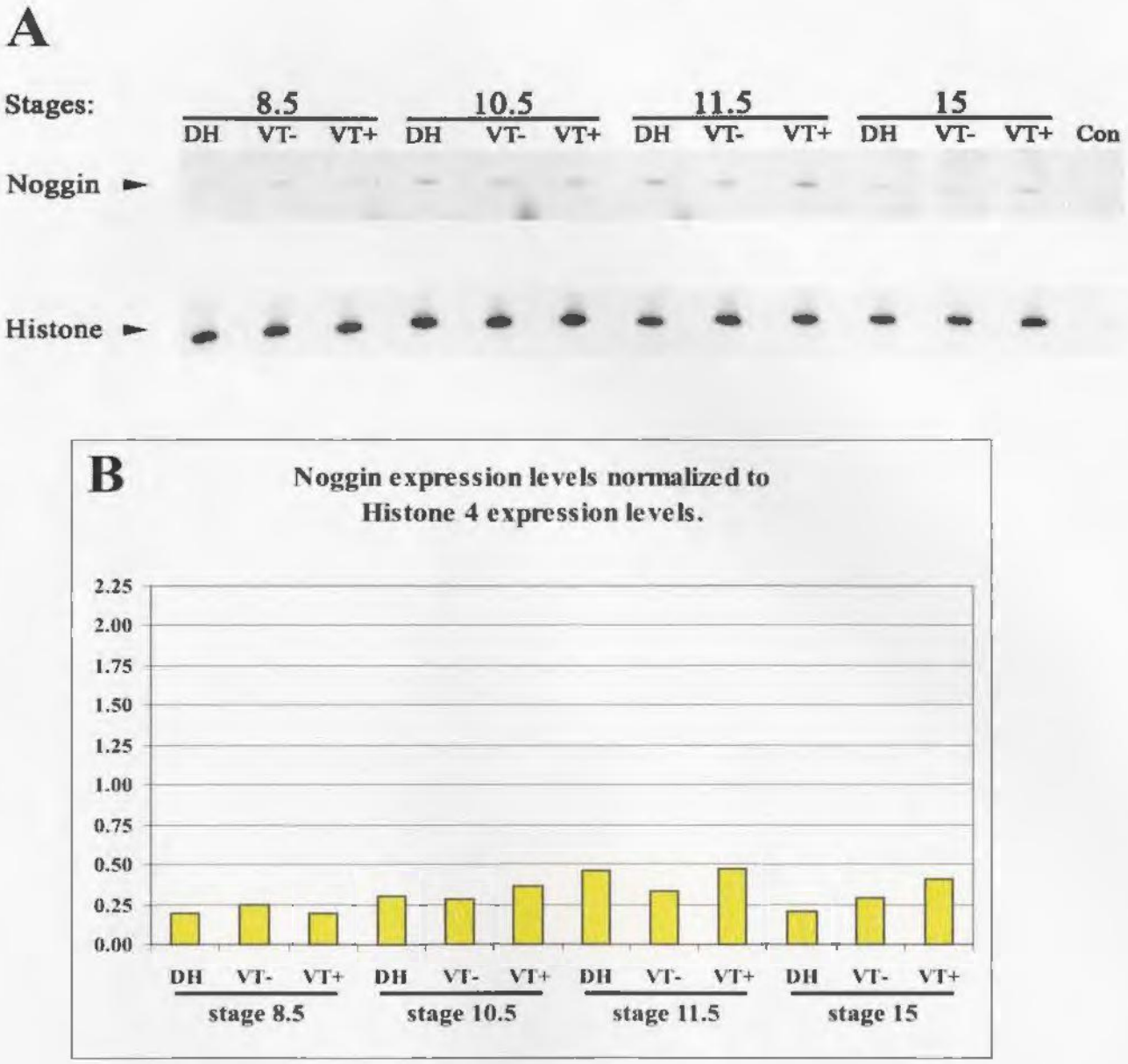

Figure 3.8: **A.** RT-PCR analysis of Noggin expression in stage 8.5, 10.5, 11.5 and 15 *Xenopus* embryos injected with DEPC-H_2O (DH) or overexpressing FGFR-VT+ (VT+) or FGFR-VT- (VT-). Total RNA was extracted and analyzed from five embryos for each injection set at each stage indicated. Histone (H4) levels were used to normalize the cDNA input for each PCR reaction. PCR cycles: 22 Histone; 26 Noggin. (Con) represents a negative control, PCR reaction without cDNA. **B.** Densitometric analysis of the expression level of Noggin normalized to H4 for each sample presented in Figure 3.8A. Duplicate PCR analysis was performed on two separate injection experiments and a representative gel is shown above.

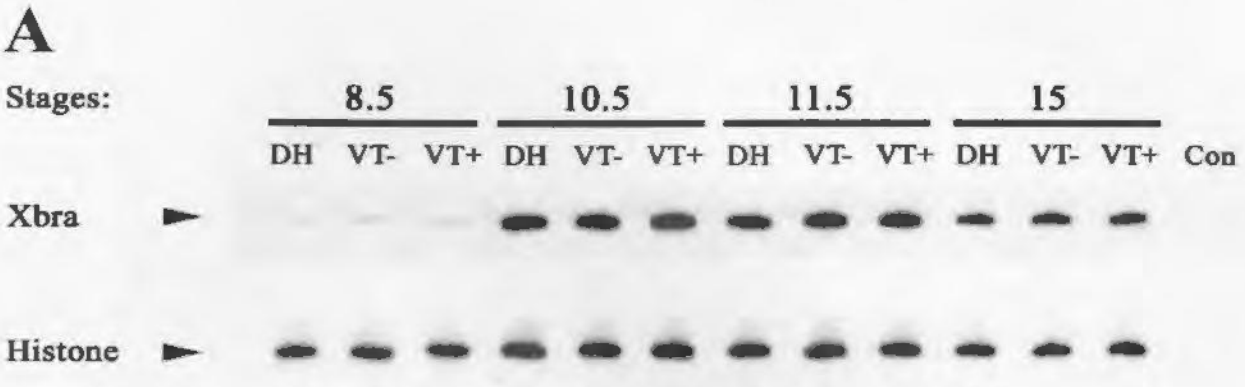

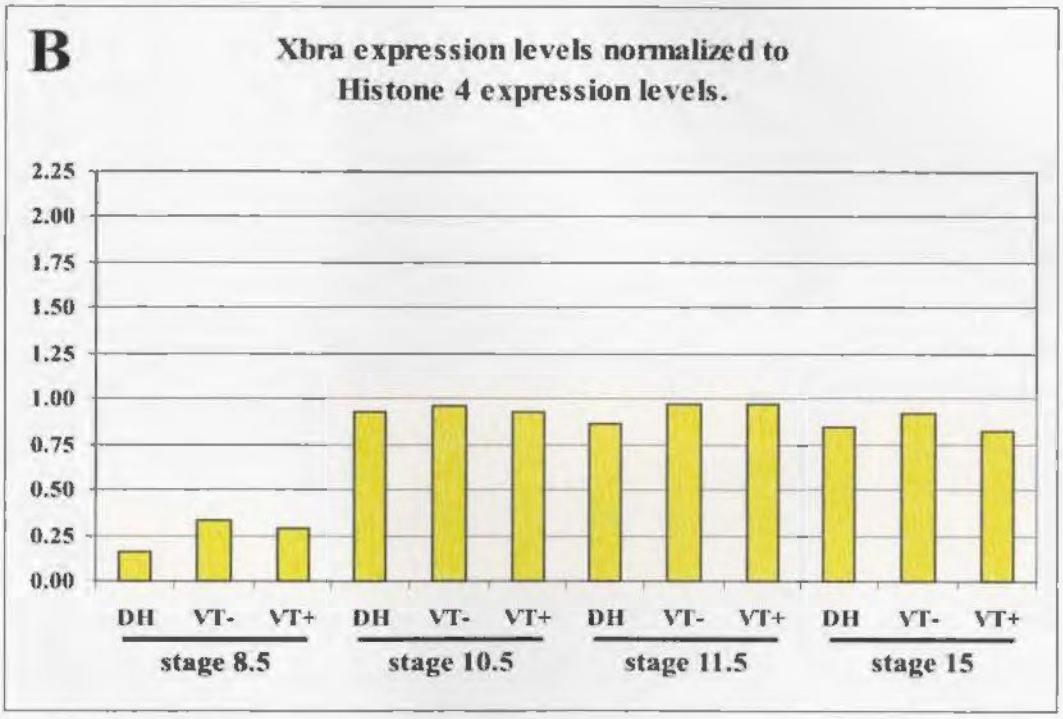

Figure 3.9: **A.** RT-PCR analysis of *Xenopus* Brachyury (Xbra) expression in stage 8.5, 10.5, 11.5 and 15 *Xenopus* embryos injected with DEPC-H_2O (DH) or overexpressing FGFR-VT+ (VT+) or FGFR-VT- (VT-). Total RNA was extracted and analyzed from five embryos for each injection set at each stage indicated. Histone (H4) levels were used to normalize the cDNA input for each PCR reaction. PCR cycles: 22 Histone; 26 Xbra. (Con) represents a negative control, PCR reaction without cDNA. **B.** Densitometric analysis of the expression level of Xbra normalized to H4 for each sample presented in Figure 3.9A. Duplicate PCR analysis was performed on two separate injection experiments and a representative gel is shown above.

expression levels occurring during gastrulation (Stage 10.5 and 11.5) and expression levels declining after gastrulation into neurulation (Stage 15) (Smith et al. 1991).

Xwnt-8 expression levels are presented in Figure 3.10A and Figure 3.10B provides graphical representation of the data. It is shown that only subtle differences in expression levels are detected within stages 8.5 and 10.5 of development for all three experimental conditions. Stage 11.5 displays an apparent decrease in Xwnt-8 expression for the DEPC H_2O (Control) sample. At stage 15 only subtle differences are detected between the three experimental conditions and as expected all samples show lower expression than stage 11.5. The pattern of expression between the DEPC H_2O (Control) samples for the four stages examined followed the normal pattern of expression for Xwnt-8 as reported in the literature. Expression is initially detected in the stage 8.5 sample (blastula), expression has increased dramatically by stage 10.5 (gastrula) and expression levels begin to decline by stage 15 (neurula) (Christian et al. 1991).

Xenopus posterior (Xpo) expression levels are presented in Figure 3.11A and graphically represented in Figure 3.11B. No differences are observed in Xpo expression levels within each stage of development for all three experimental conditions. The pattern of expression in the DEPC H_2O (Control) samples for the stages examined followed the normal pattern of expression for Xpo as reported in the literature. Expression is initially detected around MBT (stage 8.5), expression begins increasing at the onset of gastrulation (stage 10.5 and 11.5) and peaks during neurulation (stage 15) (Sato and Sargent 1991).

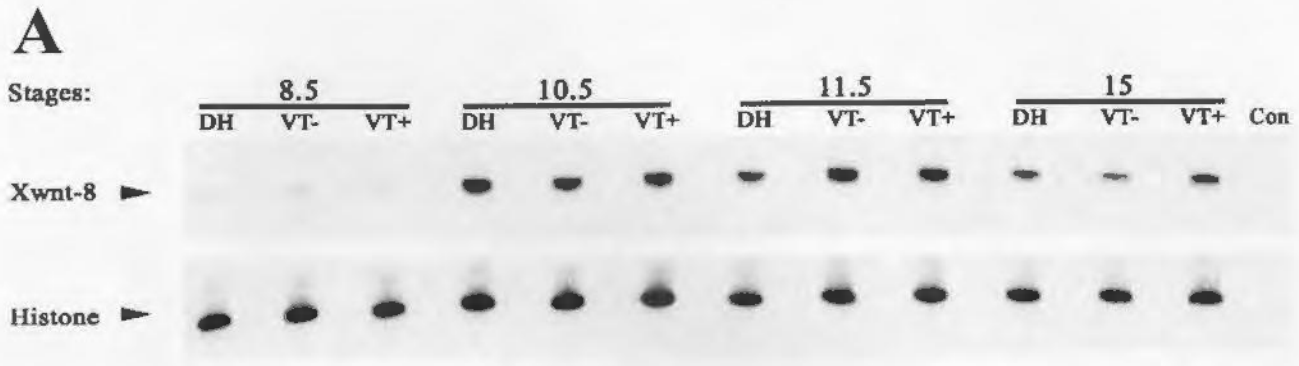

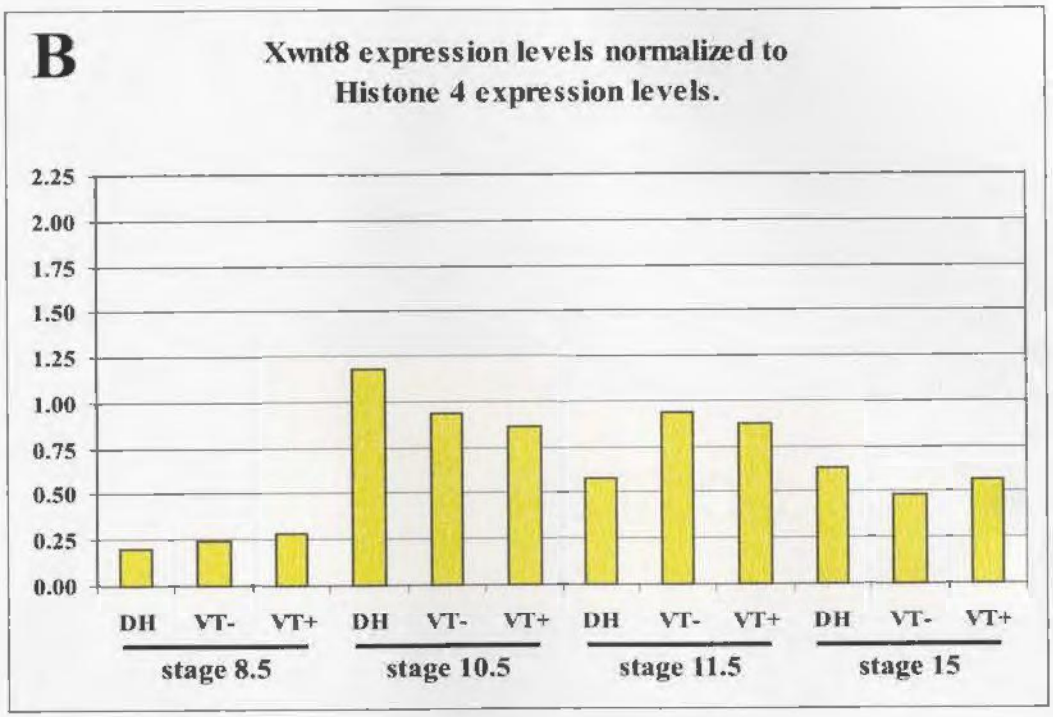

Figure 3.10: A. RT-PCR analysis of Xwnt-8 expression in stage 8.5, 10.5, 11.5 and 15 *Xenopus* embryos injected with DEPC-H_2O (DH) or overexpressing FGFR-VT+ (VT+) or FGFR-VT- (VT-). Total RNA was extracted and analyzed from five embryos for each injection set at each stage indicated. Histone (H4) levels were used to normalize the cDNA input for each PCR reaction. PCR cycles: 22 Histone; 26 Xwnt-8. (Con) represents a negative control, PCR reaction without cDNA. **B.** Densitometric analysis of the expression level of Xwnt-8 normalized to H4 for each sample presented in Figure 3.10A. Duplicate PCR analysis was performed on two separate injection experiments and a representative gel shown above.

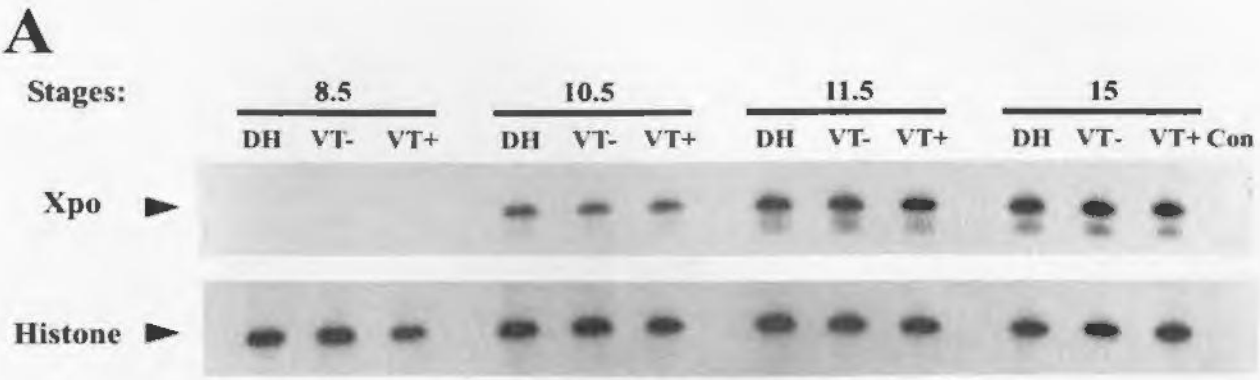

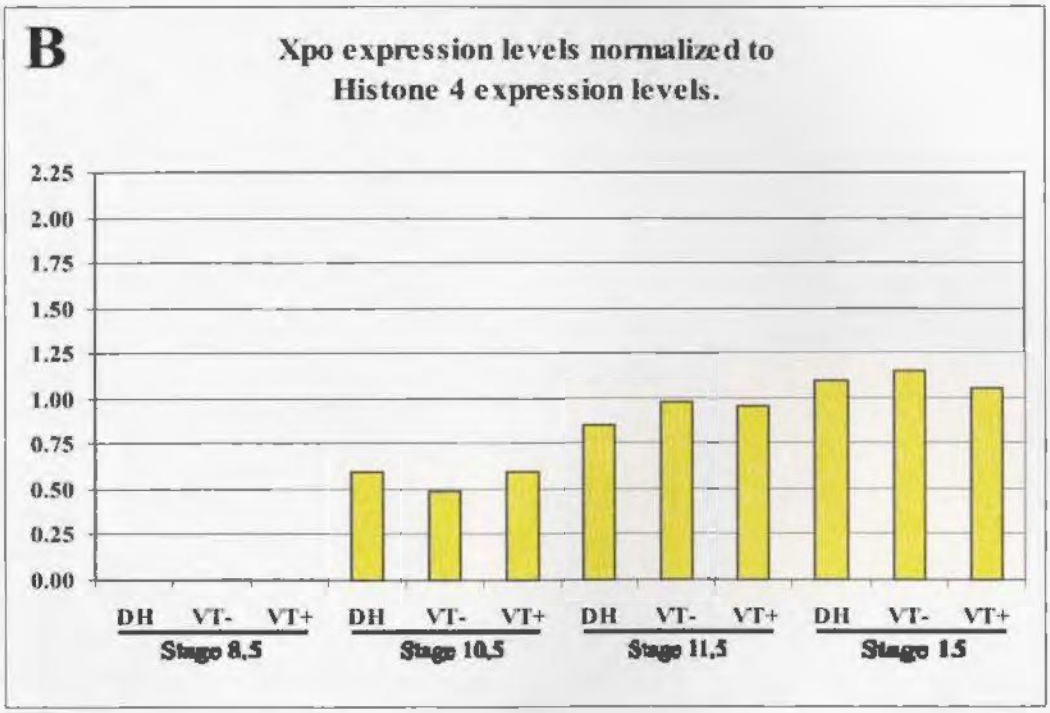

Figure 3.11: A. RT-PCR analysis of *Xenopus* posterior (Xpo) expression in stage 8.5, 10.5, 11.5 and 15 *Xenopus* embryos injected with DEPC-H_2O (DH) or overexpressing FGFR-VT+ (VT+) or FGFR-VT- (VT-). Total RNA was extracted and analyzed from five embryos for each injection set at each stage indicated. Histone (H4) levels were used to normalize the cDNA input for each PCR reaction. PCR cycles: 22 Histone; 26 Xpo. (Con) represents a negative control, PCR reaction without cDNA. **B.** Densitometric analysis of the expression level of Xpo normalized to H4 for each sample presented in Figure 3.11A. Duplicate PCR analysis was performed on two separate injection experiments and a representative gel is shown above.

In summary, there was very little or no difference in the molecular marker expression pattern between the FGFR-VT+, FGFR-VT- and DEPC-treated water injected embryos (Table 3.1). Some of the possible reasons for this will be discussed in Section 4.1, p. 74. Therefore, I did not pursue investigation of the molecular mechanisms involved in the abnormality caused by overexpression of FGFR-VT+.

Table 3.1: Summary of molecular marker expression pattern observations.

Molecular Marker	Observation
BMP-4	Subtle differences between samples; overall, the controls display no difference from expected pattern.
Xenopus Forkhead	No differences between samples; overall, the controls display no difference from expected pattern.
Goosecoid	Subtle differences between samples; overall, the controls display no difference from expected pattern.
Mix-1	Subtle differences between samples in stages 8.5, 10.5 and 11.5, not expressed at stage 15; overall, the controls display no difference from expected pattern.
Noggin	Subtle differences between samples; overall, the controls display no difference from expected pattern.
Xenopus brachyury	No differences between samples; overall, the controls display no difference from expected pattern.
Xwnt-8	Decreased expression in control sample at stage 11.5, compared to VT- and VT+ samples; overall, the controls display no difference from expected pattern.
Xenopus posterior	No differences between samples; overall, the controls display no difference from expected pattern.

3.3 Expression Analysis of Additional FGFR Variant Forms

As previously mentioned, the secondary objective of this project was to investigate the expression patterns of other known FGFR isoforms that may have functional significance. The next FGFR1 variant examined differs from the reported FGFR1

sequence by Proline^{442}-Serine^{443} deletion, an aspect of interest as the serine residue represents a potential phosphorylation site. The final variant examined, actually a variant pair, represent the α- and β-forms of FGFR, an aspect of interest as these receptor forms may have different FGF binding affinities and/or specificities. To accomplish this analysis, total RNA samples were collected solely from normally developing *Xenopus laevis* embryos at stages 1-8, 8.5, 9, 10, 10.5, 11, 11.5, 12, 13, 16, 25, 38 and 42. For this experiment, *Xenopus* eggs were obtained via artifically induced ovulation and subsequently *in vitro* fertilized, but were not otherwise manipulated until time of collection and processing for RNA. This RNA panel was subsequently reverse transcribed and used to analyze the temporal expression patterns of the FGFR isoforms indicated. The product bands were also analyzed by densitometry using AlphaEase™ Stand Alone Software Version 3.2 on the ChemiImager 4000 Digital Imaging and Analysis System (Alpha Innotech Corporation) to determine a ratio of expression levels within each stage.

The first analysis looked at the expression of FGFR1 isoform that differed from the reported sequence by the deletion of Pro^{442}-Ser^{443}, subsequently referred to as FGFR-PS-. For the purpose of this analysis, the reported sequence containing Pro^{442}-Ser^{443} is referred to as FGFR-PS+. Figure 3.12A represents the temporal expression pattern of the FGFR-PS+ and FGFR-PS- isoforms at the various stages throughout early *Xenopus* development previously mentioned. Duplicate PCR analysis was performed on a single set of embryo RNAs collected as described above. The results of this analysis compare the ratio PS-:PS+ within each sample as indicated (Figure 3.12); for this reason, an input control such

as Histone-4 levels was not used in this analysis. The expression pattern observed in Figure 3.12 show that during early development the PS- variant expression level is 1.3-1.8X higher than that of the PS+ variant at the same stage of development. By stage 11.5, the ratio of the expression level of the variants approaches 1.0.

The second analysis looked at the expression of two variants of FGFR1 that involve differences in the immunoglobulin-like (Ig-like) domains. The use of alternative splice sites results in either the inclusion or exclusion of the first of the three immunoglobulin-like domains. For the purpose of this analysis these FGFR isoforms are termed α-FGFR (3 Ig-like domains) and β-FGFR (2 Ig-like domains). Using the previously mentioned panel of total RNA from various stages throughout early *Xenopus* development, the temporal expression of α-FGFR and β-FGFR were examined, comparing the ratio of α:β within each stage but not between stages, therefore an input control such as Histone 4 was not used in this analysis. The results of this analysis (Figure 3.13) indicated that the α-FGFR variant is the predominantly expressed isoform through early development (stages 1-13), with an expression level approximately 2.5-4.1X higher than that of β-FGFR. By tadpole stages (stages 38-42) the β-FGFR variant shows an increase in expression levels approaching that of the α-FGFR variant at the same stage of development, with the ratio of α-FGFR to β-FGFR approaching 1.0.

A

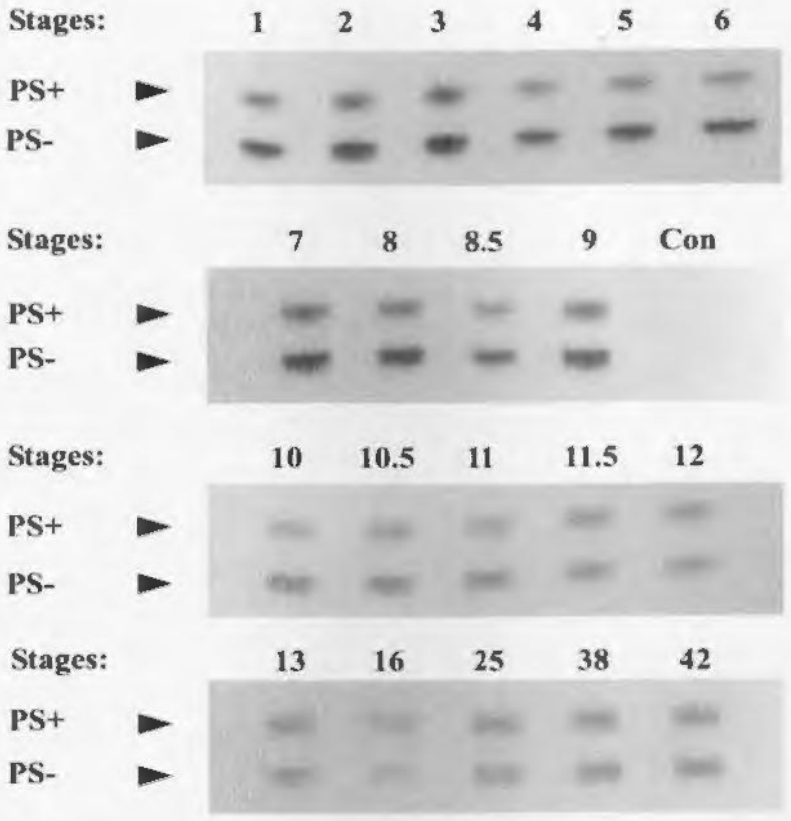

B **Densitometery Results for Temporal Expression Analysis of FGFR-PS+ and FGFR-PS- Variants**

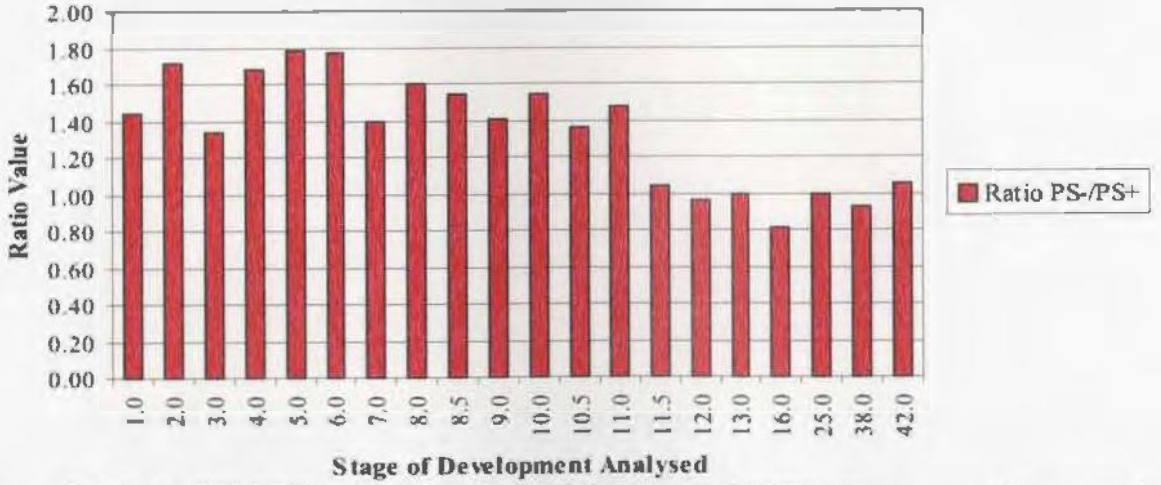

Figure 3.12: A. RT-PCR analysis of FGFR-PS+ and FGFR-PS- temporal expression patterns during *Xenopus laevis* development. Total RNA was extracted and analyzed from five embryos for each stage of development indicated. Stage numbers represent the Nieuwkoop and Faber (1967) stages of development from which the sample was taken; PS+, FGFR-PS+; PS-, FGFR-PS-. Duplicate PCR analysis was performed on a single RNA set and a representative gel is shown. **B.** Densitometric analysis of the PS-:PS+ ratio for each sample presented in Figure 3.12A.

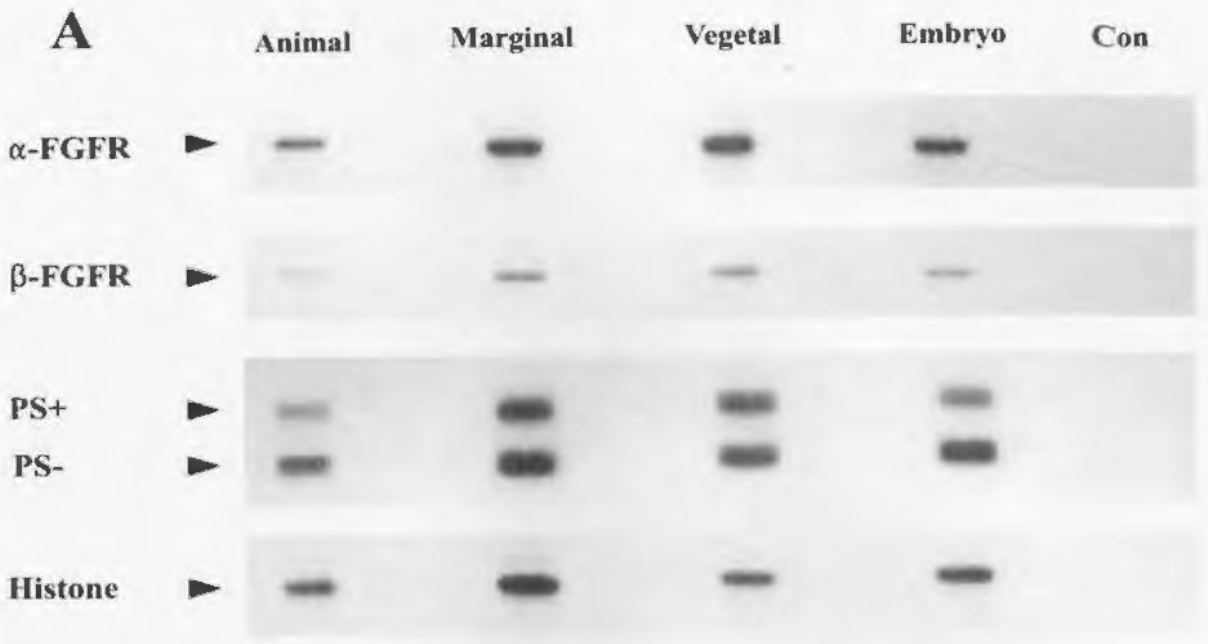

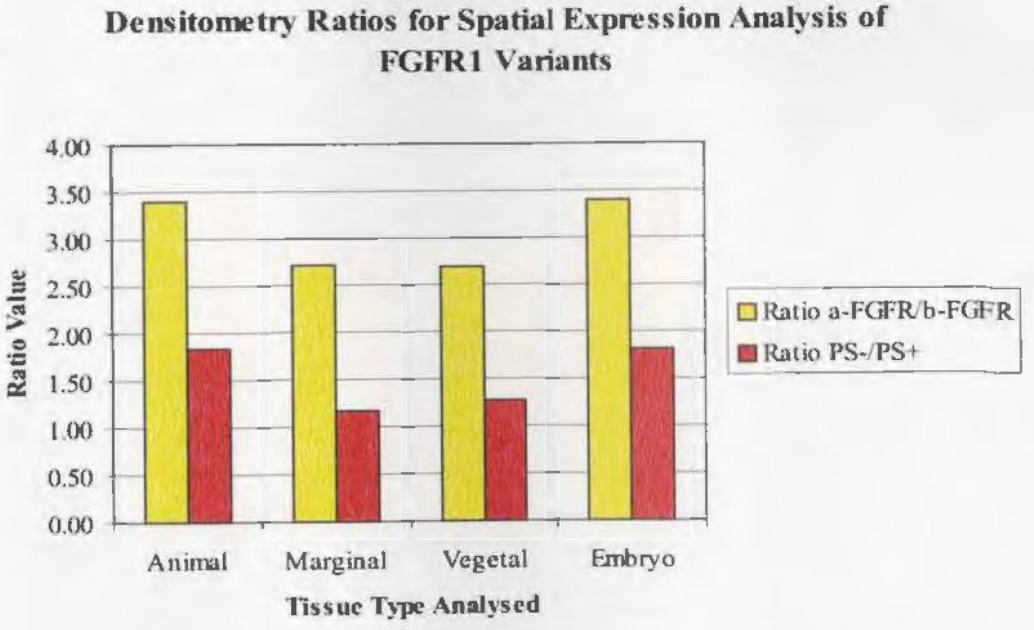

Figure 3.13: A. RT-PCR analysis of α-FGFR and β-FGFR temporal expression patterns during *Xenopus laevis* development. Total RNA was extracted and analyzed from five embryos for each stage of development indicated. Stage numbers represent tbe Nieuwkoop and Faber (1967) stages of development from which the sample was taken. Duplicate PCR analysis was performed on a single RNA set and a representative gel is shown. **B.** Densitometric analysis of the α-FGFR:β-FGFR ratio for each sample presented in Figure 3.13A. a, α; b, β.

In addition to the temporal patterns, spatial expression patterns for these variant FGFR isoforms were also analyzed. Total RNA samples were collected from normally developing *Xenopus laevis* embryos (stage 8.5) that were dissected into Animal Cap, Marginal Zone and Vegetal Cap. Total RNA was also collected from whole embryos from the same batch. Figure 3.14A represents the spatial expression pattern observed for the FGFR-PS-, FGFR-PS+, α-FGFR and β-FGFR isoforms. The results of this analysis suggest that FGFR-PS- is the predominant form in the Animal cap tissues being expressed at approximately 1.8X higher levels (Figure 3.14B) when compared to FGFR-PS+. The ratio of FGFR-PS- to FGFR-PS+ expression levels approaches 1.0 in both the Marginal zone and Vegetal cap tissues (Figure 3.14B). The expression in the whole embryo sample suggests that FGFR-PS- is expressed at a higher level (~1.8x) than the FGFR-PS+ form (Figure 3.14B). The spatial expression patterns of α-FGFR and β-FGFR presented in Figure 3.14A indicate that the α-FGFR variant is predominantly expressed in all three spatial zones examined as well as the whole embryo sample. The expression levels of α-FGFR are approximately 2.5-3.5X higher than the β-FGFR isoform expression levels (Figure 3.14B) for all four samples examined. The potential implications of these findings will be discussed later.

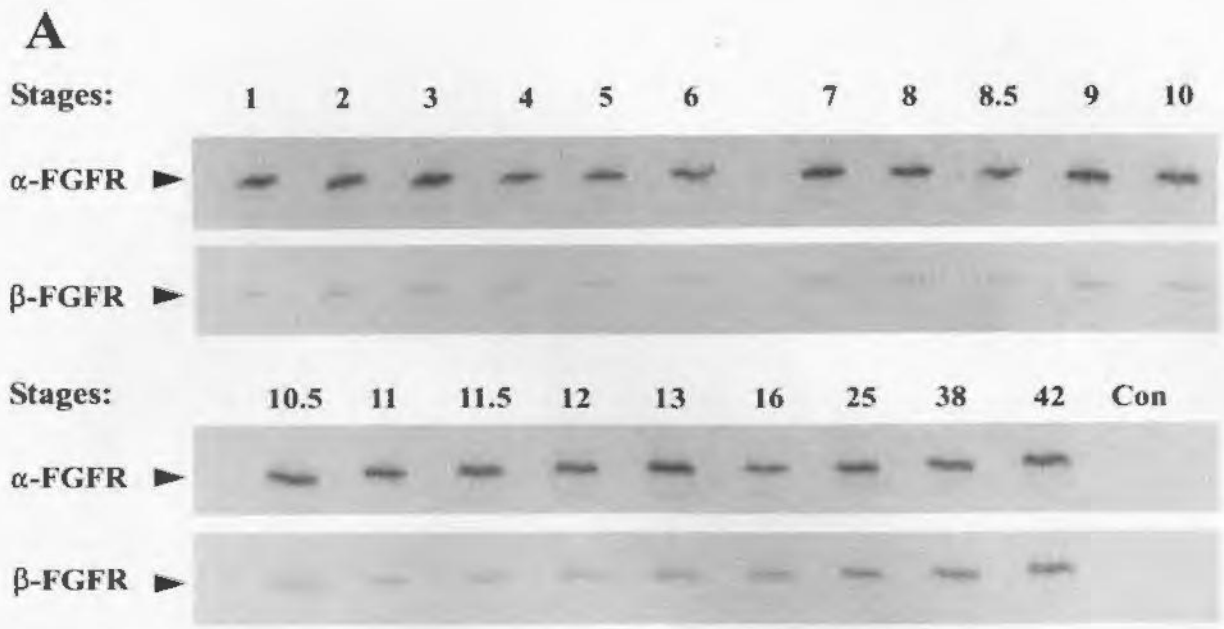

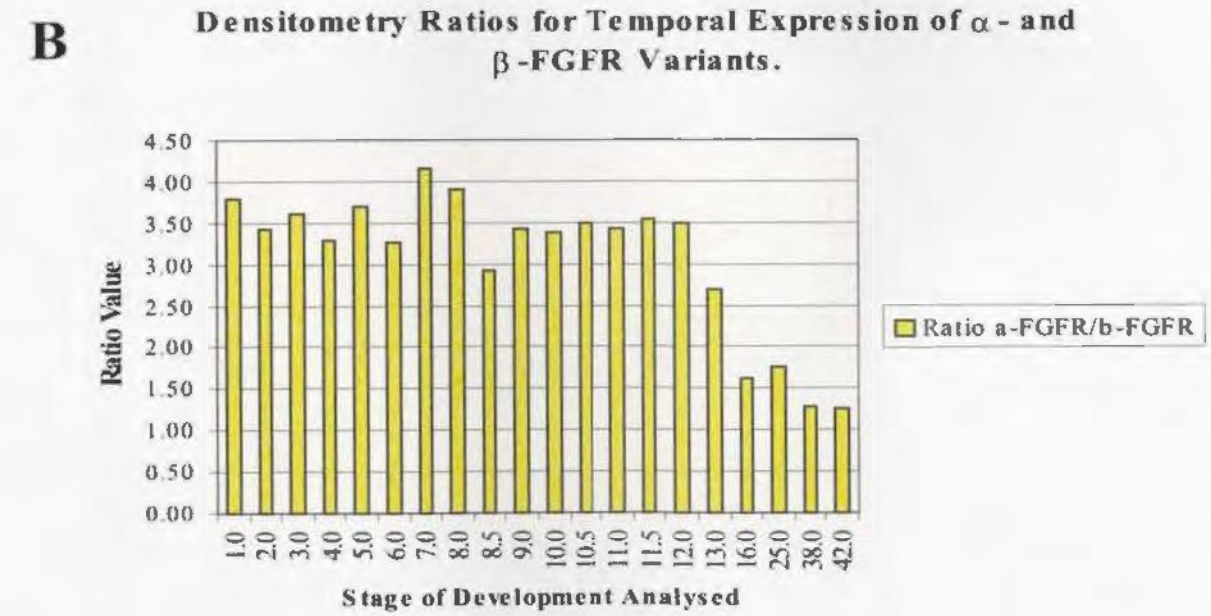

Figure 3.14: A. RT-PCR analysis of α-FGFR, β-FGFR, FGFR-PS+ and FGFR-PS- spatial expression patterns. Total RNA was extracted and analyzed from animal caps (Animal), marginal zone (Marginal), vegetal caps (Vegetal) and whole embryos (Embryo). Histone (H4) levels were used to normalize the cDNA input for each PCR reaction. PS+, FGFR-PS+; PS-, FGFR-PS-. Duplicate PCR analysis was performed on a single RNA set and a representative gel is shown. **B.** Densitometric analysis of the PS-:PS+ ratio and the α-FGFR:β-FGFR ratio for each sample presented in Figure 3.14A. a, α; b, β.

Chapter 4
Discussion

4.1 Molecular Marker Expression Analysis of Embryos Overexpressing FGFR-VT- and FGFR-VT+.

The abnormal phenotype observed in *Xenopus* embryos overexpressing FGFR-VT+ may be a consequence of a deficiency in mesoderm formation (Paterno et al. 2000), therefore the markers being studied all represent early markers of mesoderm induction (Table 4.1). The set of markers representing various regions of the mesoderm were assessed for potential deviations from normal expression patterns, in an effort to elucidate the molecular pathway that was adversely affecting development in the embryos overexpressing FGFR-VT+.

Table 4.1: Region of Expression of the Molecular Markers Examined.

Marker	Expressed in
BMP-4	Ventral-lateral mesoderm
Xenopus Forkhead	Organizer
Goosecoid	Organizer
Mix-1	Presumptive endoderm and mesoderm
Noggin	Organizer
Xenopus brachyury	Early mesoderm
Xwnt-8	Ventral-lateral mesoderm
Xenopus posterior	Posterior mesoderm

As previously stated, the complete set of markers examined for this project displayed only subtle deviations from their normal, expected pattern of expression. This may in part be due to any one or combination of factors, such as: no effect on this particular set of markers, or limitations on the methodology employed, or consistency of the RNA sample.

It is conceivable that there is no effect on any of the markers in the set evaluated. However, this was not anticipated as *Xbra* expression had previously been observed to be undetectable or only very faintly detectable in embryo samples overexpressing FGFR-VT+, when compared to controls, as determined by *in situ* hybridization (Paterno et al. 2000). It poses some question as to whether or not the RT-PCR results for the remaining molecular markers are reliable. Additional means of re-examining these markers might include procedures such as whole mount *in situ* hybridization, northern blot analysis, or RNase protection assay. These procedures will be discussed in further detail in the potential future directions of this research, Section 4.3.1, p.81.

Limitations on the methodology used include translational efficiency; RNA may be present but is it translated? The RT-PCR procedure would amplify RNA that is present but the question of whether or not this RNA is being translated into protein *in vivo* remains. In addition, the RT-PCR procedure amplifies target messages as well as any errors or contaminations present, subsequently affecting the accuracy and reliability of the data. Therefore, consistency of the RNA sample collected represents another possible limitation. This project investigated the molecular basis of the abnormal phenotype observed in embryos overexpressing FGFR-VT+. Therefore embryos collected were phenotypically normal for the control samples (DEPC-H_2O and FGFR-VT- injected embryos) and phenotypically abnormal for experimental samples (FGFR-VT+ injected embryos). The reason for this selection method is that we were looking directly at the RNA pool of these embryos for possible gene misexpression, that is differences in gene expression patterns between the control (normal) and experimental (abnormal) embryos.

The potential for a problem presents itself in that if a single normal embryo is collected with the abnormal sample, it may "contaminate" this sample with copies of genes that are being misexpressed in the abnormal embryos. The methodology employed, radiolabeled RT-PCR would amplify these normal copy genes and the expression pattern presented would not be a truly representative pattern. The reason that this represents a possible problem is that the abnormal phenotype does not present until gastrulation at which time it can present as a severely abnormal exogastrulation event or as a subtle slowing of gastrulation movements. All embryos collected prior to gastrulation appear normal and as development proceeds to gastrulation and beyond, abnormal development becomes obvious. While much care was taken during sampling to avoid this, it remains as a possible reason for lack of differences observed. Furthermore, PCR analysis may have been too sensitive a method to employ in analyzing marker expression under the sampling protocol implemented, i.e. for pooled embryo samples. Subsequent analysis should consider the plausibility of sampling individual embryos as controls or for comparison to pooled embryo samples.

4.2. Expression Pattern Analysis of FGFR Variant Forms.

4.2.1 Analysis FGFR-PS+ and FGFR-PS- Isoforms.

Study into the expression pattern of this variant pair was undertaken as Serine^{443} represents a potential phosphorylation site and therefore differential expression of these isoforms may be functionally significant. As determined by NetPhos 2.0 predictions, amino acid position 443, occupied by serine residue in the PS+ variant is located within a

phosphorylation consensus sequence (Blom et al. 1999). Comparison with consensus sequences for several Ser/Thr kinases revealed that amino acid position 443 was located within a consensus sequence for phosphorylation by PKA (Kennelly and Krebs 1991). In FGFR-PS+, a serine is located in position 443, however in the FGFR-PS- form a Lys occupies this position.

Temporal expression of FGFR-PS variants revealed that the PS- variant is the predominant form up until stage 11.5 after which time little or no difference in expression levels between the two forms is detected. The spatial expression analysis revealed that the PS- variant is the predominant form present throughout the stage 8.5 embryo. This raises question into the possibility of functional differences between these receptor isoforms.

It has been previously demonstrated for receptor isoforms that differ from each other by a dipeptide sequence, FGFR-VT+ and FGFR-VT-, when one of these amino acids positions falls into a phosphorylation consensus site, the isoforms can differ in their ability to be regulated by phosphorylation (Gillespie et al. 1995). Phosphorylation represents an important mechanism for regulating FGFR activity, for this reason these variants, FGFR-PS+ and FGFR-PS- may function differently in addition to being expressed differently. To date there is no evidence in the literature for a differential role of these isoforms (PS+ and PS-) during mesoderm induction specifically or during development in general.

4.2.2 Analysis of α-FGFR1 and β-FGFR1 Forms.

The expression analysis of the FGFR1 variants that differ in their number of immunoglobulin-like (Ig-like) domains, the α-form (3 Ig-like domains) and the β-form (2 Ig-like domains) is of interest because they may also differ in their ligand binding specificities and affinities. The second Ig loop, the linking sequence and the NH_2 terminus of the third Ig loop comprise the minimal structural requirement for the binding of FGF family ligands in general. The COOH-terminus of the alternatively spliced third Ig loop determines the specificity for particular FGFs (Wang et al. 1995a; Wang et al. 1995b). It has been demonstrated that human and rat α-FGFR shows an affinity for FGF-1 that is 12.5 % of that of β-FGFR in the presence of heparin and shows no affinity for FGF-1 in the absence of heparin (Shi et al. 1993).

The results of this analysis indicate that both the α-FGFR1 and β-FGFR1 variants are expressed through early development (stages 1-16), however the α-FGFR1 isoform displays a greater than 2.5-fold increase in expression level as compared to the β-FGFR1 isoform during this timeline. By tadpole stages (stages 38-42) the β-FGFR1 variant shows an increase in expression levels approaching that of the α-FGFR1 variant at the same stage of development. The spatial expression pattern results indicated that the α-FGFR1 variant is predominantly expressed in all three spatial zones examined as well as the whole embryo sample.

These results may be a consequence of ligand availability. The α-FGFR1 form may be predominantly expressed during early stage *Xenopus* development in response to the presence of FGFs that preferentially bind α-FGFR1. As development stages progress and

additional FGFs begin to accumulate, the β-FGFR1 form may be up regulated to respond to these new ligands. In evaluating the concept of differential expression of α- and β-FGFR1 in the early stages of *Xenopus* development being related to ligand preference and availability, a review of current literature is required. Presently, *Xenopus* homologues of FGFs 2, 3, 4, 8, 9 and 20 have been shown to exist and their expression patterns documented (Isaacs et al. 1992; Kimelman et al. 1988; Kiefer et al. 1993; Slack and Isaacs 1989; Tannahill et al. 1992; Kimelman and Kirschner 1987; Song and Slack 1996; Slack et al. 1996; Christen and Slack 1997; Koga et al. 1999), these are summarized in Table 4.2. Unfortunately, little information seems to have been published in the literature to-date regarding α- or β-FGFR binding specificity of the *Xenopus* homologues, with the sole exception of XFGF3. XFGF3 has been shown to interact with α–XFGFR2 IIIb and IIIc isoforms with high affinity and are suggested to be the most likely partner for XFGF3 at physiological conditions (Mathieu et al. 1995). The same report (Mathieu et al. 1995) also showed that XFGF3 affinities for mouse α- and β-FGFR2-IIIc were very similar, which contrasts results by Shi et al. (1993) that reports FGF1 has an 8-fold higher affinity for β-FGFR1 than for α-FGFR1.

All six of the known *Xenopus* FGF homologues are present from gastrulation (stage 12) to neurula (stage 16) (referenced in Table 4.2), the timeframe in which we have reported α-FGFR1 as the predominant transcript. This could suggest that the α-form may be the principle receptor for these ligands. However, XFGF-2, XFGF-4, XFGF-8 and XFGF-20 all display decreased expression later in development when β-FGFR1 is more abundant. This might be suggestive of the β-FGFR1 receptor being the most likely

partner for these FGFs. A decrease in FGF expression occurring concurrently with an increase in FGFR expression, would maintain a likelihood of an FGF-FGFR interaction. Undoubtedly, further research into the binding affinities between these prospective ligand-receptor partnerships will be required.

Table 4.2: Documented Expression Patterns of *Xenopus* FGF Homologues.

Xenopus FGF homologue	Expression	Reference(s)
XFGF-2	abrupt increase at MBT and maintains a stable level through gastrulation and neurulation.	Kimelman et al. 1988; Kimelman and Kirschner 1987
XFGF-3	expressed just before the onset of gastrulation through to pre-larval stages.	Tannahill et al. 1992
XFGF-4	sharp increase at onset of gastrulation and falls after stage 12.	Isaacs et al. 1992
XFGF-8	first strong expression in early gastrula, persists into late neurula, decreases at early tailbud, further decrease at late tailbud.	Christian and Slack 1997
XFGF-9	detected from early cleavage (indicative of maternal expression), detected at neurula and tailbud stages as zygotically expressed.	Song and Slack 1996
XFGF-20	initial detection at blastula, strongest intensity at gastrula, decreases a neurula and continues to decrease subsequently.	Koga et al. 1999

4.3 Future Considerations

4.3.1 In Investigating the Abnormal Phenotype Presented in Embryos overexpressing FGFR-VT+.

This project has many different directions it can follow as a means to accomplishing the goal of uncovering the molecular basis of the observed abnormal phenotype in FGFR-VT+ overexpressing embryos. Presented here are some of the methodologies that might be considered in continuing this project.

Characterization of the stock FGFR1 cRNAs was conducted using an *in vitro* translation system. While this provided a measurement of translation in an *in vitro* system, it does not provide any information on how efficiently the message will be translated *in vivo*. A subsequent check could have been conducted using a myc-tagged construct which could be injected into embryos, total embryo protein could then be extracted from the sample extract and subjected to western analysis using an anti-myc antibody to determine the efficiency of *in vivo* translation.

An initial step that might be considered in future work on the marker analysis is to increase the pool of markers being analyzed. For obvious reasons, increasing the test pool would increase the likelihood of uncovering a gene misexpression pattern. Some markers that might be considered include: *chordin* a gene whose expression can be activated by organizer-specific homeobox genes and which is initially expressed in the dorsal lip and subsequently tissues derived from the organizer (Sasai et al. 1994); Xnr3, is member of the TGF-β superfamily that is expressed specifically in the Spemann organizer (Smith et al. 1995); Xnot, a homeobox gene that is initially expressed throughout the embryo but whose expression becomes restricted to the organizer region

and presumptive mesoderm as development proceeds, transcription peaks at the onset of gastrulation, show a marked decrease by the end of gastrulation but remain detectable into tailbud stages (von Dassow et al. 1993); Xcad3 is an immediate early target of the FGF-signaling pathway that is required for normal posterior development in *Xenopus* embryos (Isaacs et al. 1998).

An additional consideration in determining what other markers to study might be to conduct histological analysis on the embryos presenting the abnormal phenotype in an effort to elucidate what tissues may be missing or deformed. Observing the phenotype in conjunction with such a histological analysis may aid in the selection of additional markers to screen. As some of the FGFR-VT+ overexpressing embryos are observed to have what could be described as a "kink" in the spine or tail region. It is conceivable that this phenotype results from a disruption in a pathway that regulates bone/cartilage or somite development. This phenotypic observation and a histological analysis may provide evidence for selecting different sets of candidate molecules for analysis, such as: Xmyf-5 a gene expressed in dorsolateral marginal zone in early gastrula and is later found in the most dorsal and ventral tips of the somites (Hopwood et al. 1991); XmyoD, zygotic expression of XmyoD begins in early gastrula. XmyoD is shown to be restricted to the gastrula mesoderm and to the somites of neurulae and tailbud embryos. Transcription is activated following mesoderm induction, and XmyoD is early muscle-specific response to mesoderm-inducing factors (Hopwood et al. 1989). The intital activation of MyoD transcription has been shown to require eFGF (*Xenopus* homologue of FGF4) (Fisher et al. 2002).

RT-PCR offered a means of analyzing a large set of samples in a relatively short period. We analyzed eight known molecular marker expression patterns in three different embryo injection sets (FGFR-VT-, FGFR-VT+ and DEPC-H_2O) through four stages of development. As previously mentioned, additional methodologies might be employed to further examine this set of molecular markers. These could include, but are not limited to, northern blot analysis, RNase protection assay and whole mount *in situ* hybridization. Northern blot analysis can be used to determine the size and amount of any specific RNA and therefore represents another means of studying the collected RNA pools. RNase protection is a sensitive technique used for the quantitation of specific RNA from total cellular RNA and represents another method of studying the given RNA pool. The northern blot and RNase protection assays may suffer from the same potential problem as RT-PCR for the pooled RNA samples. Therefore whole mount *in situ* hybridization may be the preferred methodology of choice. The whole mount *in situ* hybridization protocol is more detailed and time consuming than that of RT-PCR, in that it requires the synthesis of a specifically labeled nucleic acid probe, which has to then be hybridized to cellular RNA. However, it would provide a method of analyzing both temporal (stage of development) and spatial (location within the embryo) expression patterns. An additional advantage to whole mount *in situ* hybridization is that it permits analysis of individual embryos as opposed to a sample collected from a pool of several embryos.

We have been focusing our analysis at the RNA level, another consideration in future direction of this project might be to look at the proteins encoded by the RNA. Western blot analysis of total protein samples from the same type of embryo injection sets as used

in this project could yield some findings of interest. Whole mount antibody staining for the products of the molecular marker genes analyzed represents another means of focusing on the protein level as opposed to RNA levels and permits observation of spatial and temporal expression patterns in individual embryos.

Fibroblast growth factor receptor signal transduction, like other receptor tyrosine kinases, results in the activation of several intracellular signaling pathways, such as, the phosphatidylinositol 3'-kinase (PI3'K) pathway, the phospholipase C gamma 1 (PLCγ1) pathway and the Ras/MAP kinase pathway (Ryan et al. 1998; Huang et al. 1995; Umbhauer et al. 2000). Using methodologies to analyze an embryo sample for proteins known to be phosphorylated (activated) in these pathways via FGFR1 signaling, such as MAP kinases for which phospho-specific antibodies are available, one could narrow the potential search field by determining the precise pathway(s) involved.

These pathways might also be a consideration for a VT+ rescue experiment. Such an experiment would be designed to determine if activation of the FGF-FGFR signaling pathway, initiated at a point below the receptor could rescue embryos overexpressing the FGFR-VT+ form of the receptor to develop with a normal phenotype.

4.3.2 In Analyzing FGFR-PS+ and FGFR-PS- Variant Forms.

In continuing investigation into the characterization of the FGFR-PS+ and FGFR-PS- receptor forms, a similar approach to that taken by Gillespie et al. (1995) might be utilized. Analysis to determine if the predicted phosphorylation site (Ser^{443}) is in fact phosphorylated will be required. A strategy that could be used to investigate this

possibility would be to immunoprecipitate the FGFR1 from whole embryos under non-denaturing conditions and follow this with Western blotting employing an antibody that recognizes phosphoserine (eg., monoclonal Anti-Phosphoserine available from Sigma). Should it be shown that Ser^{443} is indeed phosphorylated *in vivo*, subsequent functional assays would be required to ascertain any functional differences between the isoforms due to the presence or absence of this residue.

4.3.3 In Analyzing the α-FGFR1 and β-FGFR1 Forms.

In further evaluating the concept of differential expression of α- and β- XFGFR1 being related to ligand preference and availability in the early stages of *Xenopus* development, binding assays should be conducted to determine if the isoforms display any preference for particular Xenopus FGFs. As the PCR analysis conducted for this project distinguished only between α- and β- XFGFR1, additional analysis to distinguish between the α-XFGFR1-IIIb and IIIc forms and between β-XFGFR1-IIIb and IIIc forms might he an important consideration. Finally, injection experiments using *in vitro* synthesized cRNA of the α- and β- XFGFR isoforms could be undertaken to determine, if any, the developmental effects of overexpressing the α- or the β-XFGFR isoforms in *Xenopus* embryos. As the results presented in this thesis suggest that α-FGFR is the predominantly expressed isoform through early development, the effect of overexpressing the β-form might be of some significance. Hypothetically speaking, if the α-form is the functional form during early development, overexpressing the β-form might saturate the system, resulting in primarily α-β heterodimeric complexes instead of

functional α-α homodimeric complexes. If this was the case, one might expect to observe developmental abnormalities in the β-FGFR overexpressing embryos.

While investigated as individual isoforms, it is important to point out that the variations discussed may occur in any number of combinations, such as α-FGFR-IIIc/VT+/PS- or β-FGFR-IIIb/VT-/PS+, for example. Currently, it is not known which particular combinations are expressed during development. However, this represents an important question for further research as differential expression of such receptor isoforms may provide a more precise means of regulating developmental events.

Chapter 5
References

Agius, E., M. Oelgeschläger, O. Wessely, C. Kemp, and E. De Robertis. 2000. Endodermal Nodal-related signals and mesoderm induction in *Xenopus*. Development **127**: 1173-1183.

Alberts, B. 1994 Molecular Biology of the Cell, third edition. Garland Publishing, Inc., New York, USA.

Amaya, E., T. Musci, and M. Kirschner. 1991. Expression of a dominant negative mutant of the FGF receptor disrupts mesoderm formation in *Xenopus* embryos. Cell **66**: 257-270.

Amaya, E., P. Stein, T. Musci, and M. Kirschner. 1993. FGF signalling in the early specification of mesoderm in *Xenopus*. Development **118**: 477-487.

Avivi, A., Y. Zimmer, A. Yayon, Y. Yarden, and D. Givol. 1991. Flg-2, a new member of the family of fibroblast growth factor receptors. Oncogene **6**: 1089-1092.

Baird, A. and M. Klagsbrun. 1991. Nomenclature meeting report and recommendations January 17, 1991. Annals of the New York Academy of Sciences **638**: xiii-xvi.

Basilico, C. and D. Moscatelli. 1992. The FGF family of growth factors and oncogenes. Advances in Cancer Research **59**: 115-165.

Beer, H., L. Vindevoghel, M. Gait, J. Revest, D. Duan, I. Mason, C. Dickson, and S. Werner. 2000. Fibroblast growth factor (FGF) receptor 1 IIIb is a naturally occurring functional receptor for FGFs that is preferentially expressed in the skin and the brain. Journal of Biological Chemistry **275**: 16091-16097.

Blom, N., S. Gammeltoff, and S. Brunak. 1999. Sequence- and structure-based prediction of eukaryotic protein phosphorylation sites. Journal of Molecular Biology **294**: 1351-1362.

Blumberg, B, CV. Wright, EM. De Robertis, KW. Cho. 1991. Organizer-specific homeobox genes in Xenopus laevis embryos. Science **253(5016):** 194-6.

Boterenbrood, E. and P. Nieuwkoop. 1973. The formation of the mesoderm in Urodelean amphibians. Wilhelm Roux' Archiv fur Entwicklungsmechanik der Organismen **173**: 319-332.

Burgess, W. and T. Maciag. 1989. The heparin-binding (fibroblast) growth factor family of proteins. Annual Review in Biochemistry **58**: 575-606.

Carballada, R., H. Yasuo, and P. Lemaire. 2001. Phosphatidylinositol-3 kinase acts in parallel to the ERK MAP kinase in the FGF pathway during *Xenopus* mesoderm induction. Development **128**: 35-44.

Chellaiah, A., W. Yuan, M. Chellaiah, and D. Ornitz. 1999. Mapping ligand binding domains in chimeric fibroblast growth factor receptor molecules. Journal of Biological Chemistry **274**: 34785-34794.

Cho, K., B. Blumberg, H. Steinbeisser, and E. De Robertis. 1991. Molecular nature of Spemann's Organizer: the role of the Xenopus homeobox gene *goosecoid*. Cell **67**: 1111-1120.

Christen, B. and J. Slack. 1997. FGF-8 is associated with anteroposterior patterning and limb regeneration in *Xenopus*. Developmental Biology **192**: 455-466.

Christian, J., J. McMahon, A. McMahon, and RT. Moon. 1991. *Xwnt-8*, a *Xenopus Wnt-1/int-1*-related gene responsive to mesoderm-inducing growth factors, may play a role in ventral mesodermal patterning during embryogenesis. Development **111**: 1045-1055.

Christian, JL and RT. Moon. 1993. Interactions between Xwnt-8 and Spemann organizer signaling pathways generate dorsoventral pattern in the embryonic mesoderm of *Xenopus*. Genes & Development **7(1)**: 13-28.

Clements, D, RV. Friday, and HR. Woodland. 1999. Mode of action of VegT in mesoderm and endoderm formation. Development **126(21)**: 4903-4911.

Cornell, RA. and D. Kimelman. 1994. Activin-mediated mesoderm induction requires FGF. Development **120(2)**: 453-462.

Cornell, RA., TJ Musci, and D. Kimelman. 1995. FGF is a prospective competence factor for early activin-type signals in *Xenopus* mesoderm induction. Development **121(8)**: 2429-2437.

Coutts, J. and J. Gallagher. 1995. Receptors for fibroblast growth factors. Immunology and Cell Biology **73**: 584-589.

Dale, L., J. Smith, and J. Slack. 1985. Mesoderm induction in *Xenopus laevis*: a quantitative study using a cell lineage label and tissue-specific anitbodies. Journal of Embryology and Experimental Morphology **89**: 289-312.

Dale, L. and J. Slack. 1987. Regional specification within the mesoderm of early embryos of *Xenopus laevis*. Development **100**: 279-295.

Dale, L., G. Howes, B. Price, and J. Smith. 1992. Bone morphogenetic protein 4: a ventralizing factor in early *Xenopus* development. Development **115**: 573-585.

Dale, L. and C. Jones. 1999. BMP signalling in early *Xenopus* development. BioEssays **21**: 751-760.

Dell, KR and LT. Williams. 1992. A novel form of fibroblast growth factor receptor 2. Alternative splicing of the third immunoglobulin-like domain confers ligand binding specificity. Journal of Biological Chemistry **267(29)**: 21225-21229.

DeMarais, AA and RT. Moon. 1992. The *armadillo* homologs *beta-catenin* and *plakoglobulin* are differentially expressed during early development of *Xenopus laevis*. Developmental Biology **153(2)**: 337-346.

Deuchar, E. *XENOPUS: The South African Clawed Frog*, Wiley-Interscience Publication.

Dickson, C., R. Smith, S. Brookes, and G. Peters. 1984. Tumorigenesis by mouse mammary tumor virus: proviral activation of a cellular gene in the common integration region *int-2*. Cell **37**: 529-536.

Dionne, C., G. Crumley, F. Bellot, J. Kaplow, G. Searfoss, M. Ruta, W. Burgess, M. Jaye, and J. Schlessinger. 1990. Cloning and expression of two distinct high-affinity receptors cross-reacting with acidic and basic fibroblast growth factors. EMBO Journal **9**: 2685-2692.

Dirksen, M. and M. Jamrich. 1992. A novel, activin-inducible, blastopore lip-specific gene of *Xenopus laevis* contains a *fork head* DNA-binding domain. Genes & Development **6**: 599-608.

Duan, DS, S. Werner, and LT. Williams. 1992. A naturally occurring secreted form of fibroblast growth factor (FGF) receptor 1 binds basic FGF in preference over acidic FGF. Journal of Biological Chemistry **267(23)**: 16076-16080.

Eisemann, A., J. Ahn, G. Graziani, S. Tronick, and D. Ron. 1991. Alternative splicing generates at least five different isoforms of the human basic-FGF receptor. Oncogene **6**: 1195-1202.

Fedi, P. and S. Aaronson. 2001. Signal transduction through tyrosine kinase growth factor receptors. In *Signaling Networks and Cell Cycle Control: The Molecular Basis of Cancer and Other Diseases.* pp. 27-38.

Fisher ME., HV. Isaacs, ME. Pownall. 2002. eFGF is required for activation of XmyoD expression in the myogenic cell linage of *Xenopus laevis*. Development **129(6)**: 1307-1315.

Forristall, C., M. Pondel, L. Chen, and M. King. 1995. Patterns of localization and cytoskeletal association of two vegetally localized RNAs, *Vg1* and *Xcat-2*. Development **121**: 201-208.

Friesel, R. and I. Dawid. 1991. cDNA cloning and developmental expression of fibroblast growth factor receptors from *Xenopus laevis*. Molecular and Cellular Biology **11**: 2481-2488.

Friesel, R and SA. Brown. 1992. Spatially restricted expression of fibroblast growth factor receptor-2 during *Xenopus* development. Development **116(4)**: 1051-1058.

Gilbert, SF. 1997. Developmental Biology, sixth edition. Sunderland: Sinauer Associates, Incorporated.

Gillespie, L., G. Chen, and G. Paterno. 1995. Cloning of a fibroblast growth factor receptor 1 splice variant from *Xenopus* embryos that lacks a protein kinase C site important for the regulation of receptor activity. The Journal of Biological Chemistry **270**: 22758-22763.

Godsave, S., H. Isaacs, and J. Slack. 1988. Mesoderm-inducing factors: a small class of molecules. Development **102**: 555-566.

Gospodarowicz, D. 1974. Localisation of a fibroblast growth factor and its effect alone and with hydrocortisone on 3T3 cell growth. Nature **249**: 123-127.

Gospodarowicz, D. 1975. Purification of a fibroblast growth factor from bovine pituitary. The Journal of Biological Chemistry **250**: 2515-2520.

Gospodarowicz, D., N. Ferrara, L. Schweigerer, and G. Neufeld. 1987. Structural characterization and biological functions of fibroblast growth factor. Endocrine Reviews **8**: 95-114.

Graff, JM, RS. Thies, JJ. Song, AJ. Celeste, and DA. Melton. 1994. Studies with a *Xenopus* BMP receptor suggest that ventral mesoderm-inducing signals override dorsal signals *in vivo*. Cell **79(1)**: 169-179.

Heasman, J, D. Ginsberg, B. Geiger, K. Goldstone, T. Pratt, C. Yoshida-Noro, and C. Wylie. 1994. A functional test for maternally inherited cadherin in *Xenopus* shows its importance in cell adhesion at the blastula stage. Development **120(1):** 49-57.

Herrmann, BG, S. Labeit, A. Poustka, TR. King, and H. Lehrach. 1990. Cloning the T gene required in mesoderm formation in the mouse. Nature **343**: 617-622.

Hoppler, S., J. Brown, and R. Moon. 1996. Expression of a dominant-negative Wnt blocks induction of MyoD in *Xenopus* embryos. Genes & Development **10**: 2805-2817.

Hopwood, N. 1990. Cellular and genetic responses to mesoderm induction in *Xenopus*. BioEssays **12**: 465-471.

Hopwood ND., A. Pluck, JB Gurdon. 1989. MyoD expression in the forming somintes is an early response to mesoderm induction in *Xenopus* embryos. EMBO J **8(11)**: 3409-3417.

Hopwood ND., A. Pluck, JB Gurdon. 1991. *Xenopus* Myf-5 marks early muscles ccll and can activate muscle genes ectopically in early embryos. Development **111**: 551-560.

Hoshikawa, M., N. Ohbayashi, A. Yonamine, M. Konishi, K. Ozaki, S. Fukui, and N. Itoh. 1998. Structure and expression of a novel fibroblast growth factor, FGF-17, preferentially expressed in the embryonic brain. Biochemical and Biophysical Research Communications **244**: 187-191.

Houssaint, E., P. Blanquet, P. Champion-Arnaud, M. Gesnel, A. Torriglia, Y. Courtois, and R. Breathnach. 1990. Related fibroblast growth factor receptor genes exist in the human genome. Proceedings of the National Academy of Science, USA **87**: 8180-8184.

Huang, J., M. Mohammadi, G. Rodrigues, and J. Schlessinger. 1995. Reduced activation of RAF-1 and MAP kinase by a fibroblast growth factor receptor mutant deficient in stimulation of phosphatidylinositol hydrolysis. Journal of Biological Chemistry **270**: 5065-5072.

Imamura, T, K. Engleka, X. Zhan, Y. Tokita, R. Forough, D. Roeder, A. Jackson, JA. Maier, T. Hla, and T. Maciag. 1990. Recovery of mitogenic activity of a growth factor mutant with a nuclear translocation sequence. Science **249**: 1567-1570.

Innis, M. and D. Gelfand. 1990. Optimization of PCRs. In *PCR Protocols: A guide to methods and applications.* (ed. M.Innis, D.Gelfand, J.Sninsky, and T.White), pp. 3-12. Academic Press, Inc., San Diego.

Isaacs, HV., D. Tannahill, and J. Slack. 1992. Expression of a novel FGF in the *Xenopus* embryo. A new candidate inducing factor for mesoderm formation and anteroposterior specification. Development **114**: 711-720.

Isaacs, HV., M. Pownall, and J. Slack. 1994. eFGF regulates *Xbra* expression during *Xenopus* gastrulation. The EMBO Journal **13**: 4469-4481.

Isaacs, H. 1997. New perspectives on the role of the fibroblast growth factor family in amphibian development. Cellular and Molecular Life Sciences **53**: 350-361.

Isaacs, HV., ME. Pownall, JM. Slack. 1998. Regulation of Hox gene expression and posterior development by the *Xenopus* caudal homologue Xcad3. ENMB J **17(12)**: 3413-3427.

Jaye, M, R. Howk, WH. Burgess, G. Ricca, IM. Chiu, MW. Ravera, SJ O'Brien, WS. Modi, T. Maciag, and W. Drohan. 1986. Human endothelial cell growth factor: cloning, nucleotide sequence, and chromosome localization. Science **233**: 541-545.

Jaye, M., J. Schlessinger, and C. Dionne. 1992. Fibroblast growth factor receptor tyrosine kinases: molecular analysis and signal tranduction. Biochemica et Biophysica Acta **1135**: 185-199.

Johnson, D., P. Lee, J. Lu, and L. Williams. 1990. Diverse forms of a receptor for acidic and basic fibroblast growth factors. Molecular and Cellular Biology **10**: 4728-4736.

Johnson, D. and L. Williams. 1993. Structural and functional diversity in the FGF receptor multigene family. Advances in Cancer Research **60**: 1-41.

Jones, C., K. Lyons, P. Lapan, C. Wright, and B. Hogan. 1992. DVR-4 (Bone Morphogenetic Protein-4) as a posterior-ventralizing factor in *Xenopus* mesoderm induction. Development **115**: 639-647.

Jones, C. and J. Smith. 1999. An overview of *Xenopus* development. Methods in Molecular Biology **97**: 331-340.

Keller, R, J. Shih, A. Sater, and C. Moreno. 1992. Planar induction of convergence and extension of the neural plate by the organizer of *Xenopus*. Developmental Dynamics **193(3)**: 218-234.

Kennelly, P. and E. Krebs. 1991. Consensus sequences as substrate specificity determinants for protein kinases and protein phosphatases. Journal of Biological Chemistry **266**: 15555-15558.

Kessler, D. and D. Melton. 1994. Vertebrate embryonic induction: mesodermal and neural patterning. Science **266**: 596-604.

Kiefer, P., M. Mathieu, M. Close, G. Peters, and C. Dickson. 1993. FGF3 from *Xenopus laevis*. EMBO Journal **12**: 4159-4168.

Kimelman, D. and M. Kirschner. 1987. Synergistic induction of mesoderm by FGF and TGF-β and the identification of an mRNA coding for FGF in the early *Xenopus* embryo. Cell **51**: 869-877.

Kimelman, D, MW. Kirschner, and T. Scherson. 1987. The events of the midblastula transition in Xenopus are regulated by changes in the cell cycle. Cell **48(3)**: 399-407.

Kimelman, D., J. Abraham, T. Haaparanta, T. Palisi, and M. Kirschner. 1988. The presence of fibroblast growth factor in the frog egg: its role as a natural mesoderm inducer. Science **242**: 1053-1056.

Kofron, M., T. Demel, J. Xanthos, J. Lohr, B. Sun, H. Sive, S. Osada, C. Wright, C. Wylie, and J. Heasman. 1999. Mesoderm induction in *Xenopus* is a zygotic event regulated by maternal VegT via TGF-β growth factors. Development **126**: 5759-5770.

Koga, C., N. Adati, K. Nakata, K. Mikoshiba, Y. Furuhata, S. Sato, H. Tei, Y. Sakaki, T. Kurokawa, K. Shiokawa, and K. Yokoyama. 1999. Characterization of a novel member of the FGF family, XFGF-20, in *Xenopus laevis* . Biochemical and Biophysical Research Communications **261**: 756-765.

Kornbluth, S., K. Paulson, and H. Hanafusa. 1988. Novel tyrosine kinase identified by phosphotyrosine antibody screening of cDNA libraries. Molecular and Cellular Biology **8**: 5541-5544.

Koster, M, S. Plessow, JH. Clement, A. Lorenz, H. Tiedemann, W. Knochel. 1991. Bone morphogenetic protein 4 (BMP-4), a member of the TGF-beta family, in early embryos of Xenopus laevis: analysis of mesoderm inducing activity. Mechanisms of Development **33(3)**: 191-9.

LaBonne, C. and M. Whitman. 1994. Mesoderm induction by activin requires FGF-mediated intracellular signals. Development **120**:463-472.

LaBonne C., B. Burke, M. Whitman. 1995. Role of MAP kinase in mesoderm induction and axial patterning during *Xenopus* development. Development **121(5):** 1475-1486.

Larabell, CA, M. Torres, BA. Rowning, C. Yost, JR. Miller, M. Wu, D. Kimelman, and RT. Moon. 1997. Establishment of the dorso-ventral axis in *Xenopus* embrys is presaged by early asymmetries in *beta-catenin* that are modulated by the Wnt signaling pathway. Journal of Cell Biology **136(5)**: 1123-1136.

Lee, P., D. Johnson, L. Cousens, V. Fried, and L. Williams. 1989. Purification and complementary DNA cloning of a receptor for basic fibroblast growth factor. Science **245**: 57-60.

Lemaire, P, S. Darras, D. Caillol, and L. Kodjabachian. 1998. A role for the vegetally expressed *Xenopus* gene *Mix.1* in endoderm formation and in the restriction of mesoderm to the marginal zone. Development **125(13)**: 2371-2380.

Lewin, B. 2000. Genes VII. Oxford University Press. New York.

Marics, I., J. Adelaide, F. Raybaud, M. Mattei, F. Coulier, J. Planche, O. de Lapeyriere, and D. Birnbaum. 1989. Characterization of the *HST*-related *FGF.6* gene, a new member of the fibroblast growth factor gene family. Oncogene **4**: 335-340.

Mathieu, M., P. Kiefer, I. Mason, and C. Dickson. 1995. Fibroblast growth factor (FGF) 3 from *Xenopus laevis* (XFGF3) binds with high affinity to FGF receptor 2. Journal of Biological Chemistry **270**: 6779-6787.

McWhirter, J., M. Goulding, J. Weiner, J. Chun, and C. Murre. 1997. A novel fibroblast growth factor gene expressed in the developing nervous system is a downstream target of the chimeric homeodomain oncoprotein E2A-Pbx1. Development **124**: 3221-3232.

Mead, PE, IH. Brivanlou, CM. Kelley, and LI. Zon. 1996. BMP-4-responsive regulation of dorsal-ventral patterning by the homeobox protein Mix.1. Nature **382**: 357-360.

Miyake, A., M. Konishi, F. Martin, N. Hernday, K. Ozaki, S. Yamamoto, T. Mikami, T. Arakawa, and N. Itoh. 1998. Structure and expression of a novel member, FGF-16, of the fibroblast growth factor family. Biochemical and Biophysical Research Communications **243**: 148-152.

Miyamoto, M., K. Naruo, C. Seko, S. Matsumoto, T. Kondo, and T. Kurokawa. 1993. Molecular cloning of a novel cytokine cDNA encoding the ninth member of the fibroblast growth factor family, which has a unique secretion property. Molecular and Cellular Biology **13**: 4251-4259.

Molenaar, M, M. van de Wetering, M. Oosterwegel, J. Peterson-Maduro, SF. Godsave, V. Korinek, J. Roose, O. Destree, and H. Clevers. 1996. *XTcf-3* transcription factor mediates beta-catenin-induced axis formation in *Xenopus* embryos. Cell **86(3)**: 391-399.

Moscatelli, D. 1987. High and low affinity binding sites for basic fibroblast growth factor on cultured cells: absence of a role for low affinity binding in the stimulation of plasminogen activator production by bovine capillary endothelial cells. Journal of Cell Physiology **131(1)**: 123-130.

Musci, T., E. Amaya, and M. Kirschner. 1990. Regulation of the fibroblast growth factor receptor in early *Xenopus* embryos. Proceedings of the National Academy of Science, USA **87**: 8365-8369.

Nakatake, Y., M. Hoshikawa, T. Asaki, Y. Kassai, and N. Itoh. 2001. Identification of a novel fibroblast growth factor, FGF-22, preferentially expressed in the inner root sheath of the hair follicle. Biochimica et Biophysica Acta **1517**: 460-463.

Newport, J and MW. Kirschner. 1982. A major developmental transition in early Xenopus embryos: I. characterization and timing of cellular changes at the midblastula stage. Cell **30(3):** 675-686.

Niehrs, C., H. Steinbeisser, and E. De Robertis. 1994. Mesodermal patterning by a gradient of the vertebrate homeobox gene *goosecoid*. Science **263**: 817-820.

Nieuwkoop, PD. 1969. The formation of the mesoderm in urodele amphibians. I. Induction by the endoderm. Wilhelm Roux Arch.Entw.Org. **162**: 341-373.

Nieuwkoop, PD. and J. Faber. 1967. Normal table of *Xenopus laevis (Daudin)*. A systematical and chronological survey of the development from the fertilized egg till the end of metamorphosis. Amsterdam: North-Holland Publishing Company.

Nishimatsu, S., A. Suzuki, A. Shoda, K. Murakami, and N. Ueno. 1992. Genes for bone morphogenetic proteins are differentially transcribed in early amphibian embryos. Biochemical and Biophysical Research Communications **186**: 1487-1495.

Nishimura, T., Y. Nakatake, M. Konishi, and N. Itoh. 2000. Identification of a novel FGF, FGF-21, preferentially expressed in the liver. Biochimica et Biophysica Acta **1492**: 203-206.

Ohbayashi, N., M. Hoshikawa, S. Kimura, M. Yamasaki, S. Fukui, and N. Itoh. 1998. Structure and expresion of the mRNA encoding a novel fibroblast growth factor, FGF-18. The Journal of Biological Chemistry **273**: 18161-18164.

Ohmachi, S., Y. Watanabe, T. Mikami, N. Kusu, T. Ibi, A. Akaike, and N. Itoh. 2000. FGF-20, a novel neurotrophic facto, preferentially expressed in the substantia nigra pars compacta of rat brain. Biochemical and Biophysical Research Communications **277**: 355-360.

Ornitz, D., J. Xu, J. Colvin, D. McEwen, C. MacArthur, F. Coulier, G. Gao, and M. Goldfarb. 1996. Receptor specificity of the fibroblast growth factor family. The Journal of Biological Chemistry **271**: 15292-15297.

Ozawa, M, H. Baribault, and R. Kemler. 1989. The cytoplasmic domain of the cell adhesion molecule uvomorulin associates with three independent proteins structurally related in different species. EMBO Journal **8(6)**: 1711-1717.

Padgett, RW, RD. St Johnston, and WM. Gelbart. 1987. A transcript from a *Drosophila* pattern gene predicts a protein homologous to the transforming growth factor-beta family. Nature **325**: 81-84.

Partanen, J., T. Makela, E. Eerola, J. Korhonen, H. Hirvonen, L. Claesson-Welsh, and K. Alitalo. 1991. FGFR-4, a novel acidic fibroblast growth factor receptor with a distinct expression pattern. EMBO Journal **10**: 1347-1354.

Pasquale, E. and S. Singer. 1989. Identification of a developmentally regulated protein-tyrosine kinase by using anti-phosphotyrosine antibodies to screen a cDNA expression library. Proceedings of the National Academy of Science, USA **86**: 5449-5453.

Pasquale, E. 1990. A distinctive family of embryonic protein-tyrosine kinase receptors. Proceedings of the National Academy of Science, USA **87**: 5812-5816.

Paterno, G., P. Ryan, K. Kao, and L. Gillespie. 2000. The VT+ and VT- isoforms of the fibroblast growth factor receptor type 1 are differentially expressed in the presumptive mesoderm of *Xenopus* embryos and differ in their ability to mediate mesoderm formation. The Journal of Biological Chemistry **275**: 9581-9586.

Powers, C., S. McLeskey, and A. Wellstein. 2000. Fibroblast growth factors, their receptors and signaling. Endocrine-Related Cancer **7**: 165-197.

Pownall ME., AS. Tucker, JM. Slack, HV. Isaacs. 1996. eFGF, Xcad3 and Hox genes form a molecular pathway that establishes the anteroposterior axis in *Xenopus*. Development **122(12)**: 3881-3892.

Rebagliati, MR, DL. Weeks, RP. Harvey, and DA. Melton. 1985. Identification and cloning of localized maternal RNAs from *Xenopus* eggs. Cell **42(3)**: 769-777.

Rosa, F., A. Roberts, D. Danielpour, L. Dart, M. Sporn, and I. Dawid. 1988. Mesoderm induction in amphibians: the role of TGF-β2- like factors. Science **239**: 783-785.

Rosa, F. 1989. *Mix.1*, a homeobox mRNA inducible by mesoderm inducers, is expressed mostly in the presumptive endodermal cells of Xenopus embryos. Cell **57**: 965-974.

Rubin, J., H. Osada, P. Finch, W. Taylor, S. Rudikoff, and S. Aaronson. 1989. Purification and characterization of a newly identified growth factor specific for epithelial cells. Proceedings of the National Academy of Science, USA **86**: 802-806.

Ruta, M., R. Howk, G. Ricca, W. Drohan, M. Zabelshansky, G. Laureys, D. Barton, U. Francke, J. Schlessinger, and D. Givol. 1988. A novel protein tyrosine kinase gene

whose expression is modulated during endothelial cell differentiation. Oncogene **3**: 9-15.

Ruta, M., W. Burgess, J. Epstein, N. Neiger, J. Kaplow, G. Crumley, C. Dionne, M. Jaye, and J. Schlessinger. 1989. Receptor for acidic fibroblast growth factor is related to the tyrosine kinase encoded by the *fms*-like gene (FLG). Proceedings of the National Academy of Science, USA **86**: 8722-8726.

Ryan, P., G. Paterno, and L. Gillespie. 1998. Identification of phosphorylated proteins associated with the fibroblast growth factor receptor type 1 during early *Xenopus* Development. Biochemical and Biophysical Research Communications **244**: 763-767.

Saiki, R. 1989. The design and optimization of the PCR. In *PCR Technology: Principles and applications for DNA amplification.* (ed. H.Erlich), pp. 7-16. Stockton Press, New York.

Sakamoto, H., M. Mori, M. Taira, T. Yoshida, S. Matsukawa, K. Shimizu, M. Sekiguchi, M. Terada, and T. Sugimura. 1986. Transforming gene from human stomach cancers and a noncancerous portion of stomach mucosa. Proceedings of the National Academy of Science, USA **83**: 3997-4001.

Sasai, Y, B. Lu, H. Steinbeisser, D. Geissert, L. Gont, and EM. De Robertis. 1994. *Xenopus* chordin: a novel dorsalizing factor activated by organizer-specific homeobox genes. Cell **79(5)**: 779-790.

Sato, S. and T. Sargent. 1991. Localized and inducible expression of *Xenopus-posterior* (*Xpo*), a novel gene active in early frog embryos, encoding a protein with a 'CCHC' finger domain. Development **112**: 747-753.

Schulte-Merker, S, JC. Smith, and L. Dale. 1994. Effects of truncated activin and FGF receptors and of follistatin on the inducing activities of BVg1 and activin: does activin play a role in mesoderm induction? EMBO Journal **13(15)**: 3533-3541.

Schulte-Merker, S and JC. Smith. 1995. Mesoderm formation in response to *Brachyury* requires FGF signalling. Current Biology **5**: 62-67.

Shi, E., M. Kan, J. Xu, F. Wang, J. Hou, and W. McKeehan. 1993. Control of fibroblast growth factor receptor kinase signal transduction by heterodimerization of combinatorial splice variants. Molecular and Cellular Biology **13**: 3907-3918.

Shiozaki, C, K. Tashiro, M. Asano-Miyoshi, K. Saigo, Y. Emori, and K. Shiokawa. 1995. Cloning of cDNA and genomic DNA encoding fibroblast growth factor receptor-4 of *Xenopus laevis*. Gene **152(2)**: 215-219.

Slack, J. and D. Forman. 1980. An interaction between dorsal and ventral regions of the marginal zone in early amphibian embryos. Journal of Embryology and Experimental Morphology **56**: 283-299.

Slack, J., L. Dale, and J. Smith. 1984. Analysis of embryonic induction by using cell lineage markers. Philosophical Transactions of the Royal Society of London **B 307**: 331-336.

Slack, J., B. Darlington, J. Heath, and S. Godsave. 1987. Mesoderm induction in early *Xenopus* embryos by heparin-binding growth factors. Nature **326**: 197-200.

Slack, J., H. Isaacs, and B. Darlington. 1988. Inductive effects of fibroblast growth factor and lithium ion on *Xenopus* blastula ectoderm. Development **103**: 581-590.

Slack, J. and H. Isaacs. 1989. Presence of basic fibroblast growth factor in the early *Xenopus* embryo. Development **105**: 147-153.

Slack, J. 1991. The nature of the mesoderm-inducing signal in *Xenopus*: a transfilter induction study. Development **113**: 661-669.

Slack, J., H. Isaacs, J. Song, L. Durbin, and M. Pownall. 1996. The role of fibroblast growth factors in early *Xenopus* development. Biochem Soc Symp **62**: 1-12.

Smallwood, P., I. Munoz-Sanjuan, P. Tong, J. Macke, S. Hendry, D. Gilbert, N. Copeland, N. Jenkins, and J. Nathans. 1996. Fibroblast growth factor (FGF) homologous factors: new members of the FGF family implicated in nervous system development. Proceedings of the National Academy of Science, USA **93**: 9850-9857.

Smith, J. and J. Slack. 1983. Dorsalization and neural induction: properties of the organizer in *Xenopus laevis*. Journal of Embryology and Experimental Morphology **78**: 299-317.

Smith, J. 1987. A mesoderm-inducing factor is produced by a *Xenopus* cell line. Development **99**: 3-14.

Smith, JC, M. Yaqoob, and K. Symes. 1988. Purification, partial characterization and biological effects of the XTC mesoderm-inducing factor. Development **103(3)**: 591-600.

Smith, J., J. Cooke, J. Green, G. Howes, and K. Symes. 1989. Inducing factors and the control of mesodermal pattern in *Xenopus laevis*. Development (Supplement) **1989 Supplement**: 149-159.

Smith, JC, BMJ. Price, K. Van Nimmen, and D. Huylebroeck. 1990. Identification of a potent *Xenopus* mesoderm-inducing factor as a homologue of activin A. Nature **354**: 729-731.

Smith, J., B. Price, J. Green, D. Weigel, and B. Herrmann. 1991. Expression of a Xenopus homolog of *Brachyury* (T) is an immediate-early response to mesoderm induction. Cell **67**: 79-87.

Smith, W. and R. Harland. 1992. Expression cloning of noggin, a new dorsalizing factor localized to the Spemann Organizer in Xenopus embryos. Cell **70**: 829-840.

Smith, WC, AK. Knecht, M. Wu, and RM. Harland. 1993. Secreted noggin protein mimics the Spemann organizer in dorsalizing *Xenopus* mesoderm. Nature **361**: 547-549.

Smith, W., R. McKendry, S. Ribisi, and R. Harland. 1995. A *nodal*-related gene defines a physical and functional domain within the Spemann organizer. Cell **82**: 37-46.

Song, J. and J. Slack. 1996. XFGF-9: a new fibroblast growth factor from *Xenopus* embros. Developmental Dynamics **206**: 427-436.

Sudarwati, S. and P. Nieuwkoop. 1971. Mesoderm formation in the anuran *Xenopus laevis* (Daudin). Wilhelm Roux' Archiv fur Entwicklungsmechanik der Organismen **166**: 189-204.

Sun, BI, SM. Bush, LA. Collins-Racie, ER. LaVallie, EA. DiBlasio-Smith, NM. Wolfman, JM. McCoy, and H. Sive. 1999. *derriere*: a TGF-beta family member required for posterior development in *Xenopus*. Development **126(7)**: 1467-1482.

Tanaka, A., K. Miyamoto, N. Minamino, M. Takeda, B. Sato, H. Matsuo, and K. Matsumoto. 1992. Cloning and characterization of an androgen-induced growth factor essential for the androgen-dependent growth of mouse mammary carcinoma cells. Proceedings of the National Academy of Science, USA **89** : 8928-8932.

Tannahill, D., H. Isaacs, M. Close, G. Peters, and J. Slack. 1992. Developmental expression of the *Xenopus* int-2 (FGF-3) gene: activation by mesodermal and neural induction. Development **115**: 695-702.

Technau, U. 2001. *Brachyury*, the blastopore and the evolution of the mesoderm. BioEssays **23**: 788-794.

Thomsen, GH and DA. Melton. 1993. Processed Vg1 protein is an axial mesoderm inducer in *Xenopus*. Cell **74(3)**: 433-441.

Tiedemann H, M. Asashima, H. Grunz, and W. Knochel 2001. Pluripotent cells (stem cells) and their determination and differentiation in early vertebrate embryogenesis. Development Growth and Differentiation **43(5):** 469-502.

Turner, PC. and HR. Woodland. 1982. H3 and H4 histone cDNA sequences from Xenopus: a sequence comparison of H4 genes. Nucleic Acids Research **10(12):** 3769-80.

Ullrich, A. and J. Schlessinger. 1990. Signal transduction by receptors with tyrosine kinase activity. Cell **61**: 203-212.

Umbhauer, M. CJ. Marshall, CS. Mason, RW. Old and JC. Smith. 1995. Mesoderm induction in *Xenopus* caused by activation of MAP kinase. Nature **376 (6535):** 58-62.

Umbhauer, M., A. Penzo-Mendez, L. Clavilier, J. Boucaut, and J. Riou. 2000. Signaling specificities of fibroblast growth factor receptors in early *Xenopus* embryo. Journal of Cell Science **113**: 2865-2875.

Vanhaesebroeck, B., SJ. Leevers, G. Panayotou, and MD. Waterfield. 1997. Phosphoinositide 3-kinases: a conserved family of signal transducers. Trends in Bichemical Sciences **22**: 267-272.

van der Geer, P., T. Hunter, and R. Lindberg. 1994. Receptor protein-tyrosine kinases and their signal transduction pathways. Annual Review in Cell Biology **10**: 251-337.

Vincent, JP and J. Gerhart. 1987. Subcortical rotation in *Xenopus* eggs: an early step in embryonic axis specification. Developmental Biology **123(2)**: 526-539.

von Dassow, G., J. Schmidt, and D. Kimelman. 1993. Induction of the *Xenopus* organizer: expression and regulation of *Xnot*, a novel FGF and activin-regulated homeobox gene. Genes & Development 7: 355-366.

Wang, F., M. Kan, J. Xu, G. Yan, and W. McKeehan. 1995. Ligand-specific structural domains in the fibroblast growth factor receptor. Journal of Biological Chemistry **270**: 10222-10230.

Wang, F., M. Kan, G. Yan, J. Xu, and W. McKeehan. 1995. Alternatively spliced NH_2-terminal immunoglobulin-like loop I in the ectodomain of the fibroblast growth factor (FGF) receptor 1 lowers affinity for both heparin and FGF-1. Journal of Biological Chemistry **270**: 10231-10235.

Weeks, DL and DA. Melton. 1987. A maternal mRNA localized to the vegetal hemisphere in *Xenopus* eggs codes for a growth factor related to TGF-beta. Cell **51(5)**: 861-867.

Wilkinson, DG, S. Bhatt, and BG. Herrmann. 1990. Expression pattern of the mouse T gene and its role in mesoderm formation. Nature **343**: 657-659.

Wilks, A. 1993. Protein tyrosine kinase growth factor receptors and their ligands in development, differentiation and cancer. Advances in Cancer Research **60**: 43-73.

Wolpert, L., R. Beddington, J. Brockes, T. Jessell, P. Lawrence, and E. Meyerowitz. 1998 Principles of Development. New York: Current Biology Ltd.

Woodland, H. 1989. Mesoderm formation in *Xenopus*. Cell **59**: 767-770.

Xie, M., I. Holcomb, B. Deuel, P. Dowd, A. Huang, A. Vagts, J. Foster, J. Liang, J. Brush, Q. Gu, K. Hillan, A. Goddard, and A. Gurney. 1999. FGF-19, a novel fibroblast growth factor with unique specificity for FGFR4. Cytokine **11**: 729-735.

Yamasaki, M., A. Miyake, S. Tagashira, and N. Itoh. 1996. Structure and expression of the rat mRNA encoding a novel member of the fibroblast growth factor family. The Journal of Biological Chemistry **271**: 15918-15921.

Yamashita, T., M. Yoshioka, and N. Itoh. 2000. Identification of a novel fibroblast growth factor, FGF-23, preferentially expressed in the ventrolateral thalamic nucleus of the brain. Biochemical and Biophysical Research Communications **277**: 494-498.

Yayon, A, Y. Zimmer, GH. Shen, A. Avivi, Y. Yarden, and D. Givol. 1992. A confined variable region confers ligand specificity on fibroblast growth factor receptors: implications for the origin of the immunoglobulin fold. EMBO Journal **11(5)**: 1885-1890.

Zhan, X., B. Bates, X. Hu, and M. Goldfarb. 1988. The human FGF-5 oncogene encodes a novel protein related to fibroblast growth factors. Molecular and Cellular Biology **8**: 3487-3495.

Zhang, J, DW. Houston, ML. King, C. Payne, C. Wylie, and J. Heasman. 1998. The role of maternal VegT in establishing the primary germ layers in *Xenopus* embryos. Cell **94(4)**: 515-524.

Zhang, JD, LS. Cousens, PJ. Barr, and SR. Sprang. 1991. Three-dimemsional structure of human basic fibroblast growth factor, a structural homolog of interleukin 1 beta. Proceedings of the National Academy of Science, USA **88(8)**: 3446-3450.